Chapter 6 - Structural Geometry

CHAPTER 6 - Structural Geometry

6.1 INTRODUCTION

The primary aim of this chapter is to establish a deformation event hierarchy that can be integrated into the Tawallah Group palaeo-geographic model proposed in Chapter 3. The structural evolution of the southern McArthur Basin has received little attention in the past, with previous studies focussed on basin-scale tectonic modelling (eg. Plumb, 1979). More recently, detailed structural analysis at the McArthur River Pb-Zn deposit (Hinman; 1995) has shown that the presence, timing and geometric characteristics of major deformational events in the southern McArthur Basin are factors that need to be considered before any reasonable geodynamic model can be proposed.

To determine the structural history of the study region, palaeostress tensors were calculated from fault-slip data collected in the Batten, Scrutton and Tawallah Ranges using the methods of Etchecopar *et al.* (1981). In this chapter, 1:25 000 scale geological field mapping, kinematic resolution of primary and secondary brittle structures and inverse palaeostress analysis were used to determine the relative timing, palaeostress-field orientations and geometric characteristics of each deformation event.

6.2 STRUCTURAL DOMAINS

The study region comprises a series of discrete, N- to NNW-trending fault-blocks that are bound by large-scale primary faults (Fig. 6.1). Dimensions of individual fault-blocks are characterised by high length-to-width ratios (5:1), reflecting the narrow spacing of primary bounding faults (5-10 km). Based on the spatial geometry of primary fault segments, and on the structural geometry in adjacent fault-blocks, the western McArthur River region is divided into three main structural domains (Fig. 6.1).

6.2.1 Southern domain

The southern domain is a coherent fault block that covers approximately 1500 km^2 in area, and includes the Batten Range on its eastern margin (Fig. 6.1). The southern Tawallah Fault segment forms the eastern boundary of the domain, has a consistent, sub-vertical dip and varies in orientation from N-S in the north, to strike NNE along the south-eastern margin of the Batten Range. The Tawallah Group and lower McArthur Group units exposed in the Batten Range mostly young westward, and

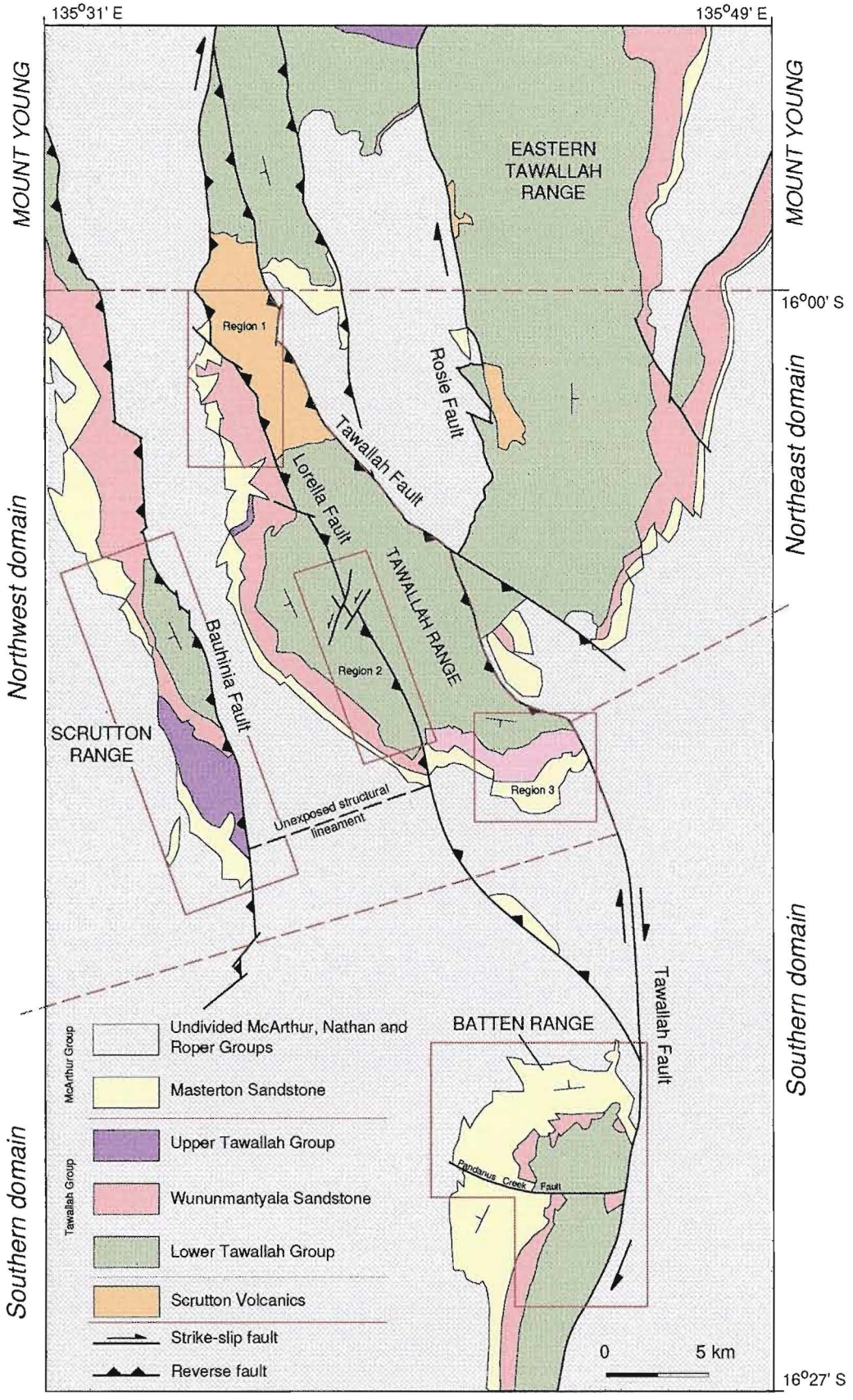

Fig. 6.1 Simplified geology, regions of detailed structural investigation (solid lines) and structural domains (dashed lines) of the study region. Lower Tawallah Group includes the Yiyintyi Sandstone, Seigal Volcanics, Sly Creek Sandstone and Aquarium Formation. Upper Tawallah Group includes the Settlement Creek Volcanics, Wollogorang Formation, Gold Creek Volcanics, Warramana Sandstone, Tanumbirini Rhyolite and Nyanantu Formation.

are juxtaposed against younger Palaeoproterozoic formations along the Tawallah Fault. Two sets of regional-scale, open and upright folds occur in the southern domain. N-S-trending regional-scale folds with shallowly dipping western limbs (20°) and short, steeply dipping eastern limbs (60°) have been gently refolded about an E-W axis. In the Batten Range, the interference of N-S- and E-W-trending folds has produced a broad, asymmetric dome (Appendix 4b).

6.2.2 Northwest domain

The northwest domain covers an area of approximately 600 km^2 and contains two structural blocks that are bound by primary fault segments (Scrutton Range and western Tawallah Range; Fig. 6.1). The internal structural geometry of each fault-block is characterised by the repetition of Tawallah Group stratigraphy across NW-trending reverse to oblique-reverse faults.

In the Scrutton Range, Tawallah Group formations typically dip and young towards the southwest, and are juxtaposed with lower McArthur Group stratigraphy along the NW-striking and moderately SW-dipping (50 to 60°) Bauhinia Fault (Appendix 4c). Vertical stratigraphic offset across the Bauhinia Fault decreases towards the southern margin of the Scrutton Range. Stratigraphic repetition in the Scrutton Range fault-block occurs across NW-trending reverse faults, where vertical displacements of up to 200 m may be preserved. Folding in the Scrutton Range fault-block is restricted to southern parts of the range, where an anticline-syncline pair occur in upper Tawallah Group stratigraphy (Appendix 4c). The folds are open and asymmetric with moderately dipping (25-40°) west-facing limbs and a shallowly dipping (12-26°) east-facing limb. Axial traces of the folds strike parallel to the Bauhinia Fault and plunge shallowly southeast. The anticlinal closure has been juxtaposed with the synclinal closure along a NW-striking reverse fault, so that the mutual east-facing fold limb has been mostly removed.

The western Tawallah Range is a fault-bound inlier that contains Scrutton Volcanics and lower Tawallah Group formations (Fig. 6.1). In general, these rock types are juxtaposed with younger Tawallah Group or McArthur Group formations along both western (Lorella Fault) and eastern margins (northern Tawallah Fault segment) of the inlier. However, complex stratigraphic juxtapositions occur in the southwest Tawallah Range where a change from SW- to NE-directed reverse movement along the Lorella Fault is interpreted to have occurred across a one kilometre wide corridor of NNW-trending oblique-sinistral faulting (Fig. 6.1). The northern end of the NE-verging Lorella Fault segment has been progressively offset within the oblique-sinistral fault zone, and terminates in a broad, open and upright antiform (Fig. 6.1). To the south, the Lorella Fault trace is terminated by the Tawallah Fault. A return to SW-directed reverse

displacement is inferred to have occurred along the Lorella Fault south of the Tawallah Range and north of the intersection with the Tawallah Fault. (Fig. 6.1).

6.2.3 Northeast domain

The third structural domain covers an inlier of Scrutton Volcanics and Tawallah Group rock types in the northeast part of the study region (Fig. 6.1). The Rosie Fault forms the western margin of inlier, where Yiyintyi Sandstone lithologies are juxtaposed with various lower McArthur Group formations. Sedimentary units young and dip towards the east within the inlier, in contrast to the stratal geometries west of the Rosie Fault. Structural investigation of the north-eastern domain was limited compared to the detailed mapping conducted for regions of the Batten, Scrutton and western Tawallah Ranges.

6.3 THE INVERSE METHOD OF PALAEOSTRESS ANALYSIS

Numerical analysis of fault-slip data in brittle terranes can be a powerful tool for interpreting palaeostress orientations and related tectonic events. Fault-slip data collected during this study included the fault plane orientation, orientation of the slip direction and the sense-of-slip. These were obtained from field measurements of slickenside lineations or fault striations (Petit, 1987). Fault striations were present on most of the secondary fault surfaces in the study region (Plate 6.1a, b and c), and their measurement was the principal method used to determine kinematic sense in the field. Where possible, observed stratigraphic displacement or extension-fibre vein orientations were measured to aid fault sense determination.

The aim of any investigation in palaeostress reconstruction is to determine the 'reduced stress tensor', which is a linear function of the actual average stress tensor responsible for the fault slips (Angelier, 1989). Although the reduced stress tensor does not provide the magnitude of the principle stresses (σ_1 - maximum compressional stress > σ_2 - intermediate stress > σ_3 - minimum stress), their orientations are identical to those of the actual stress tensor. Compression or extension directions that were operative during tectonism can therefore be determined.

Theoretical studies of rock mechanics have shown that, for a given stress tensor and fault plane orientation, the sense and orientation of slip is determined by the orientation of resolved shear stress acting on the plane (Wallace, 1951; Bott, 1959). The inverse problem involves calculation of the stress tensor from the orientations and slip-senses (orientations of resolved shear stress) on a number of faults.

Algebraic and/or graphical methods that resolve regional palaeostress directions from fault-slip data have been proposed by Etchecopar *et al.* (1981); Angelier (1981, 1984); Reches (1987); Gephart (1990); Will and Powell (1991); Yin and Ronalli

Plate 6.1 Kinematic indicators preserved on fault surfaces in the study region and silicification of the Sly Creek Sandstone in the Batten Range.

a) Quartz fibres preserved on the lee side of a ripple crest from a reverse fault surface in the Bauhinia Fault Zone (Sly Creek Sandstone, Scrutton Range; 5625E - 82136N).

b) Quartz striations preserved on a dextral strike-slip fault surface in the Batten Range (Masterton Sandstone; 5788E - 81916N).

c) Quartz striations preserved on a dextral strike-slip fault surface in the Tawallah Range (Sly Creek Sandstone; 5675E - 82157N).

d) Aerial photograph of the northeast Batten Range showing the characteristic lighter colouration of the (silicified) Sly Creek Sandstone (Ptl) relative to the younger Tawallah Group and McArthur Group sandstones (Ptn - Wununmantyala Sandstone; Pms - Masterton Sandstone).

Plate 6.1

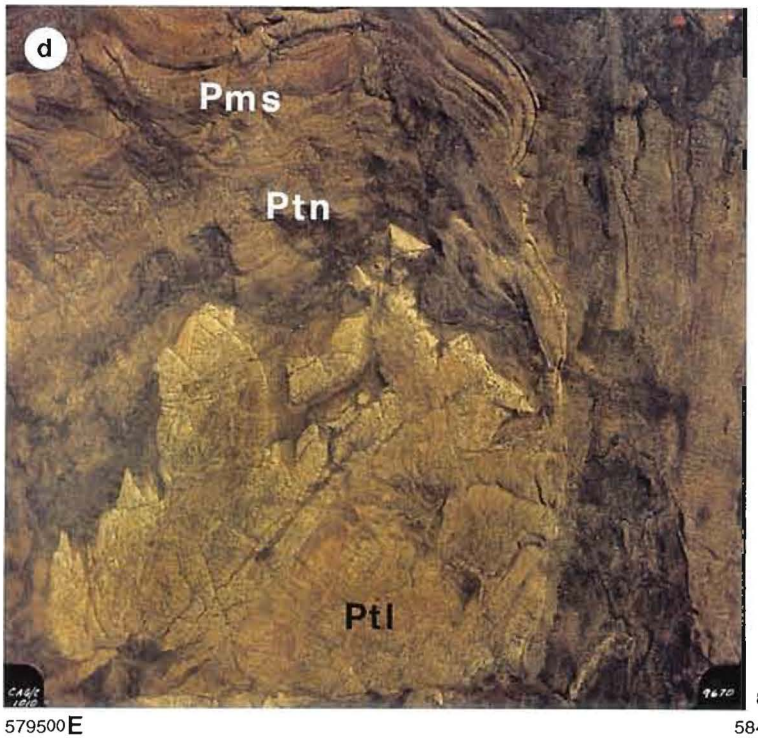

8193000 N

8188800 N

579500 E

584700 E

(1993); and Dupin *et al.* (1993). The main assumption common to all methods is that a given tectonic event is characterised by one, regionally homogenous stress field. In other words, each fault-slip has the direction and sense of shear stress that corresponds to a unique common stress tensor (Angelier, 1989). Variations in regional stress patterns due to mechanical interaction between faults are assumed to be negligible. However, recent studies have shown secondary that faults, and particularly those that form part of a larger fault zone, mechanically and kinematically influence their nearest neighbours to generate local perturbations in the stress field (Bürgmann *et al.*, 1994). Although this may seem problematical, especially where fault spacings are small or faults intersect, large deviations of stress relative to the homogenous far-field stress are rare (Dupin *et al.*, 1993). Computer-generated fault-slip models suggest that the angular discrepancy between the slip direction and resolved regional shear stress are generally within the precision of stress inversion analysis (Pollard *et al.*, 1993). Large fault-slip data sets that include many fault orientations are necessary to validate the homogenous stress field assumption. A further implication of the assumption is that faults with no resolved shear stress (ie. those that develop parallel to σ_1), such as transfer faults in extensional settings or tear faults in thrust terranes, cannot be discerned using the inverse method of fault-slip analysis.

Fault-slip data collected in this study were used to derive palaeostress-field orientations following the methods of Etchecopar *et al.* (1981; Appendix 2). This method aims to determine the reduced stress tensor that minimises the angular deviation between the predicted shear stress direction and the measured slip direction for each fault plane. The algorithm used in the analysis; (a) sorts and attributes the data to a tectonic phase, and (b) defines the characteristics of the stress tensor related to this phase. In this way, superimposed tectonic phases can be separated from the total fault-slip data. The polyphased data method used in this study was divided into three successive steps (Etchecopar *et al.*, 1981);

Step 1: The initial step involved a 'first pass' estimation of the reduced stress tensor for a given initial σ_1 value. One hundred different tensors were applied to the data using randomly chosen parameters (directions of σ_1, σ_3 and R). For each tensor, theoretical fault-slip directions were calculated for each fault plane. Fault planes that had the smallest angles between predicted and actual slip orientation were selected and the quadratic sum (S) of these angular deviations were calculated. The tensor (T_o) with the smallest value of S was retained.

Step 2: The parameters used to obtain T_o in step 1 were modified so that the quadratic sum of angular deviations was minimised for the selected data. A new selection of predicted slip orientations were then calculated using the modified parameters. Using a non-linear optimising procedure, data not consistent with the new estimated tensor were either dropped or replaced by the data rejected in step 1.

Step 3: The final step refined the solution using least squared regression analysis of the angular deviations. Measured data up to 0.6 radians (34.4°) from the calculated fault-slip orientations were deemed to have developed during the same tectonic phase. Data that were not explained by the computed tensor corresponded to a different tectonic phase and were re-analysed separately from step 1.

6.4 PALAEOSTRESS ANALYSIS: RESULTS

More than 150 fault-slip measurements were recorded from secondary faults in the Batten Range (Appendix 4b). Most of the secondary faults had preserved evidence for strike-slip motion, and in general, were characterised by minor amounts of lateral displacement (< 50 m). Three distinct fault generations, each corresponding to a separate compressional episode, were determined for the Batten Range region by inverse palaeostress analysis (Appendix 2). Approximately 150 fault-slip measurements were collected from a 70 km^2 area of the Scrutton Range (Appendix 4c). Palaeostress analysis of measured fault-slip data has been interpreted to indicate that the Scrutton Range structural geometry was formed by two separate compressional deformation events (Appendix 2).

Three regions of the western Tawallah Range were chosen to investigate the structural evolution of the southern Lorella Fault and northern Tawallah Fault segments (Fig. 6.1). Region 1 covers approximately 32 km^2 immediately south of the 1:250 000 *BAUHINIA DOWNS/MOUNT YOUNG* map sheet boundary (Appendix 4d). Region 2 covers a 40 km^2 area in central-western Tawallah Range, adjacent to the NW-striking Lorella Fault segment (Appendix 4e). Region 3 covers 20 km^2 of Tawallah Group and lower McArthur Group stratigraphy adjacent to the Tawallah Fault (Appendix 4f). Palaeostress analysis of each region indicated that secondary fault patterns preserved in the western Tawallah Range were formed by two brittle deformational events (Appendix 2).

6.4.1 E-W compression

Secondary faults generated during E-W compression occur in the Batten Range (σ_1: 3°→101°, σ_2: 21°→192°, σ_3: 68°→004°), and include a mutually cross-cutting, conjugate NE-striking dextral and NW-striking sinistral set, and NNE-striking reverse faults (Fig. 6.2). These structures only occur in lower Tawallah Group stratigraphy (Yiyintyi Sandstone through to Aquarium Formation). The conjugate fault pair mostly consists of dextral strike-slip faults that are characterised by moderate to steep, NW-dipping fault planes. Dip-slip faults have moderate, ESE-dipping fault planes and consistent, west-directed reverse motions.

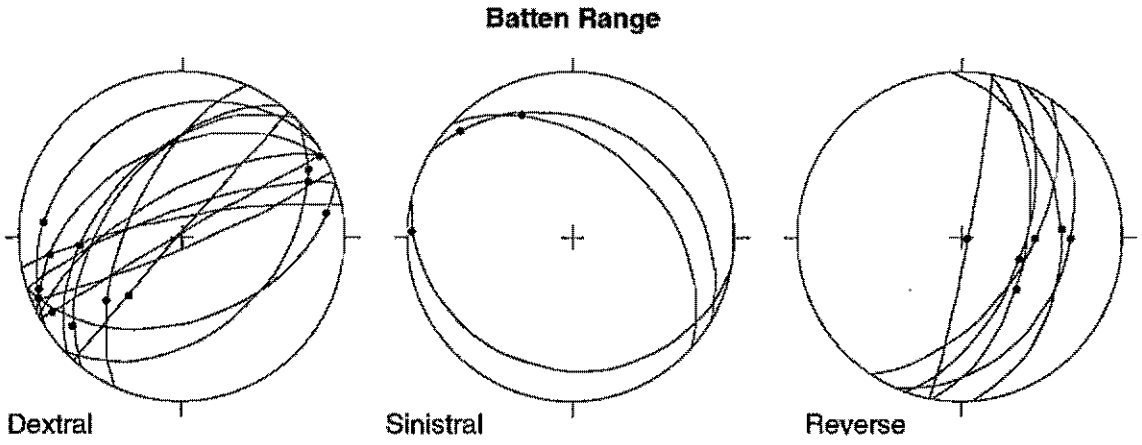

Fig. 6.2 Orientation of measured fault-slip data corresponding to E-W compression in the Batten Range.

6.4.2 NW-SE compression

Batten Range

Throughout the Batten Range region, a poorly-preserved array of secondary faults were formed in response to NW-SE compression (σ_1: 19°→167°, σ_2: 70°→326°, σ_3: 7°→75°). This array consists of orthogonal conjugate NW-striking dextral and NE-striking sinistral strike-slip faults, and ENE-striking reverse faults (Fig. 6.3a). In contrast to the faults formed by E-W compression, faults associated with this deformational phase occur in, and cross-cut all exposed stratigraphy. Dextral strike-slip faults typically have steep, NE- or SW-dipping fault planes, and are the most abundant fault type formed by NW-SE compression. Sinistral strike-slip faults are also steeply inclined, and have consistent SE dip-directions. Dip-slip faults have reverse movements, and mostly dip towards the south.

Scrutton Range

In the Scrutton Range, secondary faults formed during NW-SE compression (σ_1: 12°→162°, σ_2: 76°→001°, σ_3: 4°→253°) include conjugate NW-striking dextral and NNE-striking sinistral strike-slip faults, and NNW-striking normal faults (Fig. 6.3b). Included in this fault pattern is the normal fault which forms the western margin of the Scrutton Range (Appendix 4c). Based on the juxtaposition of lower McArthur Group formations (Masterton Sandstone and Mallapunyah Formation) with various upper Tawallah Group units, up to 250 m stratigraphic displacement is interpreted to have occurred on this structure.

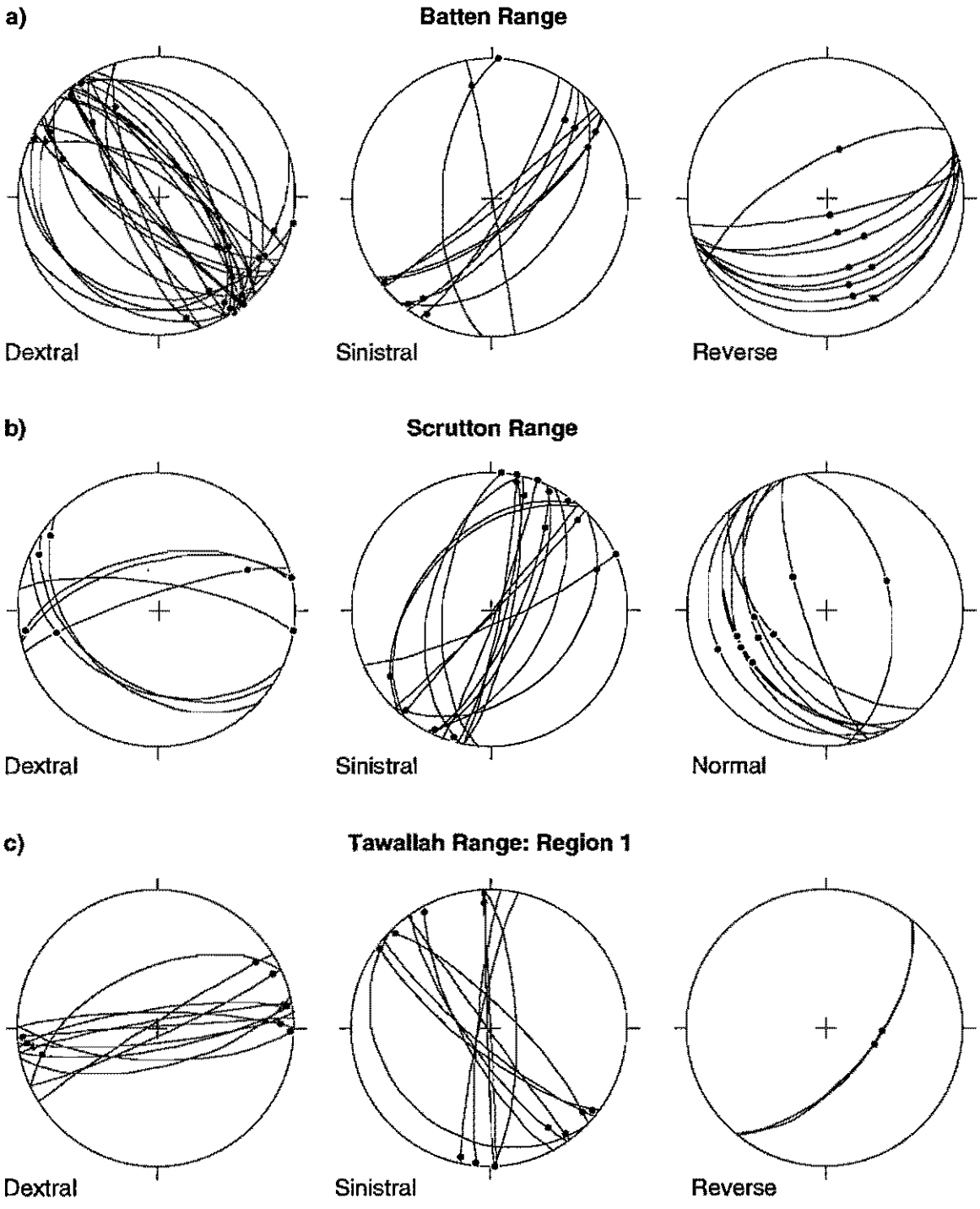

Fig. 6.3 Orientations of measured fault-slip data corresponding to NW-SE compression in the: a) Batten Range; b) Scrutton Range; and b) Tawallah Range - Region 1.

d)

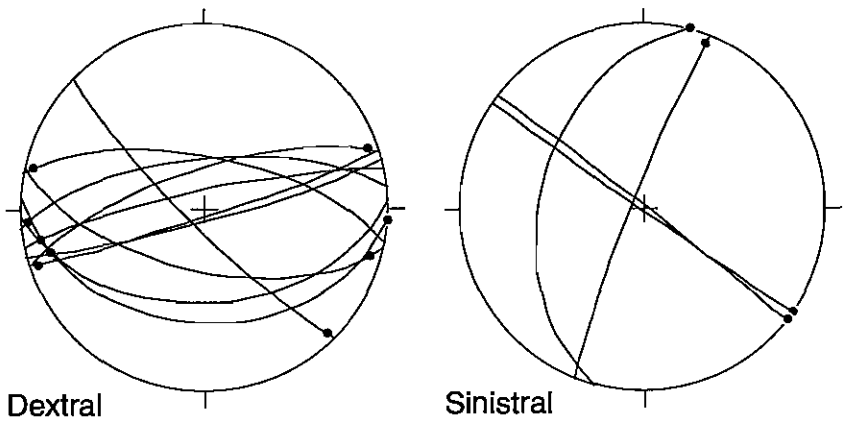

e)

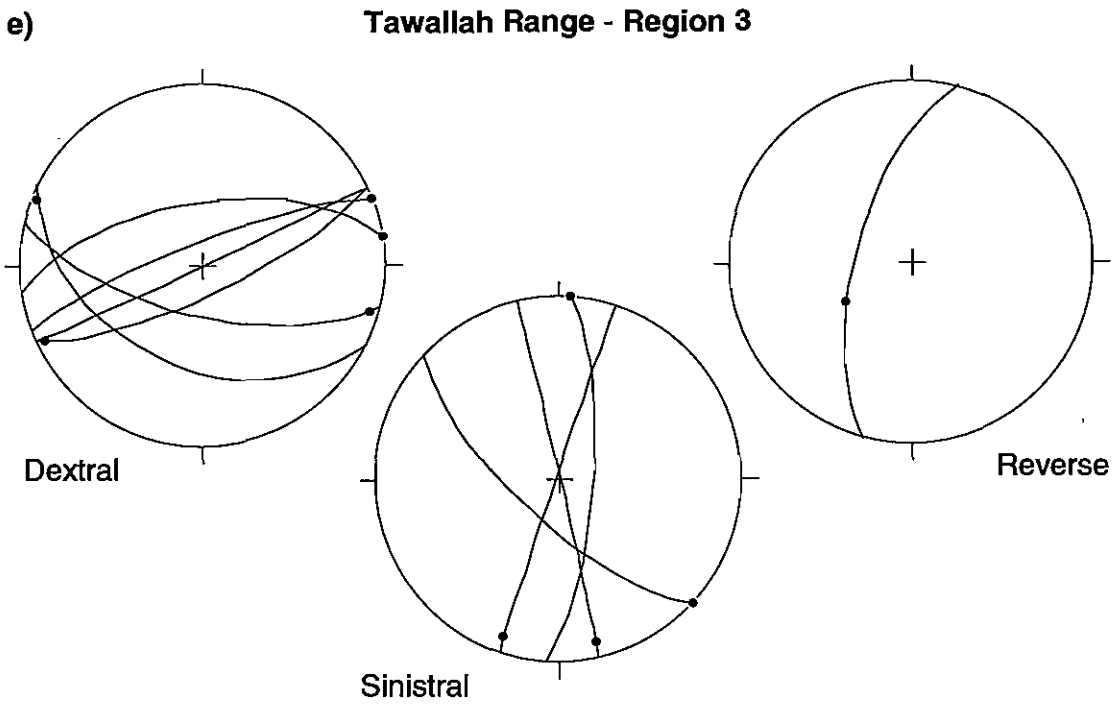

Fig. 6.3 (cont.) Orientations of measured fault-slip data corresponding to NW-SE compression in the: d) Tawallah Range - Region 2; and e) Tawallah Range - Region 3.

Tawallah Range

In the western Tawallah Range, a consistently orientated set of brittle faults have formed in response to NW-SE compression (σ_1: 1°→123°, σ_2: 78°→014°, σ3: 12°→219°). In all regions, the main secondary fault types are conjugate ENE-striking dextral and NW-striking sinistral strike-slip faults (Fig. 6.3c, d and e). Minor elements of the fault-pattern include N-striking sinistral strike-slip and NE-striking reverse structures. Most of the strike-slip faults have steeply inclined to sub-vertical fault planes (Fig. 6.3c, d and e).

6.4.3 NE-SW compression

Batten Range

Most of the fault-slip data used for palaeostress analysis in the Batten Range were collected from secondary faults formed by NE-SW compression (σ_1: 13°→231°, σ_2: 88°→086°, σ_3: 1°→321°; Fig. 6.4a). NNW-striking dextral strike-slip faults that have steeply ENE-dipping fault planes are the most abundant fault type associated with this deformational phase. NE-striking dextral faults formed by NE-SW compression mostly occur within 2 km of Tawallah Fault. Secondary faults that have preserved evidence for sinistral strike-slip motion during this event include a prominent WNW-striking set, and an ENE-striking population that occurs locally along the Tawallah Fault. Both sinistral strike-slip fault-sets have moderate to steep, north or south dipping fault planes. NW-striking reverse faults typically have shallow to moderate, NE-dipping fault planes.

Scrutton Range

Based on the results of the palaeostress analysis, most of the secondary faults in the Scrutton Range have developed in response to NE-SW compression (σ_1: 5°→254°, σ_2: 1°→164°, σ_3: 85°→063°; Fig. 6.4b). The most abundant secondary fault types formed by NE-SW compression are NW-striking reverse faults and NE-striking dextral strike-slip faults. A minor NNE to NNW-striking dextral strike-slip fault-set are interpreted to be conjugates of ESE-striking sinistral strike-slip faults. Late WNW-trending sinistral strike-slip faults offset the conjugate pair. The majority of strike-slip faults have steeply dipping fault planes, whereas the reverse faults have moderately SW-dipping fault planes (Fig. 6.4b).

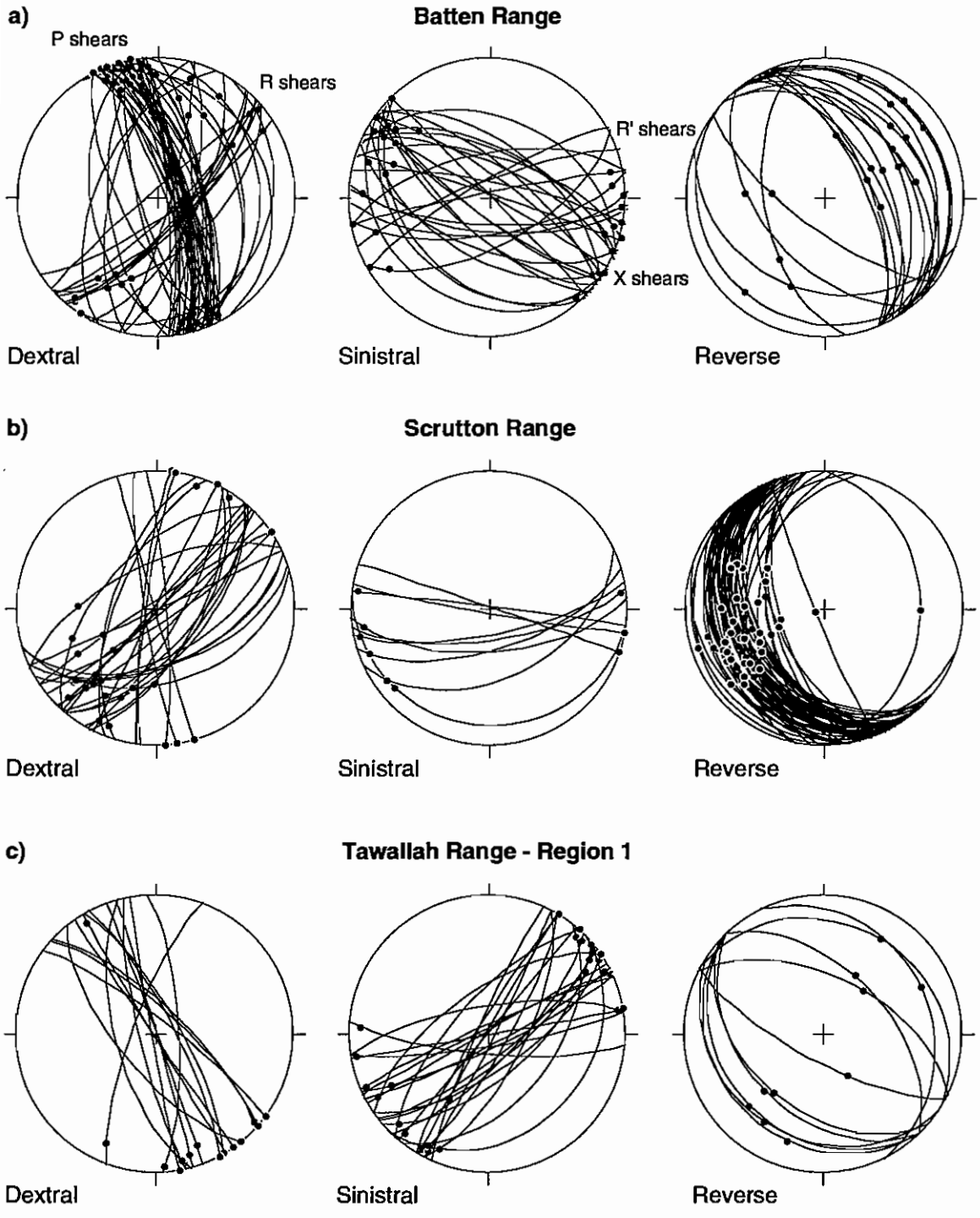

Fig. 6.4 Orientations of measured fault-slip data corresponding to NE-SW compression in the: a) Batten Range; b) Scrutton Range; and c) Tawallah Range - Region 1.

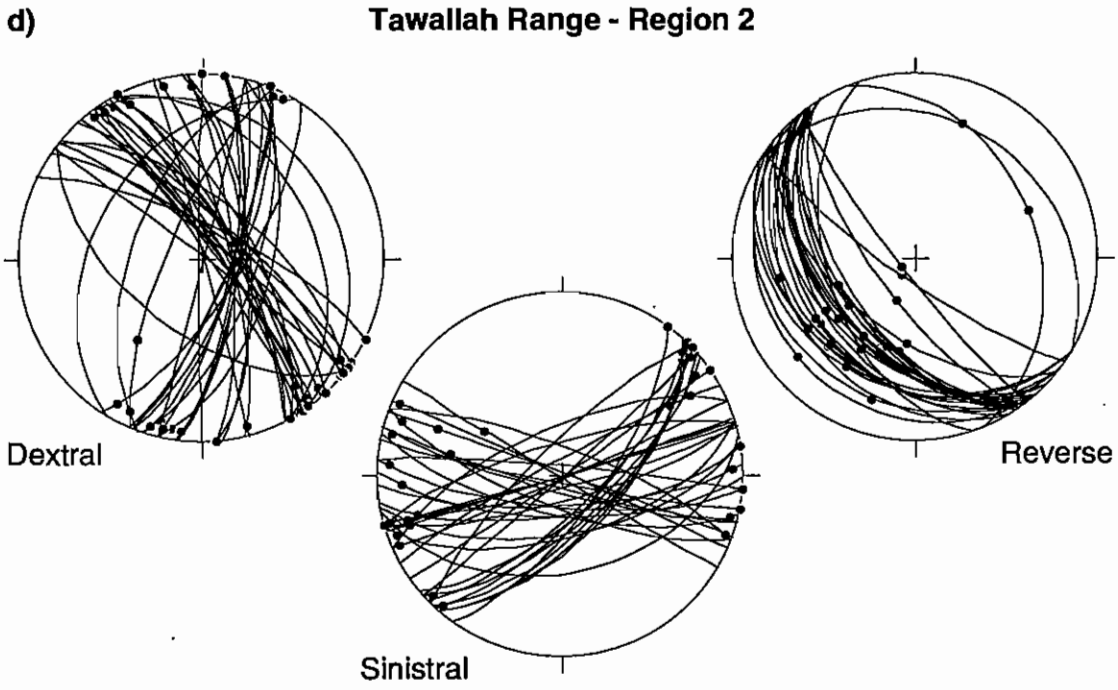

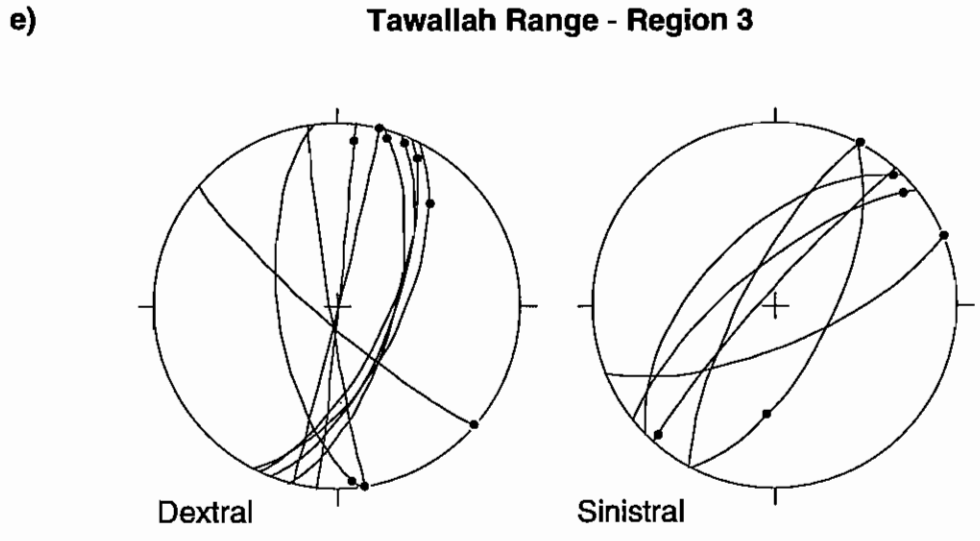

Fig. 6.4 (cont.) Orientations of measured fault-slip data corresponding to NE-SW compression in the: d) Tawallah Range - Region 2; and e) Tawallah Range - Region 3.

Tawallah Range

Most of the secondary faulting in the western Tawallah Range has developed in response to NE-SW compression (σ_1: 6°→219°, σ_2: 82°→357°, σ_3: 6°→128°; Fig. 6.4c, d and e). In each region, sub-vertical strike-slip faults are the major component of secondary fault patterns formed during this event.

In region 1, a mutually cross-cutting conjugate fault pair comprising NNW-striking dextral and NE-striking sinistral strike-slip faults have an average intersection angle of 71° (Fig. 6.5). In regions 2 and 3, the same conjugate fault pair has an average intersection angle of 70° and 58° respectively (Fig. 6.5). A second conjugate strike-slip fault pair occurs in region 2, where NNE-striking dextral and WNW-striking sinistral faults have an average intersection angle of 70° (Fig. 6.5). Although the two main conjugate pairs are easily recognised on Figure 6.5, a number of strike-slip faults cannot be attributed to one of the main conjugate orientations. Mutually cross-cutting relationships typically exist for each conjugate pair. However, only one conjugate orientation may have developed locally.

NW-striking reverse faults developed during NE-SW compression occur throughout the western Tawallah Range. In region 1, moderately NE-dipping reverse faults characterised the Lorella Fault Zone, whereas shallow to moderately SW-dipping reverse faults were typical of the Tawallah Fault Zone (Fig. 6.4c). Most of the reverse faults measured from region 2 were moderately SW-dipping, bedding-parallel structures occurring in the Lorella Fault hangingwall (Fig. 6.4d). However, the steeply SW-dipping reverse fault planes on Figure 6.4d were measured from the southern Lorella Fault segment, whereas the NE-dipping reverse fault planes were measured from the northern Lorella Fault segment.

6.5 TIMING OF DEFORMATION EVENTS

6.5.1 Syn-Tawallah Group deformation (D_1)

Evidence for overprinting, such as superimposed striations, were not observed on fault planes formed by E-W compression. However, the faults related to this event have been cross-cut and offset by later faults (Appendix 4b). E-W compression is therefore interpreted to be the oldest deformation event preserved in the Batten Range (D_1). Because the brittle structures that were generated during E-W compression occur only in the lower Tawallah Group, they are interpreted to have developed prior to Wununmantyala Sandstone deposition.

In Chapter 3, the Wununmantyala Sandstone was interpreted to have been deposited in a proximal braidplain system adjacent to the Tawallah Fault. The proximal

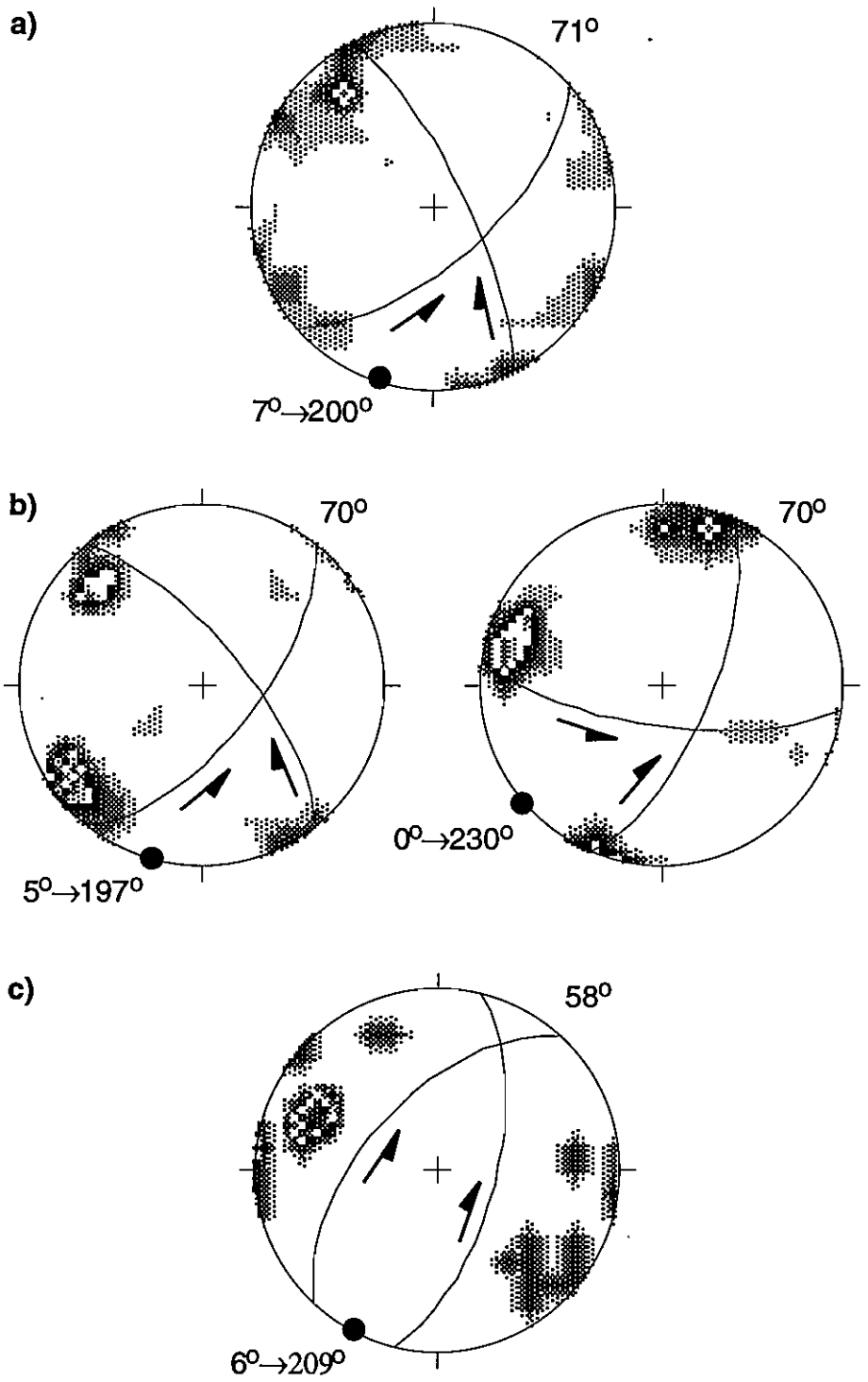

Fig. 6.5 Orientations and average intersection angles of D_3 conjugate strike-slip faults in the western Tawallah Range; **a)** Region 1, **b)** Region 2, and **c)** Region 3. Orientations of the D_3 maximum principle stress estimated for each region by palaeostress analysis are also shown (full circles).

deposits were correlated with more distal braidplain facies associations in the Scrutton Range. Intrabasinal uplift of Scrutton Volcanics and lower Tawallah Group stratigraphy was proposed to explain these local variations in the Wununmantyala Sandstone facies architecture. West-directed palaeocurrents measured from planar cross-bedded lithofacies in the Wununmantyala Sandstone were interpreted to indicate that uplift was controlled by east-block-up movements along the N-striking Tawallah Fault (Bull, 1993). Pre-Wununmantyala Sandstone uplift along the Tawallah Fault is therefore interpreted to have occurred during D_1, E-W compression. Other indirect lines of evidence for a pre-Wununmantyala Sandstone D_1 timing include; 1) the regional and pervasive silicification of the lower Tawallah Group sedimentary package (in particular, the Yiyintyi and Sly Creek Sandstones) compared to the middle and upper Tawallah Group packages; and 2), the abundance of cataclastic and/or hydraulic breccias in post-D_1 fault zones that occur in lower Tawallah Group rock types.

Pervasive silicification is a characteristic feature of the Yiyintyi and Sly Creek Sandstones in the study region, and is responsible for their light colouration on air photographs and surface exposure (Plate 6.1d). Although the actual silicification mechanism is unknown, diagenetic (pre-D_1) or deformation-related (syn-D_1) fluid circulation and regional silicification are two possibilities. Both processes could have produced the low porosity lithofacies which characterise the Yiyintyi and Sly Creek Sandstones. The effectiveness of mechanical fracture and shear localisation in quartz arenite are thought to be enhanced for low porosity and hence, high fracture strength samples (Dunn *et al.*, 1973; Wong, 1990). Post-D_1 faults that occur in lower Tawallah Group sandstones are associated with an increased intensity of brittle deformation textures compared to those developed in middle and upper Tawallah Group units. The regional silicification and porosity reduction of pre-D_1 stratigraphy is interpreted to have promoted cataclastic and/or hydraulic fracture of these formations during the later deformation events. Although the silicification of the lower Tawallah Group may not directly relate to the D_1 event, it does highlight the stratigraphic level at which a significant change in the regional basin architecture had occurred.

6.5.1 Post-Tawallah Group deformation (D_2 and D_3)

Two fault striation sets were present on the NNW- and NW-striking faults formed by NW-SE compression in the Batten Range. Rare instances of overprinting indicated that these faults were reactivated during NE-SW compression. In the Scrutton Range, normal and strike-slip faults formed by NW-SE compression are preserved within isolated fault-blocks developed during NE-SW compression. In the Tawallah Range, overprinting relationships were interpreted to indicate that the dextral and sinistral motions measured from ENE- and NW-striking faults respectively (NW-SE

compression), were reversed during NE-SW compression. In conclusion, overprinting relationships in the study region are consistent with NW-SE compression (D_2) predating NE-SW compression (D_3).

Cross-cutting relationships in the study region are consistent with a post-Tawallah Group timing for D_2, although an absolute age for NW-SE compression is not possible. The D_2 event recognised in the study region is tentatively correlated with a NW-SE transpressional event described at the McArthur River Pb-Zn deposit by Hinman (1995). At McArthur River, the talus breccia lithofacies of the Barney Creek Formation are interpreted to have been sourced during uplift associated with NW-SE transpression along the Emu Fault Zone. If the correlation is correct, a syn-Barney Creek Formation timing for D_2 is inferred.

D_3 is the youngest tectonic phase recognised in the study region, and is interpreted to have occurred following deposition of the Roper Group. A post-Roper Group timing for NE-SW compression is inferred by the occurrence of NW-trending folds in Roper Group stratigraphy south of the study region (Abner Range). Post-Roper Group folding at this locality can be explained by proposing that the Abner Range was situated at a transpressional position along the Tawallah Fault Zone during D_3.

6.6 DISCUSSION: Structural Evolution of the Study Region

The structural architecture of the study region has developed in response to three compressional deformation events. The mechanical and kinematic constraints on the structural geometries formed during each event are discussed in the following section.

6.6.1 E-W compression (D_1)

D_1 strike-slip faults occur in a mutually cross-cutting conjugate geometry, although NE-striking dextral faults are the most abundant fault type formed by E-W compression in the Batten Range (Fig. 6.2). The predominance of one orientation in a conjugate fault pair has been recognised in active regions of distributed strike-slip faulting (eg. Salton Trough, southern California; Thatcher and Hill, 1991), and in experimental sandbox models (Gapais *et al.*, 1991). However, the D_1 secondary fault pattern in the Batten Range is interpreted to have been modified by the preferential reactivation of NW-striking sinistral faults during later compressional phases. NE-striking secondary faults are minor components of the D_2 and D_3 deformational geometries, whereas NW-striking faults were the most abundant fault type formed during the later deformation events (Figs. 6.3a and 6.4a). Martel *et al.* (1988) suggested that slip on pre-existing macroscopic surfaces may be an important factor during the

progressive development of fault zones. In the Batten Range, NW-striking faults appear to have been more favourably orientated for reaction during later deformation, resulting in poor preservation of early striations.

6.6.2 NW-SE compression (D_2)

Batten Range

In the Batten Range, D_2 strike-slip faults occur in an orthogonal conjugate geometry (Fig. 6.3a). According to two-dimensional Mohr-Coulomb criterion, conjugate faults develop by failure and slippage along planes perpendicular to the σ_1/σ_3 plane, intersect at σ_2 and are inclined at angles of ϑ_o to σ_1 (Jaeger and Cook, 1979). Experimental studies concerning the mechanics of internal rock friction suggest that ϑ_o values average between 25 to 30° (Byerlee, 1978). The intersection angle between a developing conjugate fault pair is therefore predicted to range from 50 to 60°. However, orthogonal conjugate fault geometries have been described from active extensional and compressional tectonic environments. In these settings, orthogonal conjugates were interpreted to have formed from small distributed fractures activated at Mohr-Coulomb angles (Thatcher and Hill, 1991). These fractures are thought to have progressively rotated away from the σ_1 direction, with continued growth and rotation occurring until fault orientations approached the optimum geometry for deactivation ($2\vartheta_o = 45°$; Sibson, 1985). Brittle conjugate faults may also develop with an initially orthogonal geometry, provided that they have low cohesive strength (Thatcher and Hill, 1991).

The D_2 secondary fault pattern in the Batten Range can also be explained by inferring that the Tawallah Fault was activated as a sinistral strike-slip system during NW-SE-directed compression. Using secondary fault terminology developed for simple shear Riedel models (Sylvester, 1988), NW-striking dextral and NE-striking sinistral faults are interpreted to be antithetic (R') and synthetic (P) shears respectively. The paucity of corresponding conjugate pairs, particularly synthetic Riedel (R) shears, is interpreted to have resulted from rotation and/or reactivation of D_2 faults during later deformation. The predicted orientation of R shears in a sinistral strike-slip system and the P shear orientation in a right-lateral simple shear system are identical. Because P shears are the most abundant fault type formed during D_3 in the Batten Range (section 6.6.3; Fig. 6.4a), absence of R shears in the D_2 fault pattern may have resulted from rotation and/or reactivation during D_3. Consequently, the evidence for sinistral movements on NNW-striking faults is interpreted to have been rarely preserved.

Scrutton and Tawallah Ranges

The Scrutton and Tawallah Ranges contain a similar D_2 strike-slip fault pattern. Differences in the Scrutton Range include the presence of NNW-striking normal faults, which occur as isolated segments within D_3 fault-blocks. Poor preservation of the D_2 secondary fault geometry in the Scrutton Range precludes an interpretation of the mechanisms responsible for its formation.

In the western Tawallah Range, the same D_2 fault pattern occurs in each of the regions investigated during this study (Fig. 6.3c). However, orientations of the estimated D_2 palaeostress-field and associated fault patterns have been rotated anticlockwise by 40-50° relative to the D_2 structural geometry preserved in the Batten Range. This disparity can be explained by inferring that anticlockwise rotation of the western Tawallah Range fault-block occurred during D_3. Uplift of the western Tawallah Range is interpreted to have been controlled by the formation of a contractional strike-slip duplex between the Tawallah and Lorella Faults during D_3 (Section 6.6.3). It is conceivable that some degree of rotation may have accompanied D_3 uplift, given that the average strike of bedding in the western Tawallah Range has also been rotated anticlockwise by approximately 45° relative to the Batten Range (Appendix 4b). If this interpretation is correct, the D_2 fault pattern in the western Tawallah Range could have been generated during sinistral strike-slip motion on N-striking (pre-D_3) segments of the Tawallah and Lorella Faults.

6.6.3 NE-SW-directed compression (D_3)

Most of the large-scale structural features in the study region have formed in response to late-stage NE-SW compression. Regional differences in the D_3 structural architecture are attributed to kinematic variations along the Tawallah, Lorella and Bauhinia Faults during NE-SW compression. In the Batten Range, the D_3 structural geometry is interpreted to have been formed during dextral strike-slip displacement along the Tawallah Fault. Reverse fault mechanisms appear to have been the main kinematic response to NE-SW compression in the Scrutton Range. By comparison with the Batten Range, the Tawallah Range D_3 structural geometry could have been formed in a dextral strike-slip system between the Tawallah and Lorella Faults. However, the D_3 fault pattern in the Tawallah Range contains additional elements that have developed in response to horizontal shortening (vertical σ_3), so that similarities can be also drawn with the Scrutton Range.

Batten Range

D_3 brittle faults in the Batten Range are interpreted to have formed during dextral strike-slip displacement on the Tawallah Fault. By comparison with Riedel models of right simple shear (Aydin and Page, 1984; Fig. 6.6), the D_3 fault pattern in the Batten Range consists of conjugate NNE-striking dextral (synthetic Riedel - R) and WSW-striking sinistral faults (antithetic Riedel - R'), NNW-striking dextral (synthetic P) and WNW-striking sinistral (antithetic X) faults. R and R' secondary faults are mostly restricted to within 2 km of the Tawallah Fault, so that the D_3 fault pattern typically consists of P and X shear fractures.

In experimental studies of strike-slip deformation, R and R' conjugate shear fractures are typically formed during the initial stages of wrench zone evolution (peak shear stress), and have regular orientations as predicted by Mohr-Coulomb criteria (Tchalenko, 1970; Hempton and Neher, 1986; Naylor *et al.*, 1986). R shears initiate at low angles (17°) to the main through-going structure or basement fault, whereas conjugate R' shears develop at relatively high angles (80-85°). With continued strike-slip deformation (post-peak shear stress), R and R' shears are unfavourably orientated to maintain large displacements (Tchalenko, 1970). To accommodate the increasing net displacement on the system, synthetic P shears develop at -15° to the through-going structure.

The formation of P shears involves a simultaneous reduction of shear resistance on Riedel structures, and a local increase and rotation of the principal stresses in an opposite sense to the general movement direction (Tchalenko, 1970). Local rotation of σ_1 towards the R shear direction occurs on the compressional side of R shear tips, or between overlapping R shears, to generate local stress fields in which new faults form in the P shear orientation (Naylor *et al.*, 1986). By comparison with the experimental studies of strike-slip deformation, P shears occurring in natural fault zones are interpreted to have developed by the rotation of σ_1 towards parallelism with the main through-going structure.

In strike-slip deformation experiments, X shears typically develop at high angles (-75°) to the main displacement zone (Bartlett *et al.*, 1981). According to Mohr-Coulomb failure criterion, the formation of X shears in a strike-slip system requires σ_1 to be orientated approximately normal to the main displacement zone (Swanson, 1988). The co-development of P and X shears in a strike-slip system therefore requires a 90° reorientation of the stress field to have occurred during deformation. Co-existing P-P' and X-X' shears have been described from mesoscopic strike-slip fault zones, and are interpreted to have formed during alternating periods of layer parallel shortening and extension (Swanson, 1988). The co-development of P and X shears has also been documented from strike-slip deformation experiments (Bartlett *et al.*, 1981). In these

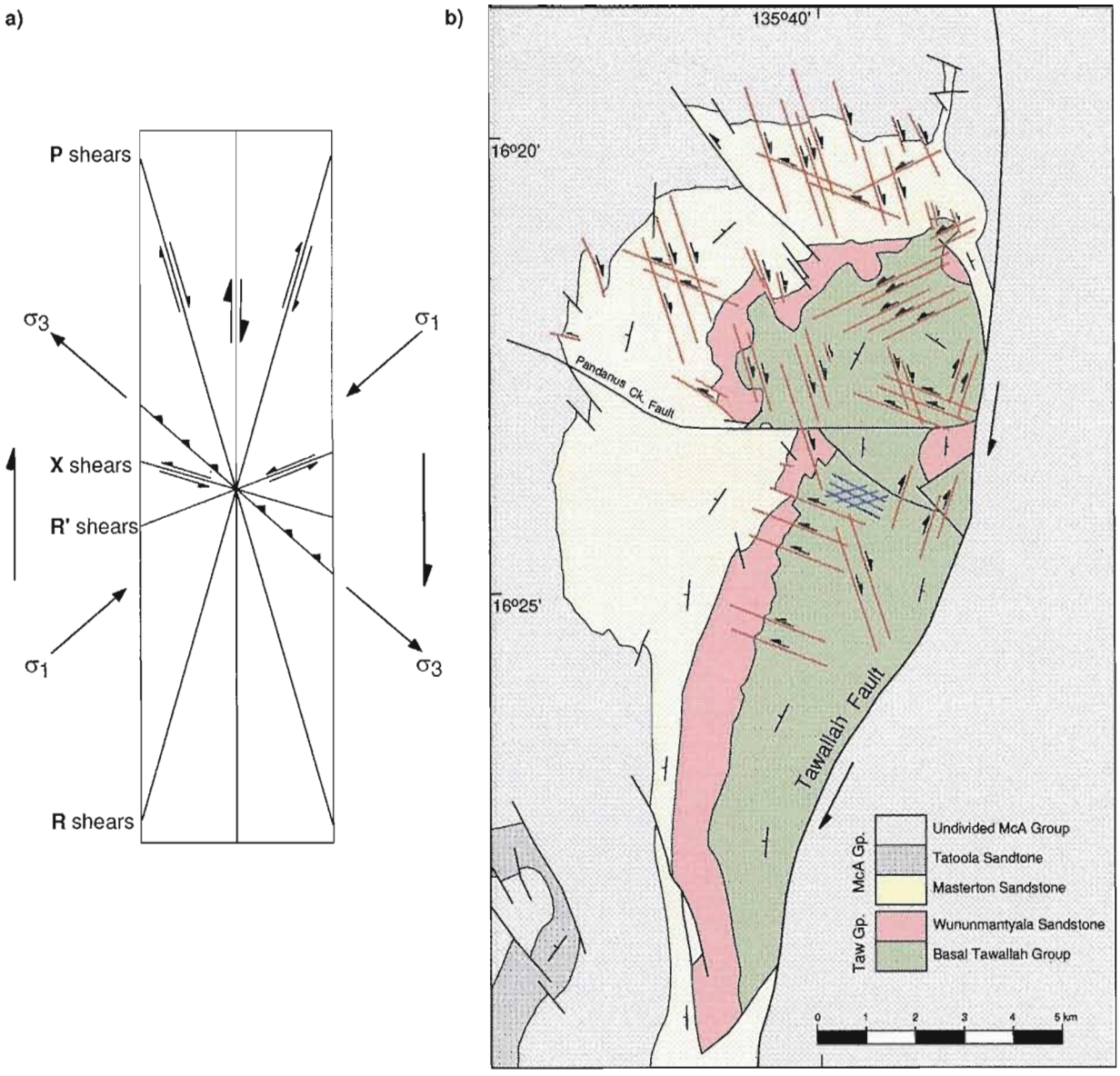

Fig. 6.7 Schematic representation of D_3 strike-slip fault orientations in the Batten Range. **a)** Shear fracture orientations within an idealised dextral strike-slip fault zone. **b)** Orientation and distribution of R, R', P and X secondary faults developed during (D_3) dextral strike-slip displacement along the Tawallah Fault (red lines). Orientations of D_1 strike-slip faults are also shown (blue lines).

experiments, P and R shears were formed simultaneously during peak shear stress. X shears were formed following peak shear stress, with additional P shears initiating to interconnect R shears. However, the X shears that developed in these experiments may have been formed by the rotation and reorientation of post-peak shear stress, R' shears (Naylor *et al.*, 1986).

Sandbox, clay-cake or limestone strike-slip deformation models are poor analogues for the D_3 fault geometry in the Batten Range, because most experimental techniques do not account for the possibility of pre-existing deformation. The restriction of (D_3) R and R' shears to within 2 km of the Tawallah Fault precludes P shear development being the subsequent response to kinematic constraint on R-R' displacement (eg. Tchalenko, 1970). Furthermore, the regular spacing and linear nature of P and X shears is interpreted to indicate that rotation of secondary faults during D_3 was negligible away from the Tawallah Fault Zone. Consequently, the formation of the D_3 secondary fault pattern in the Batten Range is interpreted to have been largely controlled by the reactivation of pre-existing (D_2) faults.

Richard and Krantz (1991) proposed that the presence of existing faults can influence the structural geometry developed during later strike-slip deformation. The early structures will accommodate later deformation in preference to the formation of new faults. The probability for reactivation on an existing plane of weakness is controlled by its orientation relative to the principle stresses (ϑ to σ_1 direction), cohesive strength (C) and internal friction coefficient (μ_i; Hobbs *et al.*, 1976). In the compressive field, these factors define a failure envelope on a Mohr diagram that is assumed to be of the linear Coulomb form;

$$\sigma_s = C + \mu_i \sigma_n$$

where σ_s and σ_n are the shear and normal stresses to the plane respectively. The slope of a failure envelope is governed by the coefficient of internal friction, which generally lies between 0.5 and 1.0 for rocks (Ramsey and Huber, 1987). Sibson (1985) used $C = 0$ for reactivation and $\mu_i = 0.75$ for both reactivation and intact rock failure to establish the kinematic conditions required for frictional reactivation of an existing weakness plane. The optimum angle for reactivation (ϑ^*) was calculated to be 26.5°. Reactivation occurring on planes orientated at $\vartheta > 2\vartheta^*$ required a progressively diminishing differential stress (ie. the relative magnitude of σ_3 decreased and ultimately became tensile) as ϑ approached 90°, so that the failure envelope for intact rock was not breached.

Orientations of D_3 strike-slip faults relative to a NE-striking maximum compressive stress and the failure envelopes for intact rock and reactivation are shown on Figure 6.7. The D_3 fault pattern in the Batten Range can be explained without the

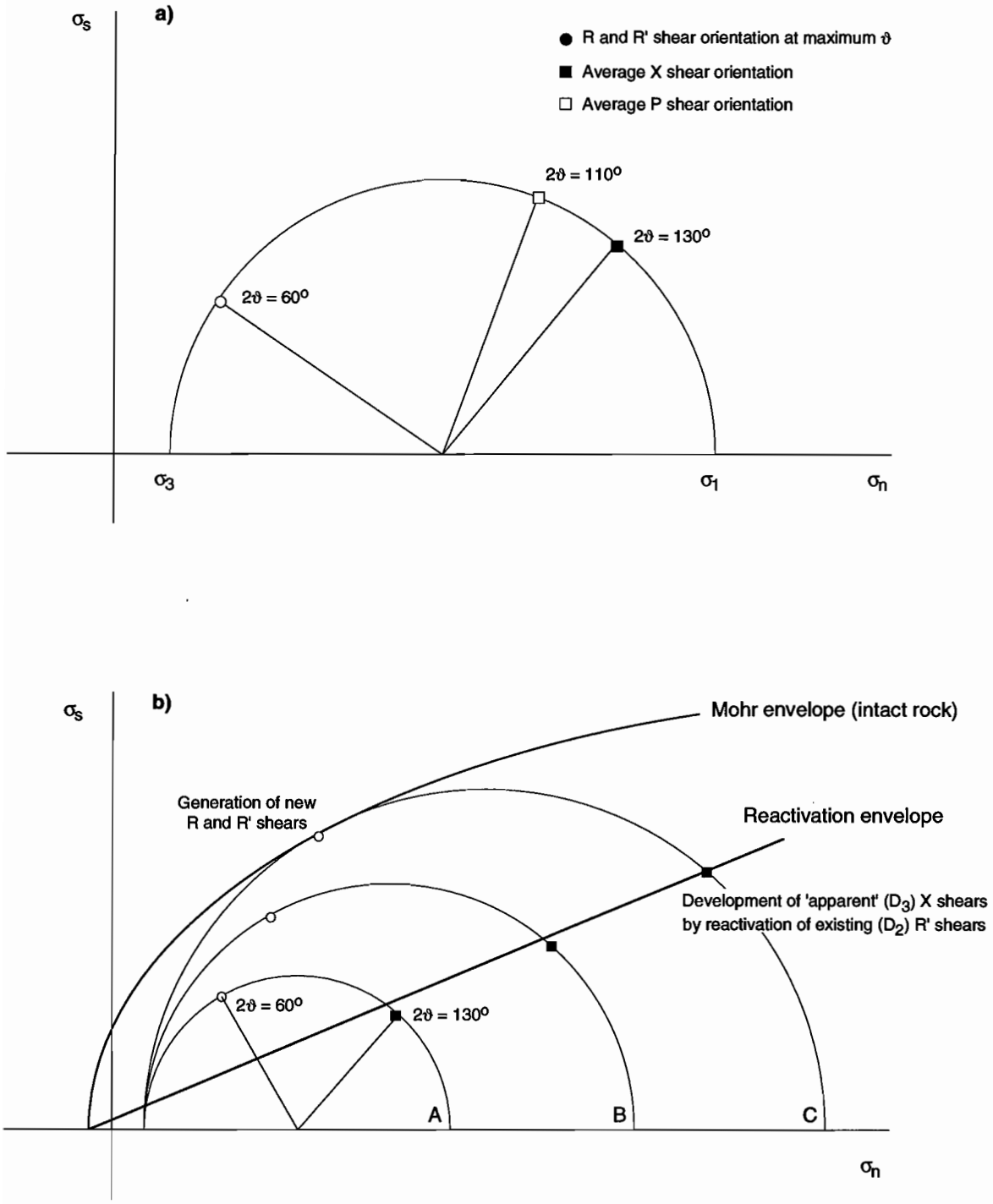

Fig. 6.7a) Mohr circle representation of average D_3 fault plane orientations relative to a NE-directed maximum compressive stress (σ_1 = 10°→230). **b)** Generation of new faults and reactivation of pre-existing structures with increasing σ_1 and constant σ_3. Mohr and reactivation envelops after Ramsey and Huber (1987).

requirement for σ_3 to be tensile, by selecting $\mu_i = 0.5$ to define the failure envelope for fault reactivation, and by allowing for minor cohesive strength on pre-existing faults (D_2 R' shears). For stress states represented by Mohr circles A and B, the existing fault plane orientated at $\vartheta = 65^o$ to σ_1 is stable (Fig. 6.7). However, for Mohr circle C, this fault plane broaches the frictional failure envelope, and reactivation occurs in an approximate X shear orientation for D_3 strike-slip deformation (Fig. 6.7). In addition, new faults orientated at $\vartheta = 30^o$ are generated as Mohr circle C intersects the failure envelope for intact rock (D_3, R and R' shears). For reactivation of existing structures orientated at $\vartheta > 65^o$, an abnormally low internal friction coefficient ($\mu_i < 0.5$) or a tensile σ_3 is required (Sibson, 1985).

Although the fault geometry developed during NE-SW compression can be explained using Mohr-Coulomb failure models, some variation in the orientations of D_3 faults occurs in the vicinity of the Tawallah Fault. These variations may have resulted from subtle differences in shear strength and/or local fluid pressure so that failure at non-optimum orientations occurred (Hobbs *et al.*, 1976). Alternatively, minor rotation of faults from optimal failure orientations may be invoked. Clockwise rotation of D_3 X shears is interpreted to have occurred in the northeast Batten Range, with a progressive change in orientation (WNW- to NNW-strike) and slip-sense (sinistral to oblique sinistral-reverse) toward the Tawallah Fault (Appendix 4b).

Scrutton Range

The Bauhinia Fault is interpreted as an emergent thrust front during D_3, a term used to classify a leading detachment structure in fold and thrust belt terranes (Boyer and Elliot, 1982; Morley, 1986). This comparison is based on the fact that the maximum vertical displacement on the exposed 40 km strike-length of the Bauhinia Fault is approximately 1300 m. The Scrutton Range fault-block forms the hangingwall to the Bauhinia Fault, and continuing the fold-thrust belt analogy, is interpreted to be an overriding thrust sheet (Boyer and Elliot, 1982).

The Scrutton Range fault-block can be sub-divided into a series of subsidiary fault-blocks that are offset by NE-striking (D_3) dextral strike-slip faults and bound by the Bauhinia Fault, or D_3 reverse faults, along their NE margins (Fig. 6.8). Individual fault-blocks that were emplaced further towards the northeast above the Bauhinia Fault have exposed deeper parts of the Tawallah Group stratigraphy. In this way, progressively younger Tawallah Group formations have been juxtaposed with McArthur Group stratigraphy towards the southern Scrutton Range margin (Fig. 6.8). The magnitude of relative displacement across the NW-striking Bauhinia Fault reduces to zero south of the Scrutton Range (southern domain; Appendix 4a).

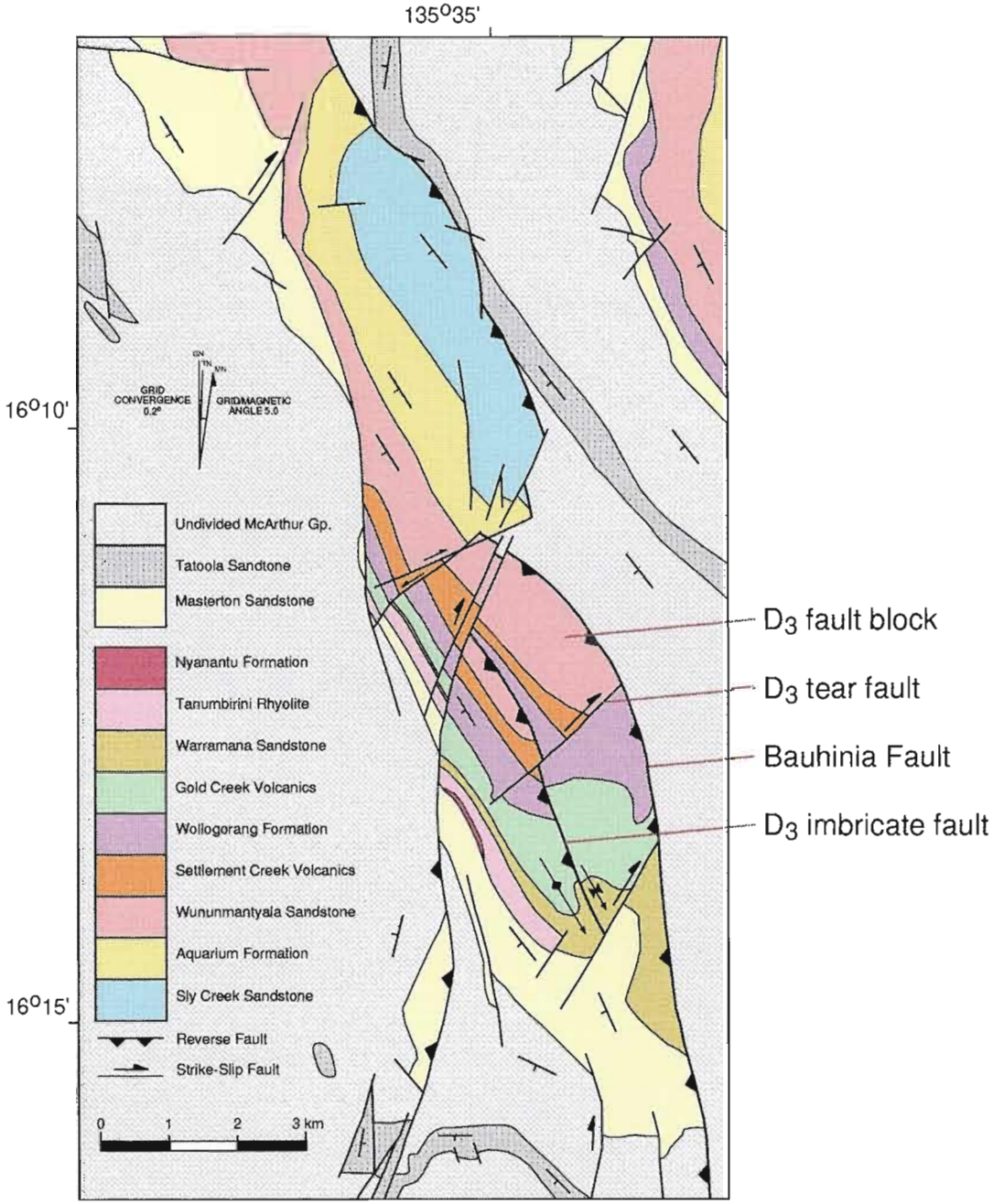

Fig. 6.8 D_3 structural geometry of the Scrutton Range. The Bauhinia Fault hangingwall is subdivided into a series of subsidiary fault-blocks that are bound by NE-striking tear faults and NW-striking imbricate faults. Minor SE-plunging folds occur in southern parts of the region.

i) Tear faults

In relatively undeformed terranes, changes in horizontal separation along the strike of a reverse fault generally implies that some degree of hangingwall rotation has occurred during transport (Ramsey and Huber, 1987). However, the change in the level of Tawallah Group stratigraphy exposed in the Bauhinia Fault hangingwall is not continuous, with abrupt vertical shifts occurring across the NE-striking (D_3) dextral faults which separate discrete fault-blocks (Fig. 6.8). These are orthogonal to the Bauhinia Fault and preserve evidence for oblique-dextral displacements (Fig. 6.4b).

For each D_3 fault-block, the average pitch of measured fault striations on bounding oblique-dextral faults is similar to the dip of the bounding reverse fault (50-60° W; Fig. 6.4b). One possible explanation for this geometry is that the bounding dextral structures are tear faults (Fig. 6.8). Wilkerson (1992) suggested that differential transport within a single thrust sheet can vary substantially along strike. In regions where displacement changes have occurred over small distances, deformation can be accommodated by intervening transverse structures (eg. tear faults). Tear faulting occurs because a continuous, non-metamorphic thrust sheet will attain a limiting value of bulk shear strain, above which, the thrust sheet cannot maintain continuity (Wilkerson, 1992). In the Scrutton Range, measured striations on tear fault surfaces are consistent with each fault-block being separated from an adjacent southern block by a dextral-reverse offset. Because the reverse component of slip was typically greater than the dip of bedding, apparent sinistral offsets were produced (Fig. 6.8).

ii) Imbrication

In addition to the generation of tear faults, internal imbrication of a competent and continuous thrust sheet can occur to accommodate excess shear strain during shortening (Mandl and Shippam, 1981; Geiser, 1988). In the Scrutton Range, most of the D_3 fault-blocks are internally deformed by NNW-striking reverse faults. Based on similarities in both orientation and slip-sense, the reverse faults are interpreted to be secondary imbricate structures that developed above the Bauhinia Fault during D_3 (Fig. 6.9).

Reverse motion on the Bauhinia Fault and secondary imbrication were probably the main controls on D_3 shortening in the Scrutton Range. However, small-scale reverse faults (< 2 m displacement) developed along bedding planes are interpreted to have accommodated some degree of shortening. Fault striations measured from the bedding-parallel structures were the source of the shallowly-dipping reverse faults shown on Figure 6.4b.

iii) Fault-propagation folding

Folding in the Scrutton Range is interpreted to have occurred during the early stages of D_3. This interpretation is based on the orientation of the anticline-syncline fold pair in the southern Scrutton Range, and on the fact that axial fold traces are offset by D_3 tear and imbricate faults (Fig. 6.8). Early D_3 fold development may have resulted from compressive buckling of the Scrutton Range fault-block, with bulk shortening accommodated by folding prior to imbrication and tear faulting. However, simple buckling of the Bauhinia Fault hangingwall cannot explain the restriction of folding to upper parts of the Tawallah Group stratigraphy (Fig. 6.8). Because the level of stratigraphy exposed in the Scrutton Range is thought to have been controlled by differential transport along the Bauhinia Fault, a mechanism that localised folding to southern parts of the region must be inferred. Fault-propagation folding associated with a secondary imbricate structure that was bound laterally by tear faults could account for the observed field relationships (Fig. 6.9).

Fault-propagation folds are thought to develop at the tip of a thrust fault, above an underlying ramp region (Suppe, 1983; Morley, 1986; Geiser, 1988; Jamison, 1987, Casas-Sainz and Simón-Gómez, 1992). They are the favoured fault-related fold type to develop in layered stratigraphy where modest ductility contrasts exist (Jamison, 1987). In the southern Scrutton Range, the underlying ramp is interpreted to have been an imbricate structure that formed above the Bauhinia Fault. Although the attitudes of both faults are unknown at depth, it is assumed that the Bauhinia Fault flattens at depth, possibly becoming bedding-parallel. Due to the shallow (< 2 km) palaeodepth of the system (Chapter 7), this assumption is supported by the observation that thrust faults generally have steeper dips close to the syntectonic erosion surface (meeting the surface at approximately 60°; Boyer and Elliot, 1982).

The progressive truncation of hangingwall strata against a thrust during fault-propagation folding results in the formation of a 'truncation anticline' (Jamison, 1987). In the Scrutton Range, a SE-plunging 'truncation anticline' and corresponding footwall syncline are well-developed along the southernmost segment of an imbricate fault (Fig. 6.8). The adjacent fault-block to the north does not contain folds, and there is an increase in vertical stratigraphic displacement across the imbricate fault. This geometry is interpreted to indicate that fold development was controlled by the degree of bulk strain accommodated in the hangingwall during differential displacement along the imbricate fault (Fig. 6.9). Larger displacements are interpreted to have occurred in the northern fault-block, so that strain was mostly accommodated by reverse motion on the imbricate fault. Lesser displacements in the southern fault-block resulted in greater strain partitioning into the hangingwall, and the formation of fault-propagation folds.

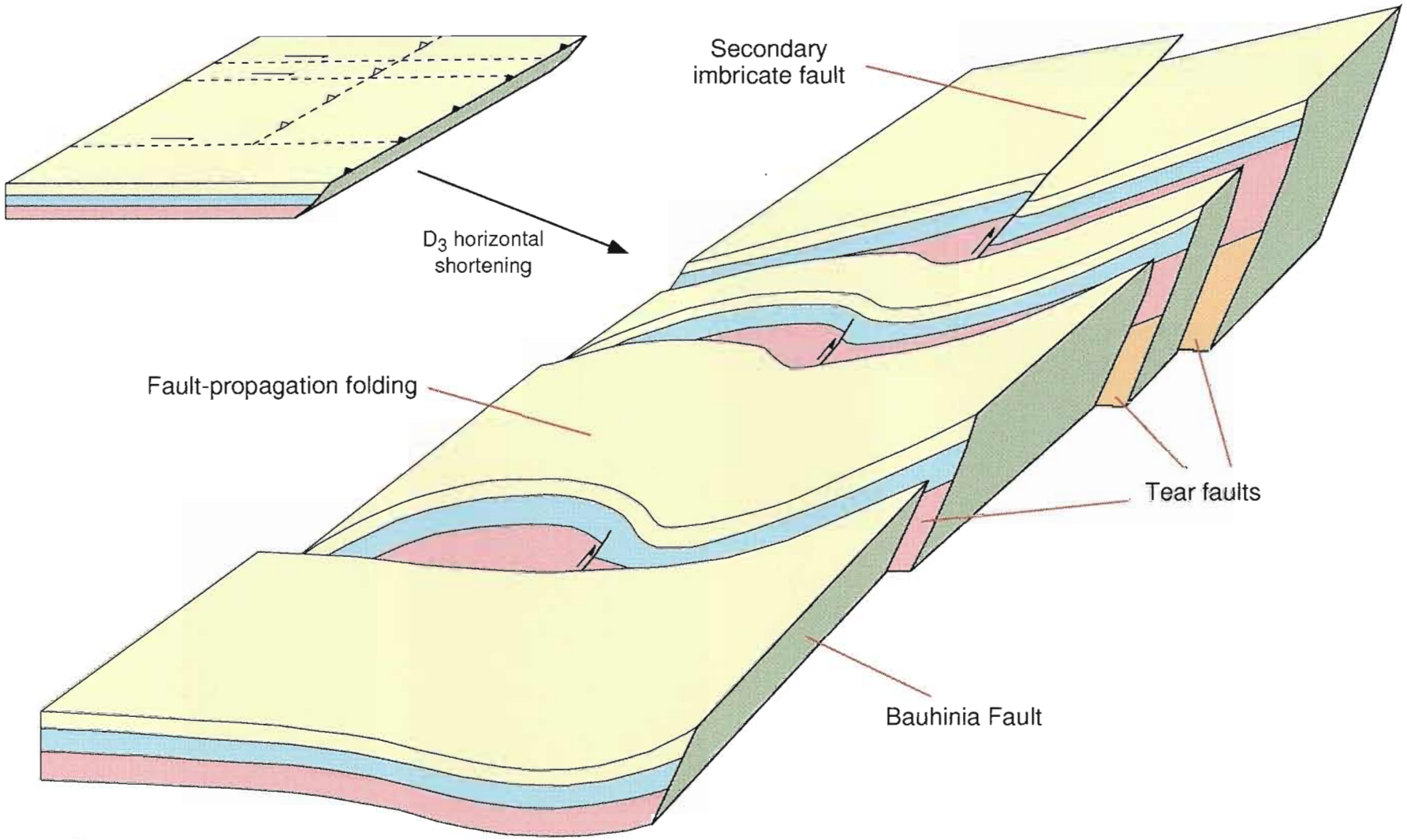

Fig. 6.7 Simplified block diagram of the southern Scrutton Range showing differential fault-block motion during D_3. Horizontal shortening in the two central fault-blocks is accommodated by fault-propagation folding. In the northern fault-block, all horizontal shortening is accommodated by the imbricate fault. Bounding tear faults have oblique dextral-reverse motions, so that net transport above the Bauhinia Fault increases towards the north.

Tawallah Range

In the western Tawallah Range, orientations of D_3 conjugate fault pairs are consistent with an approximate orientation of $5^o \rightarrow 202^o$ for the maximum principle stress direction (Fig. 6.5). However, a second orientation of $0^o \rightarrow 230^o$ for σ_1 is defined by the orientation of an additional conjugate fault pair in Region 2 (Fig. 6.5). Region 2 is also interpreted to have undergone the greatest degree of D_3 horizontal shortening in the western Tawallah Range, based on the local abundance of NW-trending reverse and oblique dextral-reverse faults (Fig. 6.4d). The formation of a transpressional zone (contractional strike-slip duplex) between the Tawallah and Lorella Faults is proposed to explain these variations in the local D_3 structural geometry.

Transpression involves a combination of pure and simple shear, and has been used to model regions of strike-slip deformation that were accompanied by components of horizontal shortening (Harland, 1971). Transpressional zones are developed locally along large-scale strike-slip systems; between convergent fault strands, between overlapping, antidilational en échelon fault segments and at restraining bends (Sanderson and Marchini, 1984). In all cases, the combination of horizontal shortening and simple shear results in crustal thickening and uplift within the transpressional zone. Uplifted domains are typically bound by convex-upward and outward branching faults that preserve evidence for both reverse and strike-slip components of displacement (Sylvester and Smith, 1976). In profile, this geometry is termed a 'palm tree' or 'positive flower structure' (Sylvester, 1988; Wilcox *et al.*, 1973; Fig. 6.10a). In plan view, a positive flower structure can be characterised by a regular geometric pattern of fault-bound lenses and slabs termed a contractional strike-slip duplex (Woodcock and Fischer, 1986; Fig. 6.10b).

Between antidilational offsets, a contractional strike-slip duplex will initiate due to shear fracture propagation from the lateral tips of the major bounding faults (Segall and Pollard, 1980). Synthetic strike-slip faults are progressively deflected towards the opposing primary fault strand in a concave inward fault pattern, developing incipient strike-slip imbricates and the isolation of an imbricate slice or horse (Woodcock and Fischer, 1986; Fig. 10b). With continued strike-slip displacement, progressive development of new horses occurs by symmetric or asymmetric outward propagation of successively younger imbricate faults from the initial fault strand (Fig. 10b). Widening of a contractional strike-slip duplex requires lateral distortion of the surrounding rock to maintain plane strain in profile (Woodcock and Fischer, 1986). Although lateral distortion can be compensated on an adjacent fault strand, some vertical accommodation generally occurs by uplift in the surrounding region, or of the duplex itself.

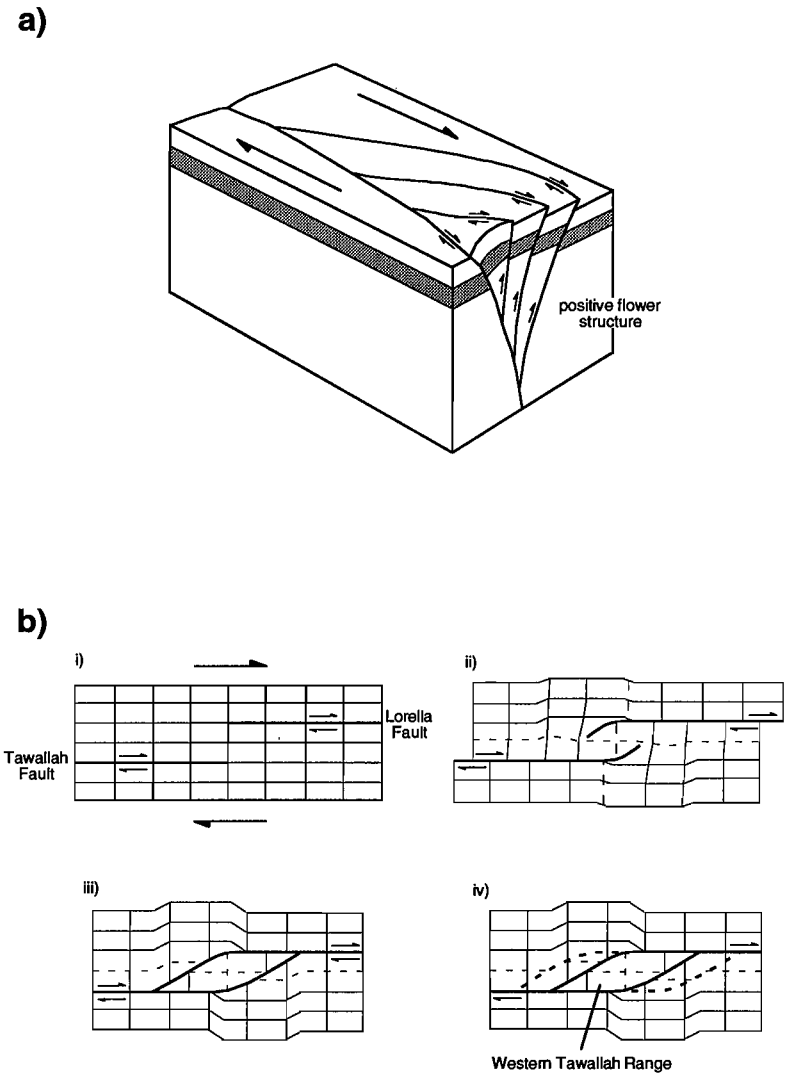

Fig. 6.11 Geometry and formation of a strike-slip duplex (after Woodcock and Fischer, 1986). **a)** Three dimensional form of a contractional strike-slip duplex. **b)** Strike-slip duplex development at an antidilational offset: **i)** antidilational offset in a dextral strike-slip fault system; **ii)** and **iii)** isolation of a horse by inward propagation of imbricate strike-slip faults from the lateral tips of the major structures; **iv)** development of a new horse by symmetric outward progression of new imbricate faults (collapse of unstrained wall).

Based on the criteria of Woodcock and Fischer (1986), and assuming that the Tawallah and Rosie Faults were part the same N-striking fault system prior to NE-SW compression, the D_3 structural geometry in western Tawallah Range is classified as a contractional strike-slip duplex. The NW-striking Tawallah and Lorella Fault segments are interpreted to have propagated from the N-striking Tawallah-Rosie and Lorella Fault systems, forming the northern and southern duplex margins respectively (Fig. 6.10b). The fault plane attitudes and slip-sense of the bounding Tawallah and Lorella Fault segments (reverse to oblique dextral-normal) are consistent with the proposed geometry for a contractional strike-slip duplex developed at an antidilational offset (Woodcock and Fischer, 1986). In this model, Regions 1 and 3 occur at the lateral margins of the duplex. Most of the local D_3 faulting is therefore interpreted to have developed in response to dextral strike-slip displacements on the N-striking Lorella and Tawallah Fault segments. The abundance of reverse and oblique-reverse faults in Region 2 (Fig. 6.4d) is consistent with its position at the centre of the transpressional zone. The 30° disparity in the orientation of σ_1 at this locality is interpreted to indicate that local rotation of the D_3 stress-field occurred during shortening and uplift. Secondary strike-slip faults that had non-optimal orientations with respect to the main conjugate trends (Fig. 6.5) may have formed to accommodate strain during the transition from a simple-shear to transpressional stress state.

One discrepancy in the model is that the direction of reverse movement on the Lorella Fault changes along the southwest duplex margin. In Region 2, a change from SW- to NE-directed transport along the Lorella Fault occurs across a kilometre-wide zone of NNW-trending oblique-sinistral faulting (Fig. 6.1). South of the Tawallah Range, the return to SW-directed transport on the Lorella Fault is interpreted to have occurred across an unexposed NE-trending structure that extends from the southern margin of the Scrutton Range (Fig. 6.1; Chapter 8). NE-directed reverse displacements were therefore restricted to an isolated segment of the Lorella Fault which paralleled the region of NE-directed uplift in the Scrutton Range (Fig. 6.1). Consequently, emplacement of the Scrutton Range fault-block to the west of the Tawallah Range during D_3 is interpreted to have influenced the development of the southwest duplex margin.

6.7 SUMMARY

Three main compressional deformation phases and complex block-faulting along major N-striking faults characterise the structural history of the study region. Results of inverse palaeostress analyses have been interpreted to indicate that each deformation event is distinguished by a unique palaeostress-field orientation and structural geometry. Early E-W compression (D_1) resulted in east-directed reverse

displacement on the Tawallah Fault, and is interpreted to have preceded Wununmantyala Sandstone deposition. NW-SE compression (D_2) post-dated Tawallah Group deposition, and was characterised by sinistral strike-slip deformation adjacent to the Tawallah and Lorella Faults. This event is tentatively correlated with syn-Barney Creek Formation transpression at the McArthur River Pb-Zn deposit (Hinman, 1995). Most of the structural features preserved in the study region were formed during post-Roper Group, NE-SW compression (D_3). In the Batten Range, D_3 was typified by dextral strike-slip deformation adjacent to the Tawallah Fault. In the Scrutton Range, NE-directed differential reverse displacement on the Bauhinia Fault formed a series of subsidiary fault-blocks that were bound laterally by tear faults and deformed internally by imbricate structures. The generation of a D_3 contractional strike-slip duplex between the Tawallah and Lorella Faults resulted in transpressional uplift of the western Tawallah Range. The role of each deformation event in the tectonic and structural evolution of the southern McArthur Basin are outlined in Chapter 8.

Chapter 7 - Fluid Dynamics

CHAPTER 7 - Fluid Dynamics

7.1 INTRODUCTION

The importance of brittle fault zones as conduits for hydrothermal fluids during deformation was discussed in Chapter 5. Characteristic brittle deformation products such as hydraulic fracture/brecciation and veining were interpreted to indicate that seismic rupture along a principal slip surface was associated with an influx of hydrothermal fluid. This chapter examines the nature of hydrothermal fluids associated with the D_3, dextral strike-slip Tawallah Fault system. Analyses of fluid inclusions from D_3 hydraulic fault breccias in the Batten Range are presented with the aims of understanding fluid processes and tracing fluid sources. The results of these analyses are used in conjunction with the geochemical models of Cooke (1993) to model the fluids that were channelled during late stage strike-slip movements on the Tawallah Fault. The principal aims of this chapter are to: (1) characterise the fluids in the Tawallah Fault system; (2) investigate fault-controlled thermal anomalies in the 'unmetamorphosed' McArthur Basin; (3) investigate processes that have led to quartz-hematite precipitation along the faults; (4) estimate possible depths of formation; (5) suggest a possible heat source for the fluids.

7.1.1 Sampling Criteria

The structural position of the Batten Range was fortuitous for high levels of fluid flow during D_3, because it was situated at a releasing bend or transtensional position along the Tawallah Fault. Seismic rupture and fault propagation at a releasing bend are characterised by rapid slip transfer, reduction of mean stress and host rock dilation (Sibson, 1986; 1994). During post-rupture, local fluid pressures are reduced to below ambient values, and favourable sites for significant fluid influx are developed. Where these processes are operative, large dilational structures can be associated with a complex array of extension veins, hydraulic breccias and subsidiary shears (Sibson, 1994). Such features are well developed along the southern Tawallah Fault segment and associated D_3 secondary structures in the Batten Range.

The pervasive and regional silicification of lower Tawallah Group stratigraphy early in the development of the basin (pre-D_1 diagenetic, or syn-D_1) has been discussed in previous chapters (Chapter 6.7.1). Early silicification is considered to have enhanced the likelihood for hydraulic brecciation during D_2 and D_3 brittle faulting in the lower Tawallah Group sandstones. Consequently, sample collection for fluid inclusion

analysis in the Batten Range has focussed on hydraulic breccias associated with D_3 structures in the Sly Creek Sandstone. Quartz-hematite breccia textures vary from jigsaw-fit clast-supported, through to matrix-supported breccias with random clast orientation (Plate 7.1a). The two end-members are referred to hereafter as fracture and open breccias respectively.

7.2 FLUID INCLUSIONS

Thirty-three doubly polished plates were prepared from fault breccia samples associated with the D_3, dextral strike-slip Tawallah Fault system. Faults sampled included the Tawallah Fault, and secondary NNW-striking dextral, NW-striking sinistral, SW-striking dextral/normal and SSW-striking dextral structures (Appendix 1d). In the following discussion, samples have been discriminated on the basis of distance away from the Tawallah Fault so that data populations may include one or more of the secondary fault types.

In the fault breccias, fluid inclusions occur as trails along healed fractures in sandstone clasts and quartz grains (Plate 7.1b), and are classified as secondary based on the criteria of Roedder (1984). All secondary fluid inclusions analysed are assumed to have been trapped during D_3 brittle rupturing of the Tawallah Fault system. The implications of this assumption are discussed further in section 7.6.

Measurements of liquid-vapour homogenisation temperatures, freezing point depressions and first melting temperatures were made on 101 chips using the procedures outlined by Roedder (1984). Salinities were calculated from freezing point depression measurements assuming an $NaCl-H_2O$ system and using the algorithms provided in Hall *et al.* (1988). Freezing point depression temperatures were measured from only 550 of the 800 fluid inclusions analysed, because the small diameter (5-20 μm) of many fluid inclusions resulted in poor viewing conditions that prevented accurate temperature measurements during the freezing procedure. All microthermometric data is provided in Appendix 3a.

7.2.1 Fluid inclusion populations

Two fluid inclusion populations have been recognised in the D_3 fault breccia samples from the Batten Range. Population I consists of secondary inclusions with constant liquid/vapour ratios (90-95% liquid; Plate 7.1c). Population II consists of fluid inclusions trails with variable liquid-vapour ratios (Plate 7.1d, e). Population II inclusions have similar homogenisation temperatures from both liquid- and vapour-rich inclusions, and are interpreted to represent the entrapment of a fluid undergoing phase separation (ie. boiling; Roedder and Bodnar, 1980). The occurrence of a fluid inclusion

Plate 7.1 Fluid inclusion types and occurrences.

a) Open (left) and fracture (right) end-member textures of the hydraulic breccia samples collected for fluid inclusion analysis (samples 93-B07 and 92-03).

b) Photomicrograph of secondary fluid inclusion trails in a hydraulic breccia sample (plain light; sample 93-B01).

c) Photomicrograph of a secondary fluid inclusion trail with constant liquid/vapour ratios (population I; plain light; sample 93-B08).

d) and e) Photomicrographs of secondary fluid inclusion trails with variable liquid/vapour ratios (population II; plain light; sample 93-B16).

Plate 7.1

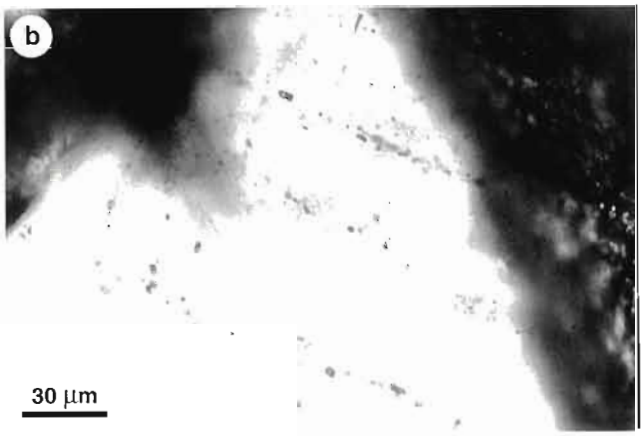

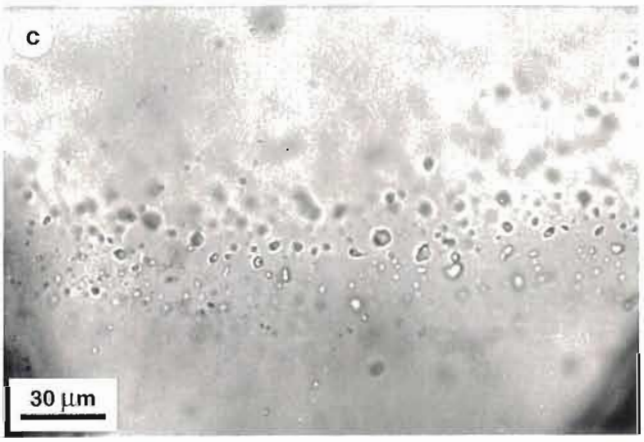

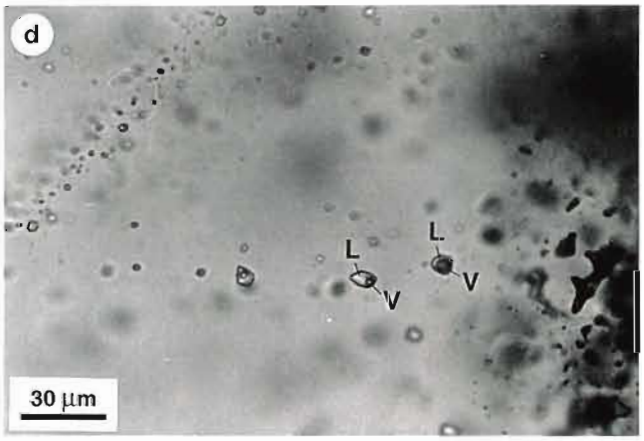

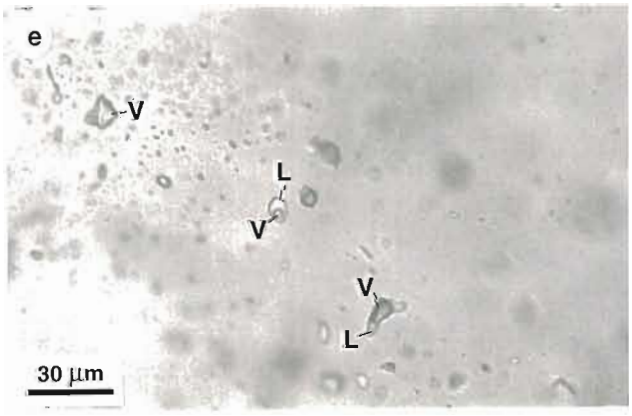

population that has preserved evidence for boiling indicates hydrostatic pressure conditions at vapour saturation (Haas, 1971). Consequently, the fluid inclusion homogenisation temperatures measured in this study were not pressure corrected. None of the fluid inclusions contain visible CO_2, and daughter minerals are rare.

7.2.2 Microthermometry

Homogenisation temperatures for populations I and II range from 90° to 400°C, with most between 120° and 220°C (Fig. 7.1; Appendix 3a). Figure 7.1 shows homogenisation temperatures of fluid inclusions in secondary faults as a function of increasing distance from the Tawallah Fault. With a mean homogenisation temperature of 210°C, fluid inclusions in Tawallah Fault breccia samples are markedly hotter than fluid inclusions from all secondary faults, which have mean homogenisation temperatures around 160°C. Figure 7.2 suggests a systematic decrease in temperature away from the Tawallah Fault. The spread of data above the mean values in Figure 7.2 is probably due to mixed entrapment of liquid and vapour phases in population II fluid inclusions during boiling rather than trapping of a single homogenous phase. Microthermometric measurements of mixed phase inclusions generally yields abnormally high values for Th (Roedder and Bodnar, 1980).

Figure 7.3 depicts the salinities of fluid inclusions with increasing distance away from the Tawallah Fault. Salinities for population I are mostly between 0.0 and 5.0 eq. wt.% NaCl, while higher values were recorded from population II fluid inclusions (10 to 20 eq. wt.% NaCl; Fig. 7.3; Appendix 3a). There is some overlap in measured salinities at homogenisation temperatures over 250°C, where values for both populations range between 8 and 13 eq. wt.% NaCl. A bimodal association of inclusions is apparent for the secondary D_3 faults, with a low salinity (0-5 eq. wt.% NaCl) and a high salinity cluster (10-20 eq. wt.% NaCl). The Tawallah Fault is distinct in that it also contains fluids with intermediate salinities (8-12 eq. wt.% NaCl).

Homogenisation temperatures and salinities of fluid inclusions in open and fracture breccias are displayed in Figure 7.4. The clast-supported fracture breccias contain a higher proportion of saline inclusions than the open breccias.

Figure 7.5 shows eutectic melting temperatures (T_e) measured for each fluid inclusion population, and the first melting temperatures for common salt-H_2O systems (taken from Crawford, 1981). The majority of T_e values recorded from both inclusion populations range between -20° and -50°C. This indicates that the liquid phase contains significant amounts of K^+, Mg^{2+} and/or Ca^{2+} ions in addition to Na^+, so that the eutectic temperature for pure NaCl-H_2O (-21.3°C) is depressed to lower values (Roedder, 1984). Depression of the NaCl-H_2O eutectic temperature can also result from quenching during the freezing procedure; ie. the failure of solid phases to nucleate during cooling. In consequence, disequilibrium assemblages may be generated at low

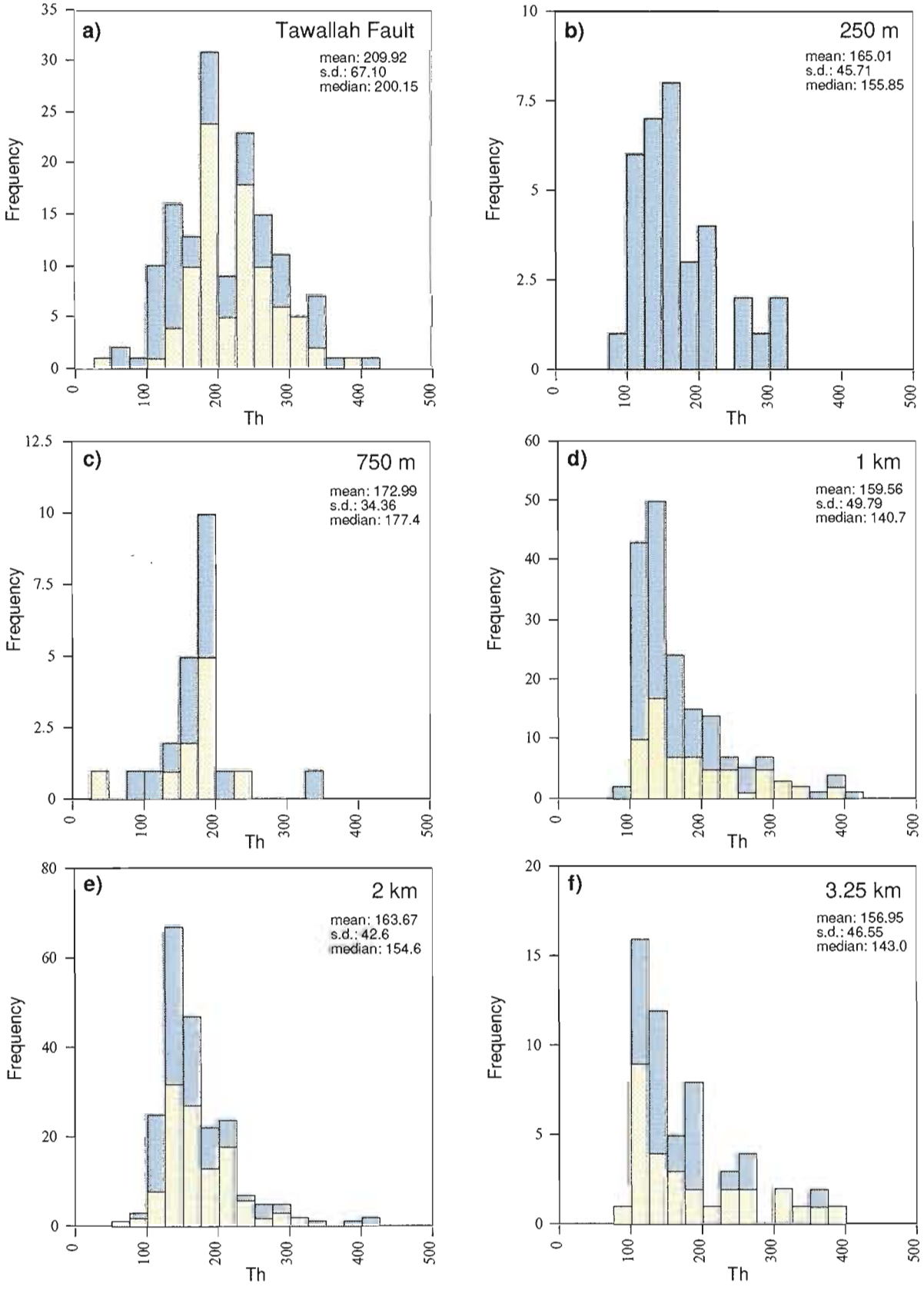

Fig. 7.1 Homogenisation temperatures of population I (yellow fill) and population II (blue fill) inclusions with increasing distance away from the Tawallah Fault.

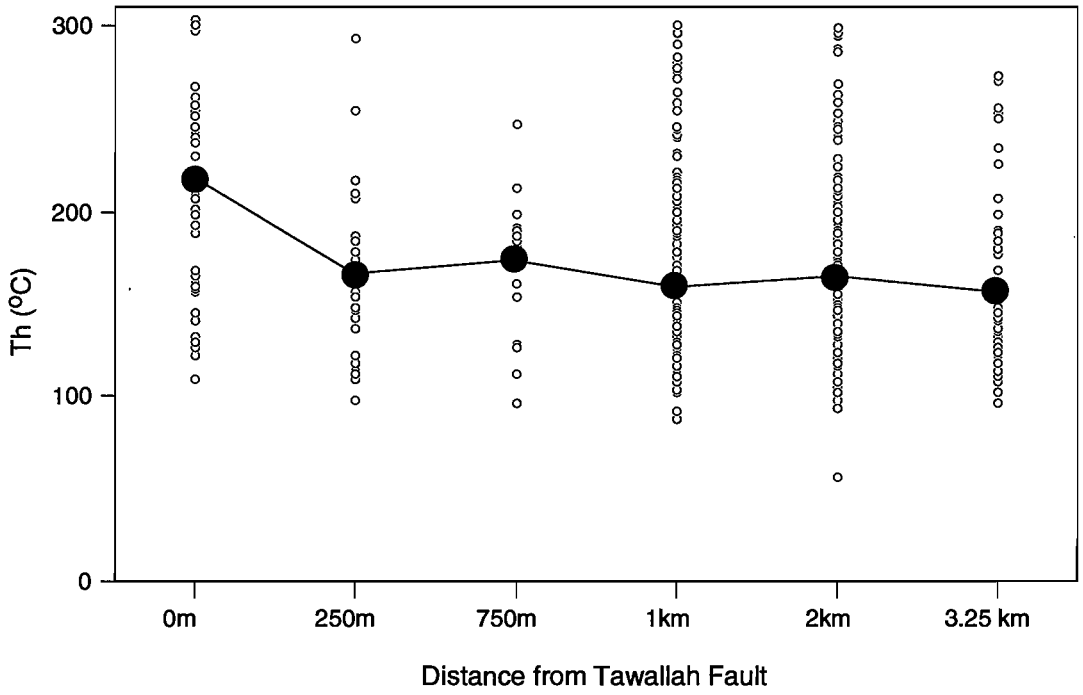

Fig. 7.2 Homogenisation temperatures of inclusions with increasing distance away from the Tawallah Fault. Filled circles represent the mean value for each population.

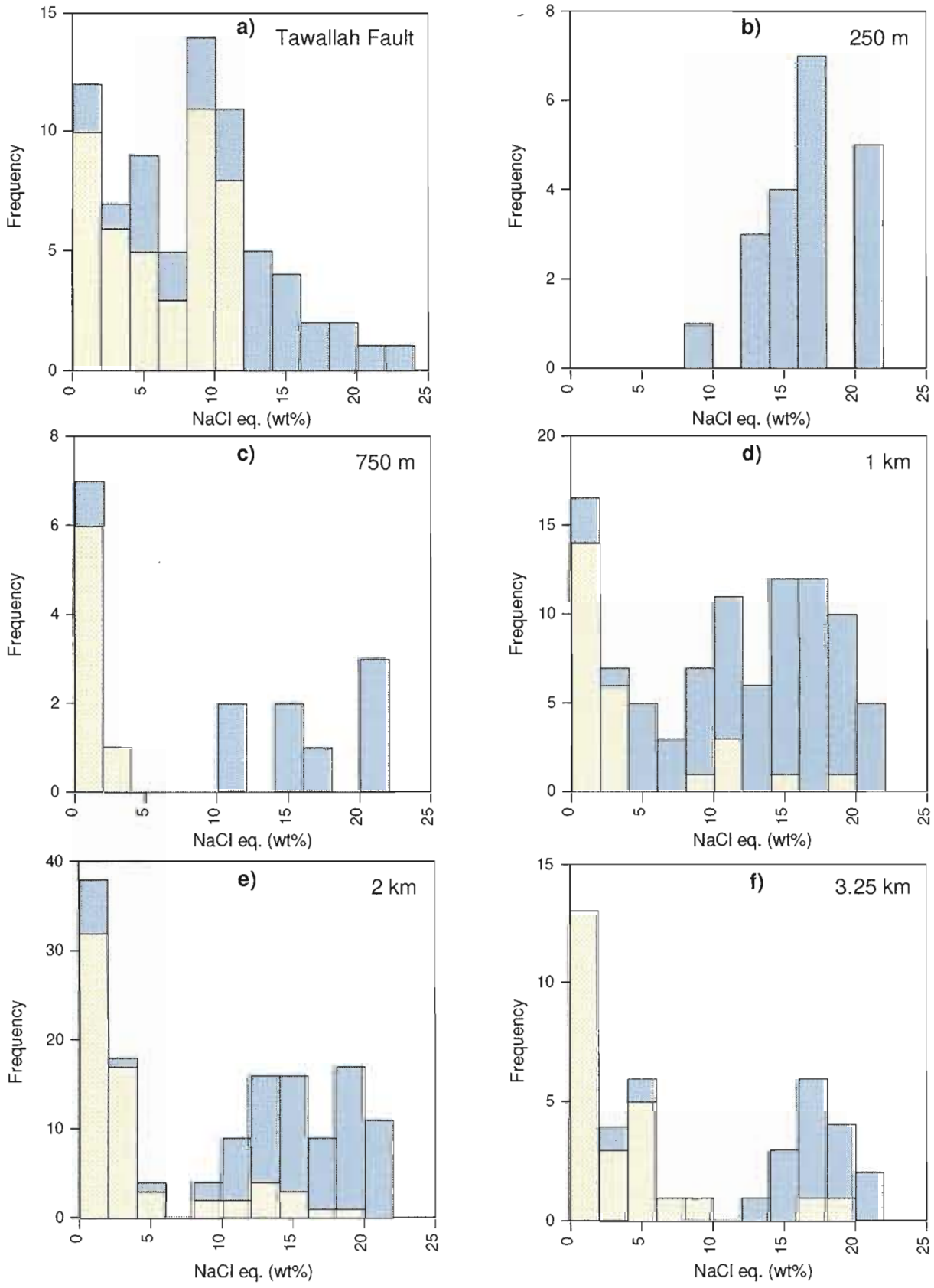

Fig. 7.3 Salinities of population I (yellow fill) and population II (blue fill) inclusions with increasing distance away from the Tawallah Fault.

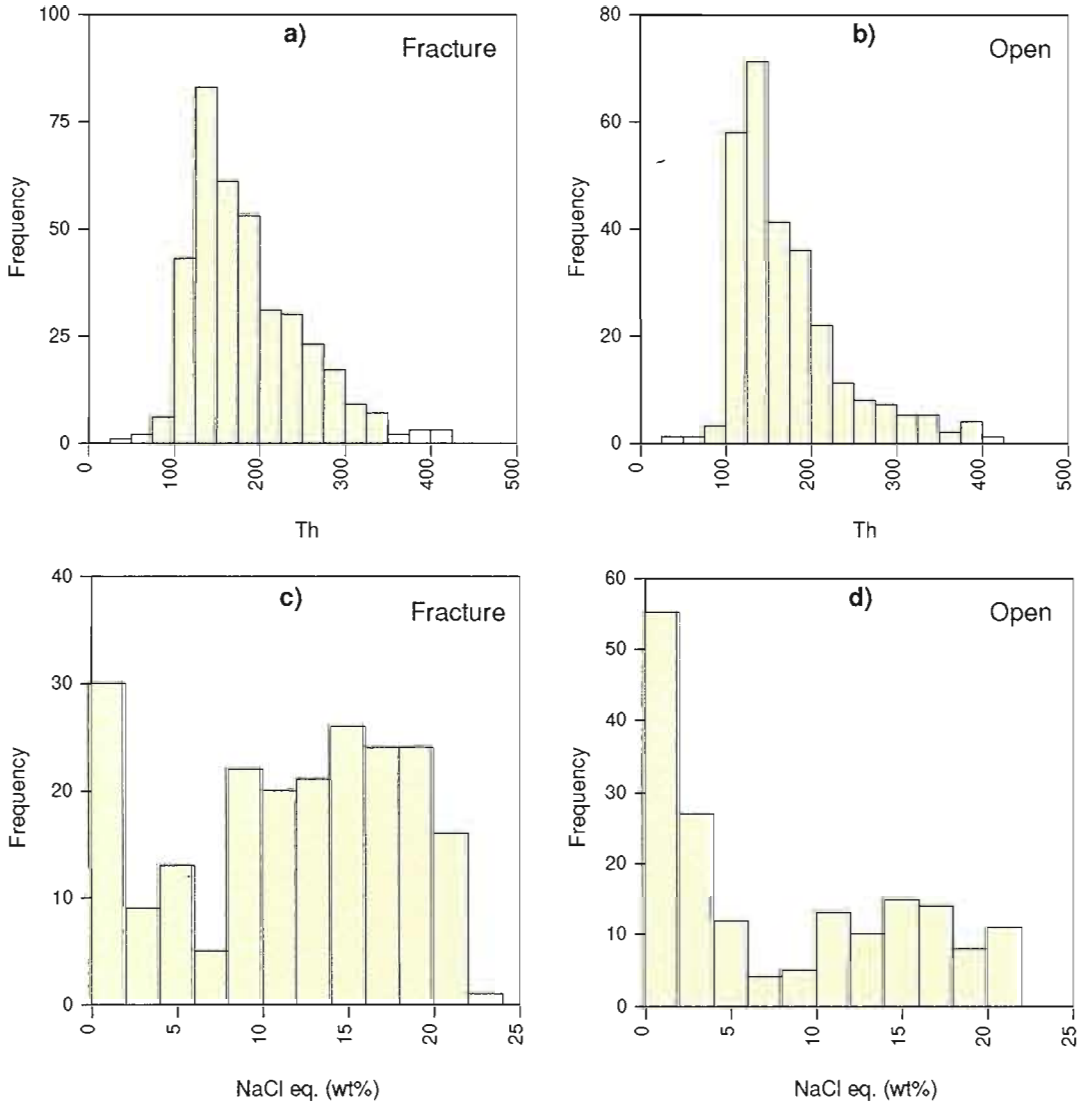

Fig. 7.4a) and b) Homogenisation temperatures, and **7.4c) and d)** salinities of fluid inclusions from fracture and open breccia (Plate 7.1).

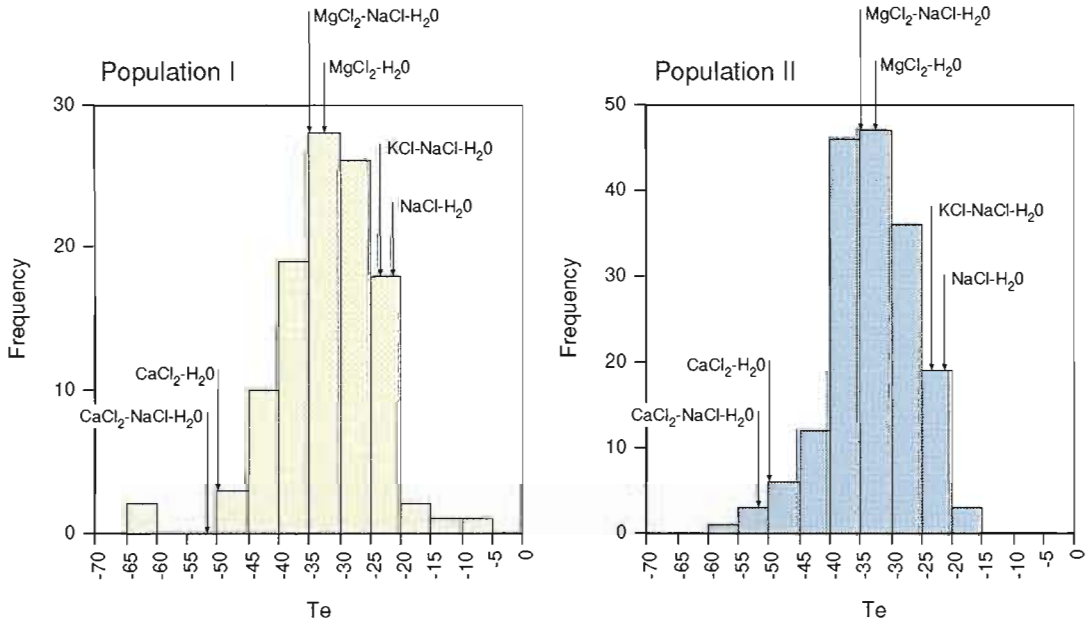

Fig. 7.5 Eutectic melting temperatures (Te). Eutectic melting temperatures for a range of chloride solutions commonly found in fluid inclusions (taken from Crawford, 1981).

temperatures and melt at the metastable eutectic temperature (approximately -28°C for the NaCl-H_2O system; Crawford, 1981). The mechanism by which Te values are depressed below the NaCl-H_2O eutectic temperature can be resolved by investigating fluid phase compositions. The compositions of fluid inclusion decrepitates from selected Batten Range breccia samples are summarised in the following section.

7.2.3 Fluid inclusion decrepitate compositions

To evaluate fluid phase compositions, eutectic melting temperatures recorded by microthermometry were complemented with an investigation of fluid inclusion decrepitate compositions. Five representative fluid inclusion chips were heated on a USGS heating/freezing stage until the majority of liquid-rich inclusions had decrepitated (maximum stage temperature: 450°C). Salt precipitates induced by thermal decrepitation were analysed using a CAMECA microprobe at the Central Science Laboratory, University of Tasmania to determine the cation compositions of forty individual fluid inclusions. Cation ratios gained by this method are considered to be semi-quantitative, as an unknown proportion of precipitated material may have been lost during decrepitation (Zaw *et al.*, 1994).

Decrepitate analyses have revealed that the fluids contain abundant Na^+, K^+, Ca^{2+} and Fe^{2+} with minor Mg^{2+} (Fig. 7.6; Appendix 3b). The depression of T_e values below the NaCl-H_2O eutectic is therefore concluded to have been largely controlled by the presence of Ca^{2+} and/or K^+ cations in the fluid. The addition of KCl to a NaCl-H_2O brine lowers the eutectic point to approximately -22.9°C (Crawford, 1981; Fig. 7.5). However, NaCl-H_2O brines containing $CaCl_2$ are associated with much greater T_e depressions; eutectic melting commences at -52°C for the $CaCl_2$-NaCl-H_2O system (Fig. 7.5). The fluids that precipitated quartz-hematite mineralisation in the D_3 Tawallah Fault system are therefore concluded to have been KCl-NaCl-H_2O brines that contained varying proportions of $CaCl_2$ and Fe.

7.2.4 Gas analyses

Raman spectroscopy of representative samples from each fluid inclusion population was conducted to evaluate vapour phase compositions. Raman spectra were recorded on a Microdil-28 laser Raman microprobe, using the 514.5 nm line from a Spectra Physics model 2020 argon ion laser at the Australian Geological Survey Organisation, Canberra. No detectable concentrations of CO_2, O_2, N_2, H_2 or CH_4 were present in any of the 10 fluid inclusions analysed. Mernagh *et al.* (1994) estimated the Raman detection limits for CO_2, O_2 and N_2 at 0.1 mole percent, and 0.03 mole percent for CH_4. These findings are consistent with low confining pressures during entrapment, because gas solubility is directly proportional to pressure (Cooke *et al.*, 1995).

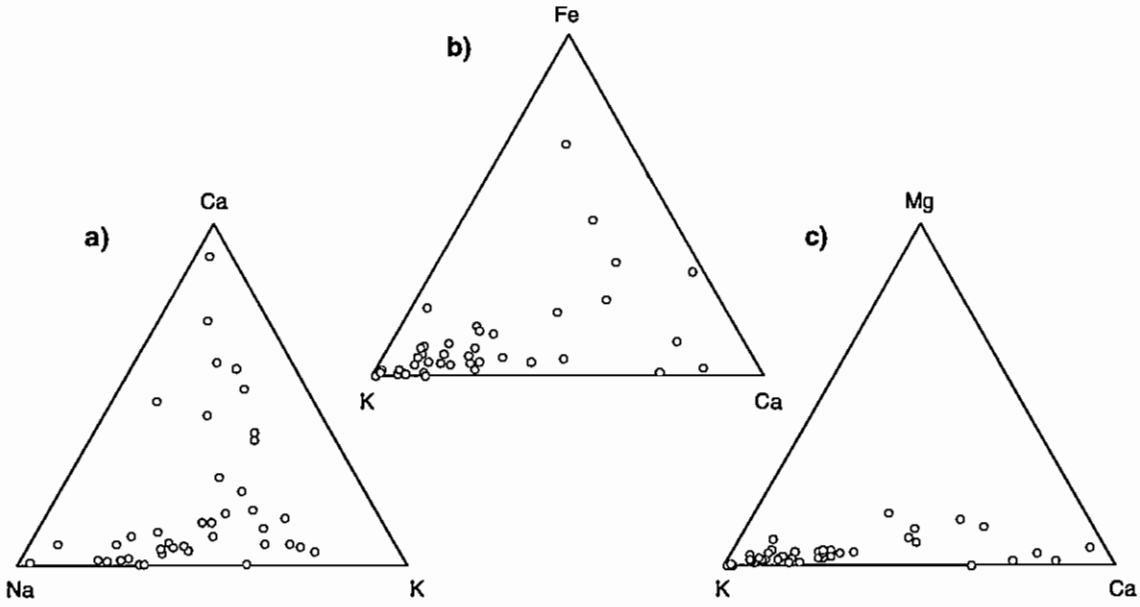

Fig. 7.6a) Ca-Na-K, **b)** Fe-K-Ca and **c)** Mg-K-Ca cation compostions of fluid inclusion decrepitates from populations I and II.

7.3 DISCUSSION

Interpretation of the microthermometric data has relied on four major assumptions: *Assumption 1*: the secondary faults formed roughly synchronous with each other, in response to dextral strike-slip movements on the Tawallah Fault (ie., they are all D_3 structures). This assumption is required to validate any attempt at modelling the fluid dynamics during D_3, dextral strike-slip deformation in the Batten Range. The Batten Range D_3 fault geometry was established by inverse palaeostress analysis of measured fault-slip data, with the reconstructed secondary fault pattern relatively well constrained by Mohr-Coulomb failure models for right-lateral displacement on the Tawallah Fault system (Chapter 6).

Assumption 2: all hydraulic breccias sampled in the Batten Range were formed during D_3 (ie., none of the breccias are derived from older, reactivated structures). In Chapter 6, the development of the Batten Range D_3 secondary fault pattern was interpreted to have been largely controlled by the reactivation of pre-existing D_2 structures. This interpretation was based on the co-existence of D_3, P and X secondary faults, which would otherwise require drastic stress reorientation to have occurred during the evolution of the Tawallah Fault strike-slip system. To help validate this assumption, D_3 hydraulic breccias that had preserved evidence for multiple episodes of brecciation were not sampled for fluid inclusion analysis.

Assumption 3: secondary fluid inclusions were trapped during or shortly after the brecciation process (ie. fluid inclusions were formed exclusively by D_3 hydraulic fracture processes). Knipe (1989) suggested that the generation of intragranular fractures during fault propagation can occur in response to variety of low-temperature

deformational processes. In the study area, cataclastic intragranular fracture and crystal-plastic deformation mechanisms are considered to have been important during brittle fault zone development (Chapter 5). The majority of microfractures in the D_3 hydraulic breccia samples collected for fluid inclusion analysis show no significant displacements, either parallel or normal to the microfracture trace, and characteristic cataclastic textures such as planar zones of pronounced grainsize reduction (microbreccia) are rare. Intragranular microfractures developed in breccia clasts are therefore interpreted to represent hydraulic fractures, formed during rupture and dilation along the D_3 Tawallah Fault system. In this case, annealing of fractures and fluid inclusion development are likely to have occurred during post-rupture fluid influx and consequent permeability destruction by mass transfer processes (Cox *et al.*, 1986; Knipe and McCaig, 1994).

Assumption 4: The fossil geothermal system, although initially under suprahydrostatic or lithostatic conditions during brecciation, evolved to hydrostatic conditions once permeability and fluid flow became established. Gray *et al.* (1994) suggested that boiling induced during seismic rupturing, dilation and fluid influx under suprahydrostatic conditions is likely to be restricted to within several hundred meters of the main fault zone. Shallow-crustal formation of quartz-hematite mineralisation in a hydrostatic environment is therefore favoured for the D_3 Tawallah Fault system, given the widespread occurrence of D_3 hydraulic breccias and population II fluid inclusions (up to 3.25 km away from the Tawallah Fault).

7.3.1 Temperature and salinity relationships

Henley *et al.* (1984) proposed that three principle processes are responsible for temperature decrease in an upwelling fluid: (1) *boiling*, whereby heat is transferred to a vapour phase that separates from an ascending liquid upon reaching a critical level in the crust. The specific depth at which boiling will occur is governed by the hydrostatic pressure imposed on the fluid; (2) *dilution* by mixing with cool groundwaters (which may also prevent the uprising fluid from boiling); (3) *conductive cooling*, whereby heat is lost to the surrounding wall rock by conduction.

Each process should result in a unique final fluid chemistry (Henley *et al.*, 1984). It is therefore theoretically possible to discern which process(es) have occurred in a fossil hydrothermal system based on salinity-temperature relationships. Boiling of a hot, saline brine will effectively concentrate salts into solution, progressively increasing the salinity of the cooler residual fluid (Henley *et al.*, 1984). In contrast, dilution due to mixing of a hot, saline brine with a relatively cool, dilute groundwater should result in a salinity decrease in the resultant hybrid fluid (Fournier, 1979). During conductive heat loss, the salinity of the fluid should remain fairly constant (Fournier, 1979).

To trace possible depositional processes, the Batten Range fluid inclusion data has been plotted on enthalpy-chloride diagrams, where enthalpy is the heat of the fluid (taken from the steam tables of Haas, 1976) and chloride is a measure of the salinity (expressed as molality; Fig. 7.7). Enthalpy-chloride diagrams were chosen for data portrayal because they allow for the simple prediction and calculation of boiling and mixing relationships (Fournier, 1979; Henley *et al.*, 1984). Figure 7.8 shows enthalpy-chloride diagrams for the Tawallah Fault, and for associated secondary faults at specific distances from the primary structure. Although there is considerable scatter, two rough trends appear to be present for the Tawallah Fault data (Fig. 7.8c); a boiling trend towards higher chloride concentrations with lower temperatures, and a mixing trend towards decreased chloride concentrations. These trends are more distinct in Figures 7.8a and b, with two fluid populations discernible at 2 km for the Tawallah Fault. Note that high enthalpy (high temperature) values were not obtained from the secondary fault samples.

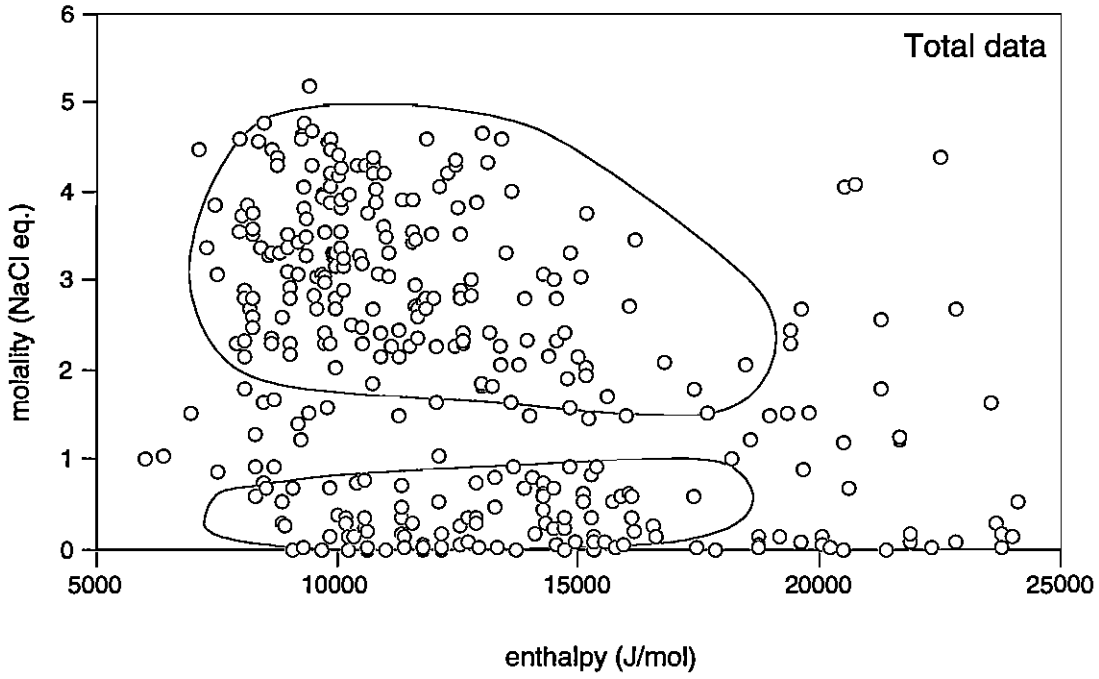

Fig. 7.7 Enthalpy-chloride diagram for the Tawallah Fault system (total data).

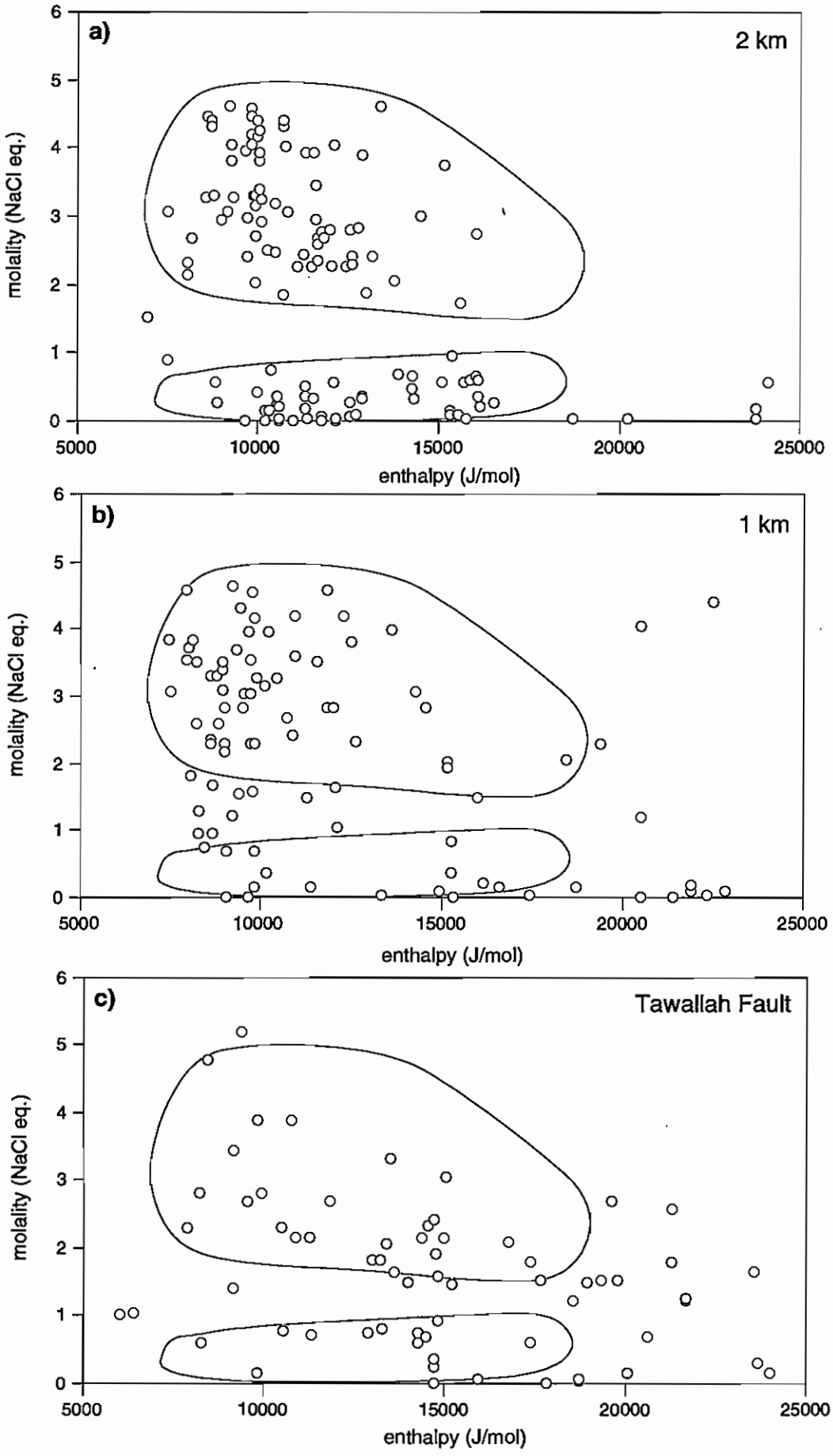

Fig. 7.8 Enthalpy-chloride diagrams for fluid inclusions at: **a)** 2 km; **b)** 1 km; and **c)** 0 km from the Tawallah Fault.

To model mixing and boiling trends, an initial temperature of 300°C and salinities of 8.06-12.75 eq. wt.% NaCl were assumed. Using the method outlined below, these fluids were numerically cooled to 100°C by isenthalpic boiling, and to 80°C by mixing with a cooler, lower salinity fluid (eg. heated ground water at 80°C, 0.5-5.0 eq. wt.% NaCl). Although the differences in the calculated mixing curves are negligible, heated ground waters, rather than surface waters at 25°C, were chosen to simulate mixing in subsurface conditions. Steam factors that separate during boiling (Table 7.1) were calculated using the following formulae;

$$y = \frac{H_{L(300^\circ C)} - H_{L(100^\circ C)}}{H_{V(100^\circ C)} - H_{L(100^\circ C)}}$$

$$C_{Cl(100^\circ C)} = \frac{C_{Cl(300^\circ C)}}{(1-y)}$$

Where H = specific enthalpy (taken from the steam tables of Haas, 1976), C_{Cl} = concentration of chloride, y = mass fraction of initial liquid which is converted to steam, subscripts L,T and V,T refer to liquid and vapour phases at the specified temperature (Henley *et al.*, 1984).

Table 7.1 Calculated enthalpy and chloride values for boiling-induced cooling of a 300°C fluid to 100°C.

	8.06 eq. wt.% NaCl		**12.75 eq. wt.% NaCl**	
Temperature (°C)	enthalpy (J/mol)	chlorinity (mol/kg)	enthalpy (J/mol)	chlorinity (mol/kg)
300	23825	1.5	23509	2.5
175	13241	2.18	13178	3.68
100	7507	2.66	7490	4.55

Mixing trends have been calculated assuming infinite dilution of the 300°C fluid upon cooling to 80°C by mixing with: (1) heated meteoric water (0.5 eq. wt.% NaCl; Table 7.2, column 1); and (2) heated seawater (5.0 eq. wt.% NaCl; Table 7.2, column 2).

Table 7.2 Enthalpy and chloride values calculated for mixing of a 300°C fluid with an 80°C heated groundwater.

	8.06 eq. wt.% NaCl		**12.75 eq. wt.% NaCl**	
Temperature (°C)	enthalpy (J/mol)	chlorinity (mol/kg)	enthalpy (J/mol)	chlorinity (mol/kg)
300	23825	1.5	23509	2.5
80	6005	0.086	6005	0.90

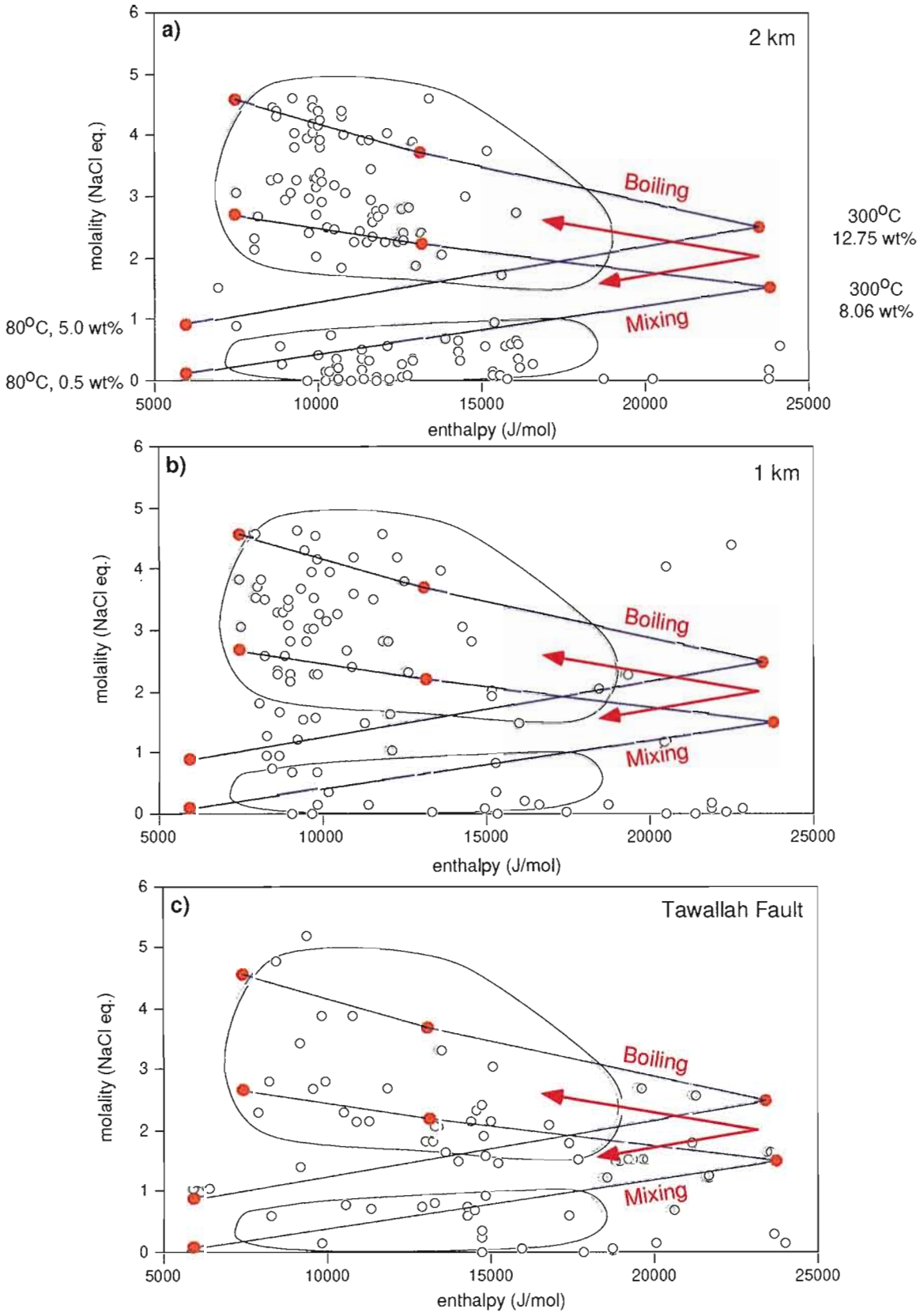

Fig. 7.9 Enthalpy-chloride diagrams and boiling/mixing curves for fluid inclusions at: **a)** 2 km; **b)** 1 km; and **c)** 0 km from the Tawallah Fault. Boiling and mixing curves have been calculated based on starting compositions of 8.06 and 12.75 wt.% NaCl at 300°C. Mixing trends assume maximum dilution by a 80°C, 0.5-5.0 wt.% NaCl heated groundwater.

Figure 7.9 shows the calculated boiling and mixing trends Tables 7.1 and 7.2 overlain on the enthalpy-chloride diagrams. Boiling of a 300°C, ≈ 10 eq. wt.% NaCl solution can account for the high salinity data at low temperatures, whereas mixing with heated seawater or meteoric water can explain the low salinity, low temperature data. Note that many other possible starting fluid compositions could have been chosen. Each would provide a set of cooling trends, and by choosing several starting fluids, the data could be accounted for by combinations of conductive cooling, boiling and mixing. However, to avoid complexity and considering that one fluid cooling by two simple processes adequately explains the data, these options are not discussed further.

The model outlined above is simplistic, in that it describes only one episode of fluid flow. In reality, multiple seismic ruptures along the Tawallah Fault system probably occurred during D_3, and each event may have been associated with fluid influx. However, the mechanisms that induce fluid flow and the physical processes associated with fluid influx will be similar for successive rupture events (Sibson, 1989). As the fluid inclusion data remains fairly consistent over the study area, it is conceivable that multiple fluid generations could be represented, provided that a similar source was utilised during each rupture event.

7.3.2 Depth Estimates

The depth at which fault-hosted hematite-quartz mineralisation formed during D_3 strike-slip motion on the Tawallah Fault can be determined from the boiling fluid inclusion populations (II) by assuming open system behaviour during rupture (Assumption 4). Based on this assumption, homogenisation temperatures can be plotted directly onto a boiling point-depth curve (Roedder and Bodnar, 1980; Fig. 7.10). A maximum depth of 210 m beneath the palaeo-water table is estimated for hydrostatic conditions (Fig. 7.10). Estimates of depth from surface are purely speculative, because the depth of the palaeo-water table and thickness of sediment above the system are unconstrained. For example, groundwater in the Cypress Plain fluid flow system in the Mesozoic Western Canada Sedimentary Basin reaches depths of 500m (Toth and Corbet, 1987). Based on this example, quartz-hematite mineralisation in the Tawallah Fault system could have formed at depths of 700m below the surface.

On Figure 7.10, two possible paths for an ascending 300°C, 8.06-12.75 eq. wt.% NaCl fluid are shown. For convective uprise, boiling would commence at approximately 1 km depth. An alternative ascent path, where overpressured fluids rose along the Tawallah Fault, is therefore inferred to enable the hot fluid to reach shallow levels (ie. 210 m below the palaeo-water table) before boiling under hydrostatic conditions.

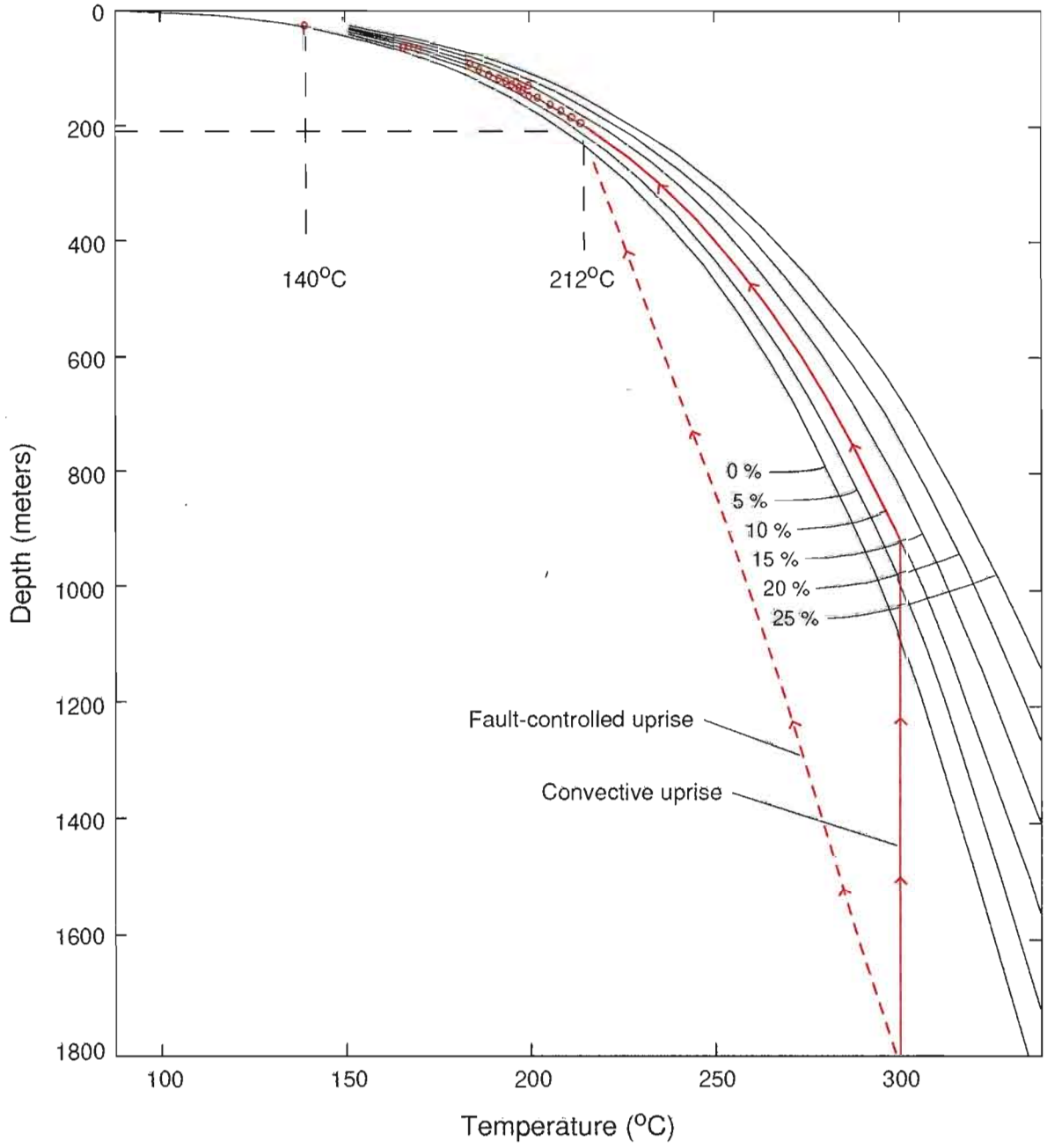

Fig. 7.10 Boiling point-depth curves for varying salanities (after Haas, 1971). Boiling populations of inclusions from the Tawallah Fault system define a maximum depth of boiling at 210 m. Source fluids at 300°C may migrate to these depths via two paths; uprise driven by temperature-induced convection (heavy line) or fault-controlled uprise (dashed line).

7.3.3 Heat Source

Geothermal gradients from a variety of sedimentary basins are shown in Figure 7.11. Based on the depth estimates from the previous section, the fluids in the D_3 Tawallah Fault system are interpreted to have cooled along a geothermal gradient similar to that of the Salton Sea system, rather than a cool cratonic basin. A basinal brine heated to 300°C in a cool cratonic basin would be required to ascend through approximately 10 km of sediment without conductive heat loss to reach the shallow crustal levels proposed for the D_3 Tawallah Fault system The 300°C source fluids introduced into the Tawallah Fault system during D_3 are therefore interpreted to have ascended from depths of 2 to 3 km. The Salton Sea geothermal gradient has been elevated however, due to widespread intrusive activity in an active extensional environment (McKibben *et al.*, 1988a). As discussed in previous chapters, the Tawallah Fault is interpreted to have been activated as a dextral strike-slip system some time after Late Palaeoproterozoic rifting and related volcanism in the southern McArthur Basin, and so magmatic input of heat is unlikely.

An alternative heat source for the fluids in the D_3 Tawallah Fault system could be high-heat-producing radiogenic granites in the Early Proterozoic basement. Solomon and Heinrich (1992) have suggested that the McArthur River Pb-Zn deposit may have formed from basement fluids that convected in response to high heat flow associated with long-lived radiogenic heat production from U-Th enriched Lower Proterozoic granites. Their rationale is that the decay rate of high initial geothermal gradients related to initial extension, crustal thinning and magmatism of the McArthur Basin is probably too rapid to have persisted through to the time of Pb-Zn mineralisation. McNaughton *et al.* (1993) suggest that high-heat-producing granites can maintain temperatures in excess of 200°C indefinitely (eg. 10^9 years) provided that their U-Th-K contents are sufficiently high and they are blanketed by a few kilometres of insulating or heat-producing cover.

Three features support a high-heat-producing granite heat source: (1) the Tawallah Fault dextral strike-slip system was activated long after rifting and magmatism had occurred in the southern McArthur Basin; (2) there is less than 2 km to the basement in the Batten Range region (Leaman, 1995); and (3) warm spring activity is still occurring 25 km to the west of the Batten Range at the Nathan Group/Roper Group unconformity. An alternative possibility is that strike-slip movement on the Tawallah Fault and related fluid inclusion entrapment was not related to the post-Roper Group deformation event, but occurred during active extension and associated volcanism earlier in the tectonic history of southern McArthur Basin (ie. Assumption 1 is invalid). However, field evidence for a late-stage development of the D_3 structural geometry (Chapter 6) makes this an unlikely option.

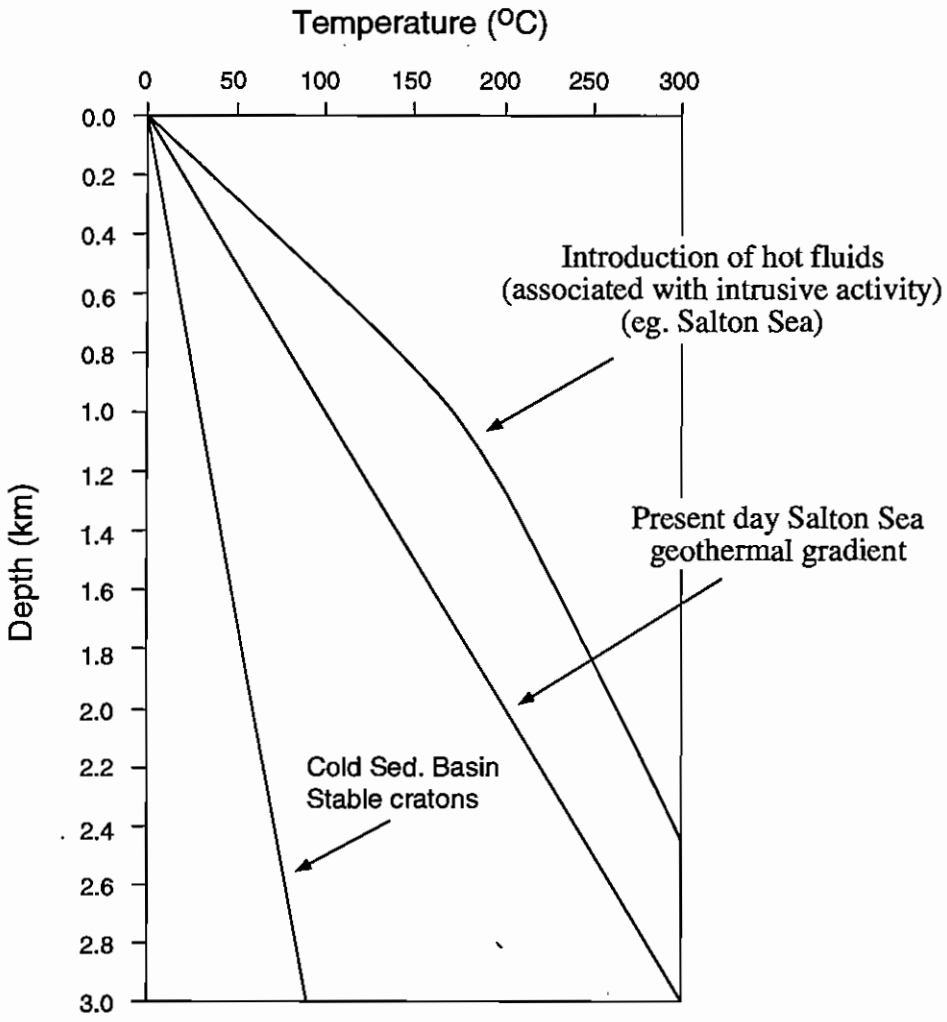

Fig. 7.11 Range of possible geothermal gradients for sedimentary basins. Salton Sea examples after McKibben *et al.* (1988); cold sedimentary basin example after Fyfe *et al.* (1978).

7.3.4 Hematite-quartz mineralisation and fluid flow model

The cation compositions of fluid inclusions analysed from D_3 hydraulic breccias in the Batten Range are comparable to the deep (1.0 to 3.0 km) saline brines of the Salton Sea geothermal system (McKibben and Williams, 1989). The principal cations in the Salton Sea brines (Na^+, K^+, Ca^{2+} and Fe^{2+}) are thought to have been derived from dissolution of evaporites (halides and sulfates) during heat-induced migration of saline connate fluids (McKibben *et al.*, 1988b). The Salton Sea geothermal system occurs in Plio-Pleistocene lacustrine-evaporite and siliciclastic sediments that are similar to the McArthur and Nathan Groups of the southern McArthur Basin. Halite, gypsum and anhydrite are the major evaporite minerals present in both successions. By analogy, dissolution of evaporites from deep-buried McArthur and/or Nathan Group carbonates during circulation of saline connate basinal brines is considered the most likely mechanism to have generated the $CaCl_2$-KCl-NaCl-H_2O fluids that were introduced into the Tawallah Fault system during D_3. High salinity basinal brines are

required to enable dissolution of Ca and SO_4 from gypsum- or anhydrite-bearing carbonates (Hanor, 1994).

Numerical modelling by Cooke (1993) predicted the effects of cooling an oxidised, 250°C, 10 eq. wt.% NaCl (Salton-Sea-type) brine by boiling and by mixing with seawater, and predicted the precipitation sequence that would result from the interaction of this brine with a hematitic quartz sandstone. Conductive or boiling-induced cooling to 100°C resulted in the precipitation of hematite and silica with traces of muscovite, chalcocite and gold. The ubiquitous quartz-hematite assemblages in the Tawallah Fault breccias and in stockwork veins adjacent to the Tawallah Fault are consistent with Cooke's (1993) predictions of mineral precipitation from an oxidised boiling brine. Cooke (1993) also noted that oxidised (hematite-stable) brines were capable of transporting significant metal loads (> 100 ppm Pb, Zn and Cu) considerable distances along faults without precipitating sulfide mineralisation. Cooling and/or boiling during transport are not predicted to initiate base metal precipitation, unless a reactive lithology or subsurface groundwater is encountered.

A schematic model to explain the fluid dynamics during D_3 rupture of the Tawallah Fault system is illustrated in Figure 7.12. This model is based on fluid inclusion data and on the numerical modelling results of Cooke (1993). Deep, oxidised, $CaCl_2$-KCl-NaCl-H_2O brines were generated by the dissolution of evaporites from McArthur and/or Nathan Group carbonates during circulation of saline formation waters. These brines were heated to temperatures of 200° to 300°C at depths of 2 to 3 km below the palaeo-water table by high-heat-producing granites in the Early Proterozoic basement (Fig. 7.12a). Rupture propagation during D_3 strike-slip movement on the Tawallah Fault is arrested at a transtensional (dilational) position along the structure (Batten Range region), leading to the creation of enhanced fracture permeability, localised pressure imbalances adjacent to the fault and the development of hydraulic implosion breccias (Sibson, 1989). In the post-rupture period (Fig. 7.12b), the deep, heated, saline fluids are interpreted to have ascended towards the surface along the Tawallah Fault and the network of secondary structures, boiling and precipitating hematite-quartz assemblages in breccia matrices and dilational veins as they rose. Phase separation during boiling may have locally increased fluid pressures to supracritical levels, resulting in secondary wall rock fracture or brecciation (Baker *et al.*, 1986). However, post-failure introduction of source fluids and subsequent quartz-hematite precipitation is interpreted to have ultimately sealed individual structures until the next rupture event. The ascending fluids are also considered to have mixed with cooler, near-surface dilute meteoric or connate waters which had filtered into the system.

The moderate salinity (8-12 eq. wt.% NaCl) and high temperature (< 300°C) fluid inclusions in Tawallah Fault hydraulic breccias are interpreted to indicate that the major upflow zone during D_3 strike-slip rupture and fluid influx occurred along the

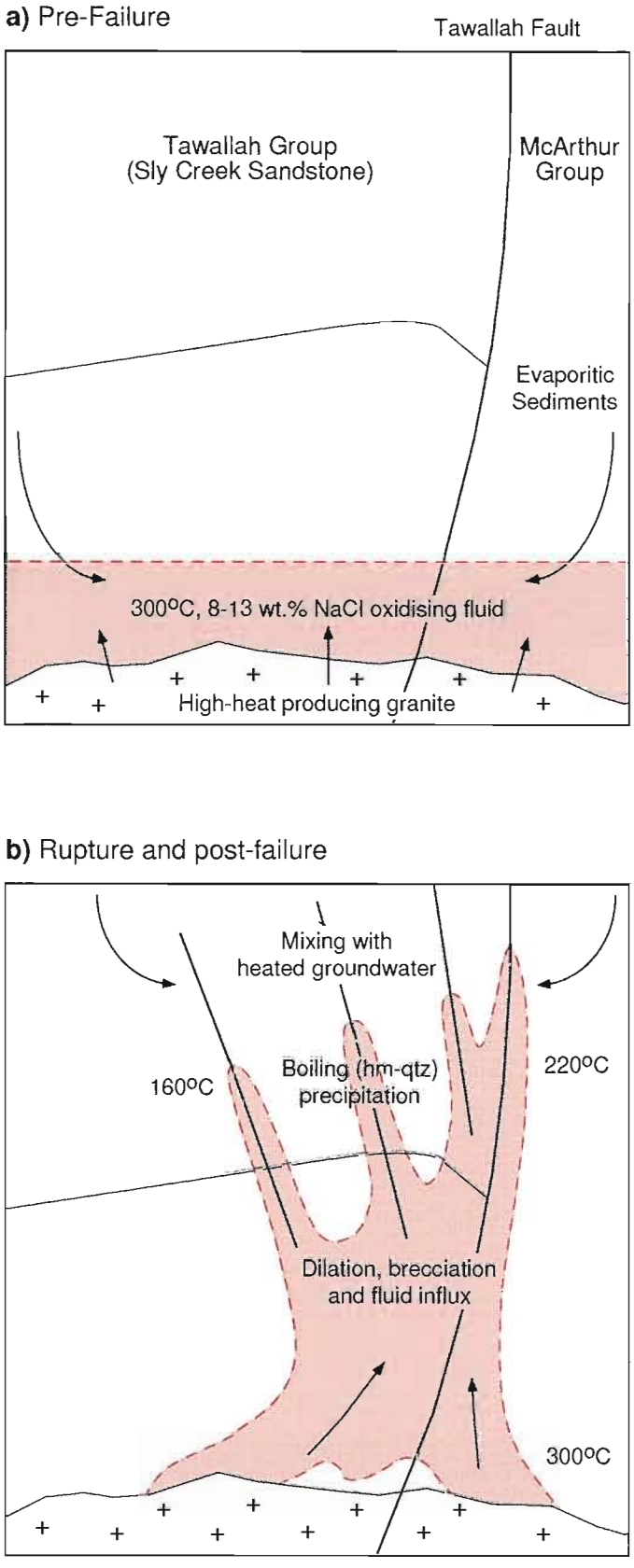

Fig. 7.12 Schematic fluid flow model for D_3 rupture of the Tawallah Fault system. **a)** Pre-failure: ponding of deep, saline fluids in sandstone aquifers. The fluids are heated by high-heat-producing granites in the basement. **b)** syn to post-rupture: cross-stratal fluid migration through the system. Diagram not drawn to scale.

primary structure. The systematic decrease in homogenisation temperatures away from the Tawallah Fault is therefore explained by more rapid cooling rates away from the major upflow zones. Along the secondary structures, fluids probably cooled quicker (ie. conductive cooling) due to lower fluid/rock ratios and greater degrees of mixing with local cooler groundwaters.

The results of the current study and the simulations of Cooke (1993) indicate that there is great potential for epigenetic base metal mineralisation throughout the entire tectonic history of the southern McArthur Basin. Basinal brine migration along the Tawallah Fault and similar fault systems may have resulted in economic mineral deposition wherever reduced (graphite and/or pyrite bearing) sediments were juxtaposed against the structures. These processes may have also been important along the Emu Fault system during the formation of base metal mineralisation at McArthur River (Fig. 1.1).

7.4 SUMMARY

Hydrothermal fluids associated with the D_3, dextral strike-slip movements on the Tawallah Fault system are characterised by moderate to high temperatures (120°-220°C) and bimodal salinities. In general, the fluids in the Tawallah Fault were hotter (≈ 210°C) than in the associated secondary structures (≈160°C). Fluid inclusions are characterised by $CaCl_2$-KCl-NaCl-H_2O cation compositions, consistent with the dissolution of halides, gypsum and/or anhydrite from deep-buried Tawallah, McArthur and/or Nathan Group carbonates by saline connate brines prior to their introduction into the D_3 Tawallah Fault system. These source fluids are interpreted to have been heated to 300°C at depths of 2-3 km. High-heat-producing granites are probably the only viable heat source for the system.

Enthalpy/chloride plots (Fig. 7.7-7.9) illustrate that cooling by boiling and by mixing of a hot (300°C), moderately saline (8-13 eq. wt.% NaCl) fluid can explain the bimodal salinity data. A combination of boiling and mixing processes are interpreted to have been responsible for the deposition of the hematite-quartz mineralisation in the hydraulic fault breccias. The mobilisation of hot, saline oxidised fluids during D_3 indicates that great potential exists for epigenetic base metal mineralisation throughout the entire tectonic history of the southern McArthur Basin, as these fluids are capable of transporting high base metal concentrations (Cooke, 1993). Potential exists anywhere along the Tawallah Fault and similar fault systems where reduced (graphite and/or pyrite bearing) sediments are juxtaposed against the structure, because these would provide favourable traps for oxidised metalliferous brines.

Chapter 8 - Discussion

CHAPTER 8 - Discussion

8.1 INTRODUCTION

A primary objective of this study has been to constrain and critically assess existing models for the early tectonic development of the southern McArthur Basin. The main aim of this chapter is to interpret each component of the Tawallah Group geology covered in previous chapters into a tectono-stratigraphic model for the southern McArthur Basin. Each phase of the model discussed in the main body of this chapter is classified according to the stratigraphic subdivision of the Tawallah Group outlined in Chapter 3.

8.1.1 Pre-Tawallah Group structural architecture

Previous models for the tectonic evolution of the southern McArthur Basin have proposed that the structural geometry of the Early Proterozoic basement was a significant factor in the generation of initial rift geometries (Plumb *et al.*, 1980; Etheridge and Wall, 1994). Major NNW- to N-trending, NW-trending and NE-trending crustal lineaments have been recognised in all Early Proterozoic domains of the North Australian Craton (Plumb, 1979). Similarly orientated fault-zones in the southern McArthur Basin are the main elements of the regional structural architecture. Consequently, it has been proposed that the tectonic development of the southern McArthur Basin was controlled by repeated reactivation of the fundamental basement fracture pattern (Plumb and Wellman, 1987). Reactivated Early Proterozoic fault systems may include the NNW to N-striking Emu, Tawallah-Abner and Four Archers Faults, which are intersected, and locally offset by, the NW-striking Mallapunyah and Calvert Faults and terminated by the NW-trending Urapunga Fault Zone.

In the study region, a number of faults with 'fundamental' structural trends can be recognised from existing regional geological maps and magnetic imagery. The NNW- to N-striking Tawallah, Lorella and Rosie Faults are associated with significant vertical displacements (up to 7.5 km; Plumb *et al.*, 1980), and are interpreted to have been active during Tawallah Group deposition (Chapter 3). In addition, a NE-trending linear feature that extends from the Tawallah Range to the southern margin of the Scrutton Range and a NW-trending lineament that transects the central Tawallah Range can be recognised from magnetic images of the northwest structural domain (Fig. 8.1). The influence of the NE-trending lineament on the local D_3 structural geometry was outlined in Chapter 6. The possibility that the NW-trending lineament was active as a

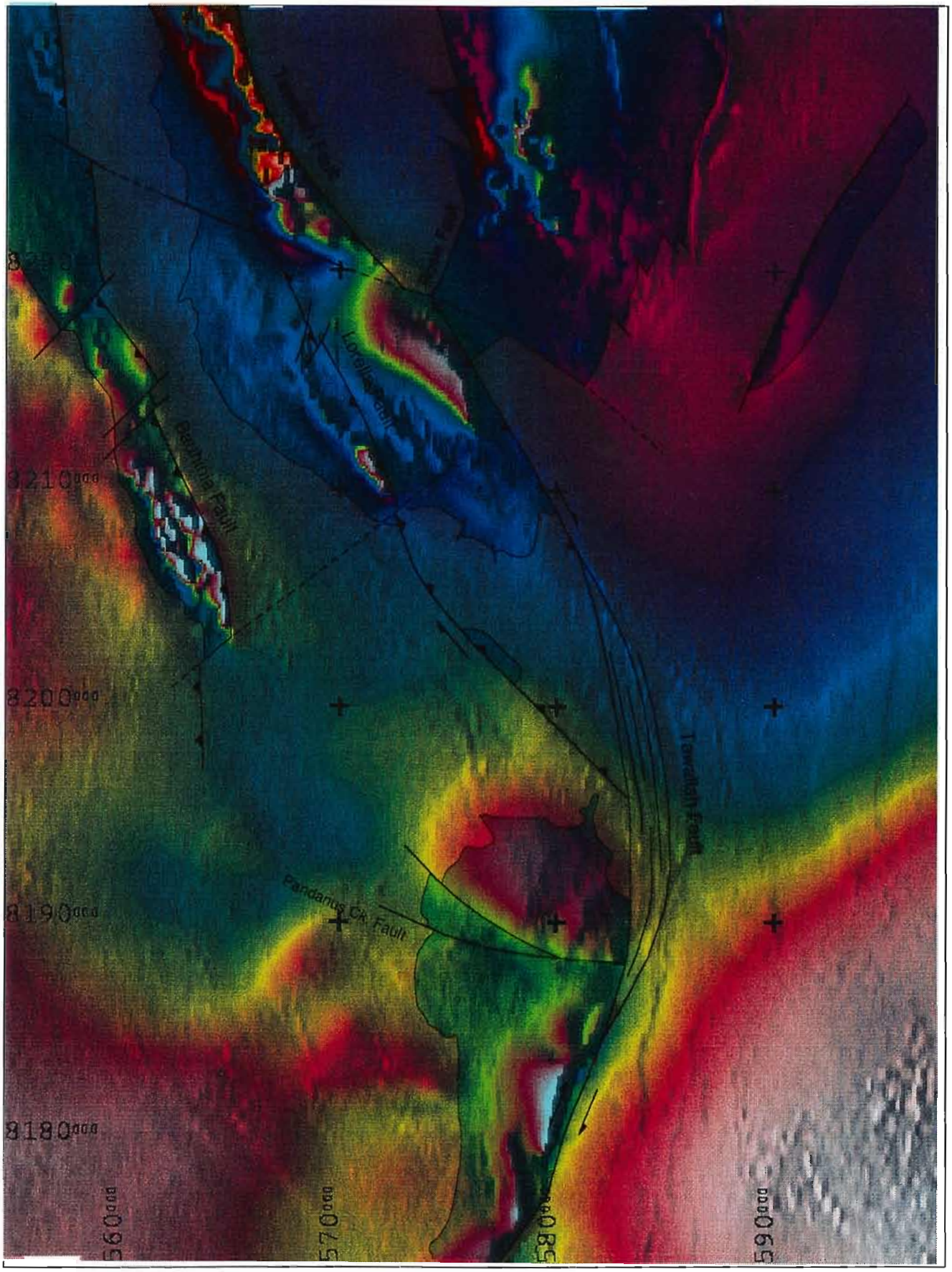

Fig 8.1 Enhanced magnetics (pseudocolour image with west sun angle illumination), major structural features and surface exposure of the Tawallah Group/ Masterton Sandstone (blue) and Scrutton Volcanics (orange) in the study region (magnetic data courtesy of NTGS).

growth structure during deposition of the basal Tawallah Group package is discussed in section 8.2.

8.1.2 Previous tectonic models for the southern McArthur Basin

As outlined in Chapter 2, opinions on the tectonic evolution of the southern McArthur Basin are divided into two opposing schools of thought. Although both groups consider that reactivation of a pre-existing structural framework was the main control on early basin geometry, the proposed orientations of initial rifting and associated transfer zones are markedly different.

(1) Etheridge and Wall (1994) suggested that the southern McArthur Basin was generated during a north-south extensional event (McArthur Event), and characterised by a series of small, approximately east-west-trending rift compartments bound by N- to NNW-trending transfer or strike-slip faults. Individual rift compartments were likely to have been preferentially localised where pre-existing WNW- to NW-trending faults (formed during the Early Proterozoic Leichhardt Event) intersected the N- to NNW-trending transfer or strike-slip faults.

Hinman (1995) noted that the Etheridge and Wall (1994) model was consistent with the structural and sedimentological architecture of the McArthur River Pb-Zn deposit. He proposed that deposition of the Barney Creek Formation occurred in a fault-bound sub-basin, generated at the intersection between the Emu Fault and an E- to ENE-trending extensional fault. The main depocentre for lower Barney Creek Formation lithologies was located parallel to the Emu Fault Zone, in an elongate trough that extended WSW, south of the ENE-trending extensional fault. Hinman (1995) proposed a transtensional tectonic environment for deposition of the lower Barney Creek Formation (NE-SW extension), with the Emu Fault system interpreted as a sinistral strike-slip transfer zone. A transpressional setting (NW-SE compression) was proposed by Hinman (1995) for deposition of the upper Barney Creek Formation, with the Emu Fault being reactivated to form a positive flower structure.

(2) Plumb and co-workers (Plumb, 1979; Plumb and Wellman, 1987; Plumb, 1994) suggested that the McArthur Basin evolved as a series of northerly-trending asymmetric rifts separated by NW-trending transfer faults and transverse ridges. Two principle rift zones, 30 to 80 km wide and 100 to 300 km long, were developed in response to approximately NW-SE oblique extension (Batten and Walker Fault Zones). The early structural geometry of the southern McArthur Basin is poorly constrained in this model. Plumb (1994) suggested that Tawallah Group deposition was largely restricted to a terrane of linked, N-trending extensional faults (eg. Emu and Tawallah Faults). This extensional terrane formed the precursor to the Batten Fault Zone, which was the principle depositional site during McArthur Group times.

The Batten Fault Zone is envisaged by Plumb *et al.* (1990) to have been a large-scale pull-apart basin during deposition of the McArthur and Nathan Groups, with NW-directed oblique extension (D_1) resulting in dextral strike-slip reactivation of N- to NNW-striking faults and large sinistral movements on NW-striking faults (Calvert and Mallapunyah Faults). Dextral strike-slip reactivation was associated with growth faulting along the Emu Fault Zone during Batten Subgroup deposition (west-block-down), indicating a basin architecture comprised of northerly-trending half-grabens flanked by broad, stable shelves. A WNW-ESE compressional event (D_2) is interpreted to have produced shallowly plunging NNE-trending folds with a poorly developed axial planar cleavage, NW-directed thrust faulting and sinistral strike-slip reactivation of N- to NNW-striking faults prior to Roper Group deposition.

Following deposition of the Roper Group, NE-directed compression (D_3) resulted in the steepening of original extensional fault blocks and the formation of conjugate NE- (dextral) and NW-trending (sinistral) faults. Syn-rift tilt blocks are believed to have been locally inverted during D_3, producing the present-day Scrutton Volcanics and Tawallah Group horst in the central Batten Fault Zone. A late N-S compressional event (D_4) is characterised by N-directed thrusting in the Murphy Inlier and Urapunga Tectonic Ridge, and may relate to a major Mesoproterozoic shortening episode in central Australia (Plumb, 1994).

Plumb (1994) incorporated his inferred deformation event hierarchy of the southern McArthur Basin into the structural framework proposed for the adjacent Mount Isa Inlier by Blake *et al.* (1990). Early Tawallah Group extension is interpreted to have been coeval with the formation of 'Cover sequence 2', whereas D_1 extension (McArthur and Nathan Group deposition) is correlated with 'Cover sequence 3'. D_2 compression in the southern McArthur Basin is interpreted to have been approximately synchronous with the Isan Orogeny, and D_3/D_4 is correlated with 'late strike-slip faulting' in the Mount Isa Inlier.

8.2 BASAL TAWALLAH GROUP DEPOSITIONAL HISTORY

The basal Tawallah Group package (Yiyintyi Sandstone, Seigal Volcanics, Sly Creek Sandstone, Rosie Creek Sandstone and Aquarium Formation) is interpreted as an intracontinental extension/subsidence sedimentary cycle, deposited during the initial phase of southern McArthur Basin tectonic evolution. The Yiyintyi Sandstone accumulated in a sandy braidplain environment in the study region, and has been correlated with the Westmoreland Conglomerate, a thick (< 1900 m) alluvial fan succession that unconformably overlies Early Proterozoic rocks along the south-eastern basin margin (Jackson *et al.*, 1987). Consequently, the initial phase of deposition in the southern McArthur Basin is interpreted to have been characterised by basin-wide clastic

sedimentation, with sandy braidplain systems formed distal (> 300 km) to alluvial fan settings on the basin margins. Clastic sedimentation was interrupted by emplacement of the thick (400 to 1600 m) Seigal Volcanics flood basalt succession, which has a regional extent comparable to some of the larger Phanerozoic flood basalt provinces (eg. Columbia River, USA; Wilson, 1989). The Seigal Volcanics have sub-alkaline tholeiitic compositions, with trace-element abundances consistent with a within-plate tectonic setting for basal Tawallah Group magmatism.

High-energy, clastic alluvial sedimentation was re-established following emplacement of the Seigal Volcanics, with the deposition of the Sly Creek Sandstone in a distal sandy braidplain environment. Continued extension and subsidence in the southern McArthur Basin is marked by a transgressive transition from the sandy braidplain system of the Sly Creek Sandstone to local braid-delta (Rosie Creek Sandstone) and eventually, to shallow marine depositional environments (Aquarium Formation). Regionally, the occurrence of low-relief shallow platform carbonates at consistent stratigraphic levels in the Aquarium formation is interpreted to indicate that the formation was deposited during a basin-wide episode of tectonic quiescence and stable platform sedimentation.

The early structural geometry and controls on the basal Tawallah Group depositional architecture are poorly constrained. However, apparent growth in the Sly Creek Sandstone, Rosie Creek Sandstone and Aquarium Formation can be inferred from Tawallah Range map patterns (Fig. 8.2). In western Tawallah Range, these formations thicken northwards toward an unexposed, WNW-trending lineament that bisects the Tawallah and Lorella Faults on regional magnetic images (Fig. 8.1). Although structurally thickened by later folding, the thickness of each basal Tawallah Group formation increases by approximately 100 m towards the WNW-trending lineament (Fig. 8.2), defining a wedge-shaped (syn-depositional growth) geometry south of the structure. The stratal geometry and scale of this growth are consistent with an extensional tilt block interpretation (Scott *et al.*, in prep.), with WNW-striking normal faults developed in response to an approximate N-S extension direction (Fig. 8.3a). The importance of N- to NNW-striking major faults during deposition of the basal Tawallah Group package is uncertain. However, given that uplift along the Tawallah Fault is interpreted to have locally controlled subsequent sedimentation patterns, a local basin geometry comprising WNW-striking normal faults and N- to NNW-striking strike-slip or transfer faults is thought to have existed during early N-S extension (Fig. 8.3a).

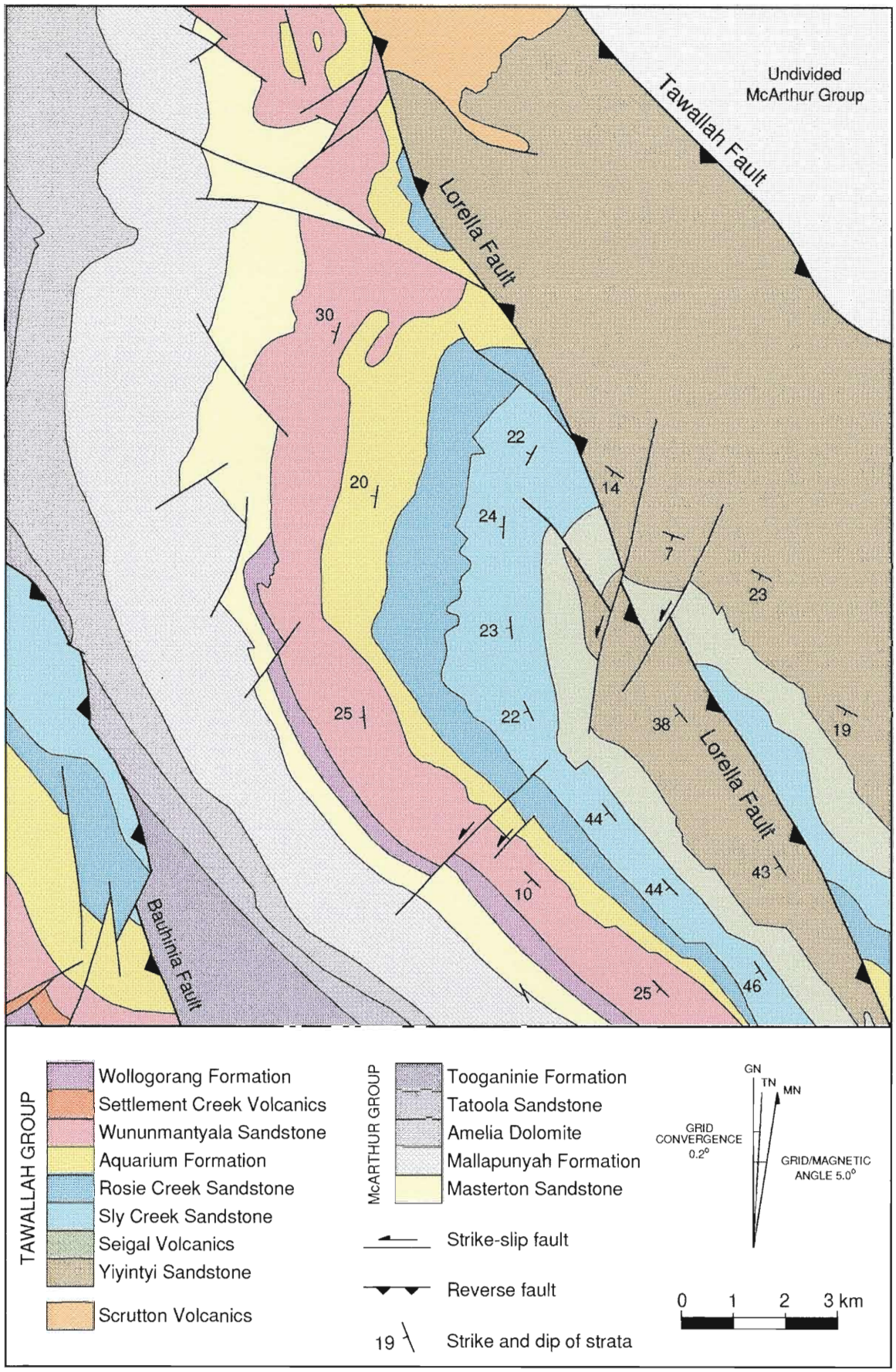

Fig. 8.2 Simplified geology of the central-western Tawallah Range showing the Sly Creek Sandstone, Rosie Creek Sandstone and Aquarium Formation increasing in thickness to the north. This stratal geometry is interpreted to represent an original growth wedge in the lower Tawallah Group, adjacent to the WNW-trending fault shown at the top of the diagram.

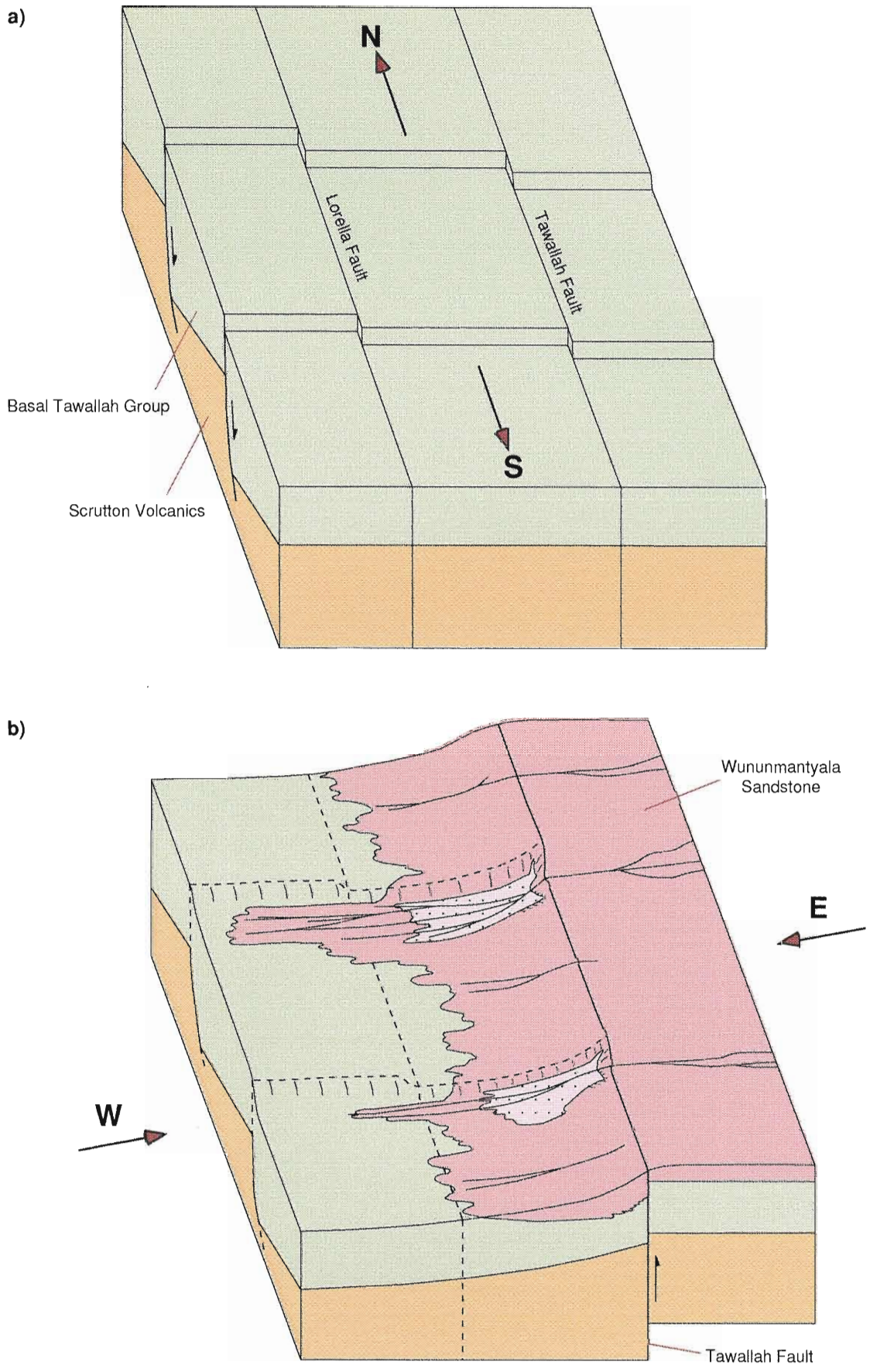

Fig 8.3 Schematic block diagrams of: **a)** possible pre-D_1 structural geometry in the vicinity of the study region (N-S extension); and **b)** Influence of pre-existing fault-geometry on the localisation of coarse-grained Wununmantyala Sandstone facies during D_1 uplift along the Tawallah Fault (E-W compression).

8.3 MID-TAWALLAH GROUP DEPOSITIONAL HISTORY (D_1)

The middle Tawallah Group package is interpreted to be the second extension-subsidence sedimentary cycle and transgressive phase during early southern McArthur Basin evolution. The boundary between the basal and middle Tawallah Group sedimentary packages is typically unconformable, with lower conglomeratic and pebbly sandstone lithologies of the Wununmantyala Sandstone marking a local transition from shallow subaqueous (Aquarium Formation) to subaerial braidplain depositional settings. The distribution of Wununmantyala Sandstone facies associations in the study area is considered to be a result of spatial and temporal variations in the braidplain depositional environment. Basal coarse-grained facies of the Wununmantyala Sandstone contain clasts derived from Scrutton Volcanics and lower Tawallah Group stratigraphy, indicating that a period of substantial intrabasinal uplift occurred subsequent to Aquarium Formation deposition. The Scrutton Volcanics and basal Tawallah Group source regions for the Wununmantyala Sandstone are thought to have been uplifted by east-block-up reverse movement along the Tawallah Fault. Uplift occurred during the E-W compressional event (D_1), and resulted in the formation of a proximal braidplain system near southwest Tawallah Range that graded to more distal settings in the Scrutton, Batten and western Tawallah Range regions (Fig. 8.3b). Largely unimodal, west-directed palaeocurrents measured from cross-bedded facies of the Wununmantyala Sandstone are consistent with the proposed post-D_1 depositional architecture (Bull, 1993). The restriction of proximal braidplain facies to the southwest Tawallah Range is interpreted to indicate that early Wununmantyala Sandstone sedimentation was localised at the intersection between the Tawallah Fault and a pre-existing WNW-striking normal fault (Fig. 8.3b).

Following D_1 and development of the Wununmantyala Sandstone braidplain depositional system, topographic erosion and the resumption of crustal extension resulted in the deposition of the Wollogorang Formation in shallow subaqueous depositional environments. The depositional geometry of the Wollogorang Formation is considered to have been topographically controlled in the study region. Elevated topography associated with D_1 uplift probably persisted throughout Wollogorang Formation times, with the Batten and Tawallah Ranges representing sites of non- or restricted deposition. Progressive onlap of shallow marine or lacustrine sediments onto the uplifted regions occurred once crustal extension and subsidence were re-established.

The uniform coarse grainsize of coherent dolerite facies in the Settlement Creek Volcanics, and the presence of marginal breccias along upper dolerite contacts is consistent with emplacement as shallow-level sills at the base of the Wollogorang Formation. A shallow intrusive mode of emplacement is also proposed for the Gold Creek Volcanics, although multiple cycles of dolerite, marginal peperitic breccia and

clastic lithologies are interpreted to indicate that volcanic activity was coeval with shallow subaqueous clastic sedimentation. The Settlement Creek Volcanics and Gold Creek Volcanics have sub-alkaline tholeiitic compositions, and have immobile element concentrations consistent with a within-plate tectonic setting for mid-Tawallah Group magmatism. They are distinguished from the Seigal Volcanics by their more restricted spatial distribution, lower volume of constituent mafic material and enrichment of TiO_2, P_2O_5, Zr, Y, Nb, Th, and LREE. These differences are attributed to the Settlement Creek Volcanics and Gold Creek Volcanics being derived from lower degree partial melting of an asthenospheric mantle source, in response to slower rates of tectonic extension following the D_1 compressional event.

Overall, the local depositional architecture of the middle Tawallah Group package was controlled by west-directed reverse displacement along the N-striking Tawallah Fault during D_1. Intrabasinal tectonic uplift of a N-S elongate fault-block of Scrutton Volcanics and basal Tawallah Group stratigraphy generated a subaerial braidplain depositional system (Wununmantyala Sandstone). Coarse-grained proximal braidplain deposits developed near the intersection of the Tawallah Fault and the NW-trending growth fault (southern Tawallah Range), and graded to more distal settings in the Batten, Scrutton and western Tawallah Ranges. Shallow subaqueous sediments (Wollogorang Formation) transgressed the subaerial depositional system once crustal extension and subsidence had resumed. However, topographic elevation was preserved in the Batten and Tawallah Range regions, resulting in restricted deposition at these localities during marine transgression.

8.4 UPPER TAWALLAH GROUP DEPOSITIONAL HISTORY

The upper Tawallah Group package (Warramana Sandstone, Tanumbirini Rhyolite and Nyanantu Formation) marks a second local transition from shallow subaqueous (Wollogorang Formation and Gold Creek Volcanics clastic facies) to subaerial depositional environments. The basal conglomeratic facies of the Warramana Sandstone is interpreted to have been deposited during sea level regression and relocation of an active beachface. Above the conglomeratic lag deposit, the Warramana Sandstone consists of a barred beachface succession, with minor siltstone intervals deposited in a lagoonal setting. A general shallowing from the subaqueous settings of the Gold Creek Volcanics is inferred prior to emplacement of the Tanumbirini Rhyolite as a series of localised subaerial lava flows and domes. The Nyanantu Formation is interpreted to have been deposited in a proximal/medial braided river environment. The abundance of felsic volcanic clasts in Nyanantu Formation facies implies that the palaeo-braided river system had developed in a terrane where the Tanumbirini Rhyolite was exposed and subject to active erosion.

Due to the lack of substantiating evidence, fault-controlled uplift is considered to be an unlikely mechanism for the period of regression that extended from late Wollogorang Formation times through to Nyanantu Formation deposition. In contrast, the basin must have retained an extensional geometry during the upper Tawallah Group regressive phase to allow regional high-level intrusion and extrusion of mafic and felsic magma. Elevation of the ambient geothermal gradient and the addition of mafic material to the crust by underplating and intrusion during post D_1-extension (Settlement Creek and Gold Creek Volcanics) is tentatively proposed as an uplift mechanism for this regressive transition. The emplacement of Settlement Creek and Gold Creek Volcanics prior to deposition of the upper Tawallah Group package, and their within-plate tholeiitic geochemistry is consistent with an underplating mechanism for uplift. Wyborn *et al.* (1987) proposed that the Proterozoic continental crustal of Northern Australia was extensively and repeatedly underplated during recurrent extensional events. In this model, mafic material accreted at the base of the Proterozoic crust either solidified at the top of large sub-crustal intrusions, or ascended to the surface to form tholeiitic basalt/dolerite suites. Cox (1980) suggested that gabbroic sill complexes emplaced during crustal underplating are eventually metamorphosed to granulite facies assemblages due to the high geothermal gradients that accompany lithospheric extension. Late Proterozoic felsic volcanic suites of Northern Australia are predominantly I-type, and are interpreted to have been sourced from granulitic lower crustal regions (Wyborn *et al.*, 1987). The Tanumbirini Rhyolite has immobile element compositions comparable to similarly aged felsic volcanic suites elsewhere in Northern Australia, and is therefore interpreted to have been derived from lower crustal partial melting of I-type source regions generated during underplating of older tholeiitic magmas.

In summary, the final phase of Tawallah Group deposition occurred during a period of regression, with a local vertical progression from nearshore (Warramana Sandstone) to braided river depositional environments in the Scrutton Range. The upper Tawallah Group formations are absent elsewhere in the study region, with the Masterton Sandstone (basal McArthur Group) separated from the Wununmantyala Sandstone by a disconformity, local erosional unconformity or palaeosol horizon in the Batten and Tawallah Ranges. Consequently, a local basin architecture similar to that proposed for Wollogorang Formation deposition is suggested for the upper Tawallah Group package. The Batten and Tawallah Ranges are considered to have remained as topographic highs and areas of non- or restricted deposition during upper Tawallah Group sedimentation and volcanic activity, which occurred in adjacent, topographically lower regions (Scrutton Range). In this model, the Masterton Sandstone is interpreted to have been a clastic blanket that unconformably covered and preserved the local Tawallah Group depositional geometry.

8.4.1 Masterton Sandstone (basal McArthur Group)

In the Batten Range, talus slope (colluvial slide) breccias interbedded with coarse-grained sandstone lithologies form the basal 150 m of the Masterton Sandstone adjacent to the Pandanus Creek Fault. The talus deposits grade laterally into conglomeratic debris flow and proximal braidplain deposits towards the south. To the north, basal conglomeratic facies of the Masterton Sandstone are approximately 50 m thick, and are interpreted to be proximal/medial braidplain deposits. Sandy alluvial braidplain deposits (upper sandstone facies) overlie the basal conglomeratic facies throughout the Batten Range (Bull, 1993). Based on palaeocurrent data measured from cross-bed foresets in the Batten Range, an interfingering relationship between the upper sandstone facies and the underlying conglomeratic deposits was proposed by Bull (1993).

The total thickness of the Masterton Sandstone increases abruptly across the Pandanus Creek Fault, from 325 m to approximately 450 m immediately south of the structure (Fig. 8.4). Masterton Sandstone exposures in the southern Batten Range attain a maximum thickness of only 50 m, defining a wedge-shaped geometry for the formation south of the Pandanus Creek Fault (Fig. 8.4). Based on the stratal geometry and local facies variations in the Batten Range, deposition of the Masterton Sandstone is interpreted to have occurred during N-S extension, with significantly thickened sections localised along E-W-striking growth faults.

Palaeocurrent directions measured from the formation indicate that the main sediment source regions were situated east of the study region (Bull, 1993). Consequently, the positive topography generated by D_1 uplift was either maintained or re-established during deposition of the Masterton Sandstone. If the Tawallah Fault was a NNW-striking transfer zone during this period, localisation of coarse-grained and/or thickened Masterton Sandstone sequences may have been controlled by local transtensional fault geometries developed along the structure. A local basin geometry of small E-W-trending extensional compartments bound by NNW-trending transfer faults is therefore proposed for Masterton Sandstone deposition. The Masterton Sandstone is interpreted to have accumulated during the initial phase of thermal relaxation following the regional uplift associated with upper Tawallah Group deposition and volcanism. Subsequent to Masterton Sandstone deposition, broad crustal extension characterised the southern McArthur Basin with carbonate and evaporite-dominated sedimentation (McArthur Group) occurring in a sag-phase tectonic setting.

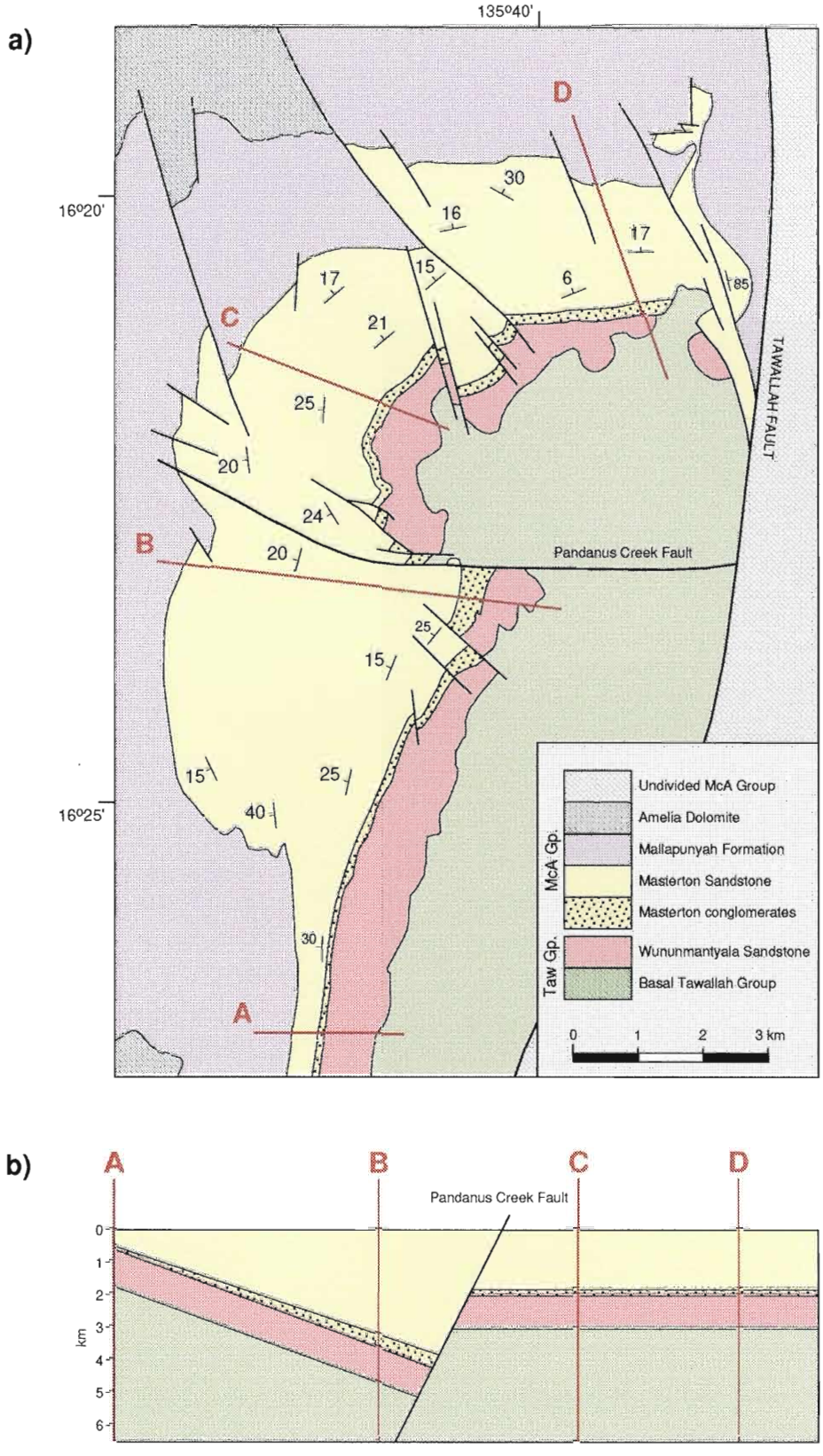

Fig 8.4 Interpreted growth wedge geometry of the Masterton Sandstone adjacent to the Pandanus Creek Fault, Batten Range. **a)** Lateral thickness variations in the basal conglomerate and upper sandstone facies of the Masterton Sandstone. **b)** Schematic N-S cross section of the western Batten Range showing thickness change of the Masterton Sandstone across the Pandanus Creek Fault.

8.5 POST-TAWALLAH GROUP DEFORMATION

Kinematic resolution of secondary fault geometries and inverse palaeostress analysis has led to the recognition of two post-Tawallah Group compressional deformation events. The structural architecture of the study region during each of these events was largely controlled by the reactivation of primary basin-forming faults (Tawallah, Lorella and Rosie Faults), resulting in a complex modification of the original basin geometry.

8.5.1 NW-SE compression: D_2

D_2 involved NW-SE compression and was characterised by sinistral strike-slip secondary deformation adjacent to the Lorella and Tawallah Faults. Variations in the estimated orientation of the D_2 stress-field throughout the study region are attributed to poor preservation of D_2 secondary faults during later deformation (ie D_3 rotation or reactivation). Although cross-cutting relationships indicate that the D_2 event post-dated Tawallah Group and lower McArthur group deposition within the study region, an absolute timing for NW-SE compression was difficult to ascertain. NW-SE-directed, syn-Barney Creek Formation transpression documented at the McArthur River Pb-Zn deposit by Hinman *et al.* (1994) is tentatively interpreted to have been synchronous with D_2 in the study region.

8.5.2 NE-SW compression D_3

Most of the secondary faulting and regional-scale structural features in the study region formed in response to D_3 NE-SW compression. D_3 is the youngest and best preserved tectonic phase in the proposed deformation event hierarchy, post-dating deposition of the Roper Group. Consequently, the D_3 event is interpreted to have marked the culmination of Proterozoic sedimentary deposition in the southern McArthur Basin. Complex block-faulting associated with the D_3 event was largely controlled by dextral and oblique dextral-reverse displacements on N- to NNW-striking regional-scale faults (Fig. 8.5).

Batten Range

D_3 secondary fault patterns in the Batten Range are consistent with a Riedel model for right-lateral simple shear on the Tawallah Fault. The local D_3 fault geometry mostly comprises P and X shear fractures, with R and R' secondary faults restricted to within 2 km of the Tawallah Fault. The co-existence of P and X shears can be

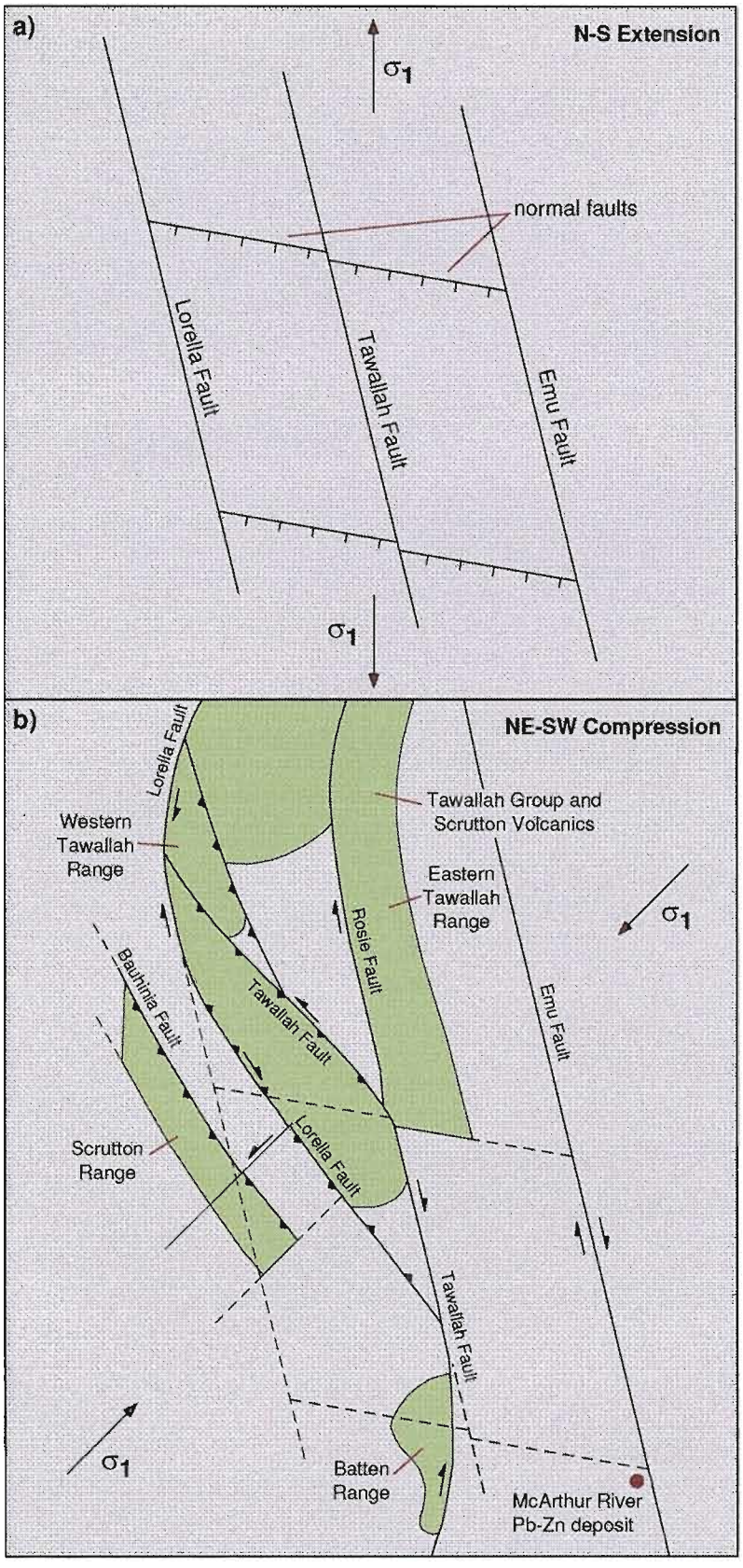

Fig. 8.5 Influence of basin-forming faults on the development of the D_3 structural geometry in the study region. **a)** Interpreted orientations of rift compartments in the southern McArthur Basin. WNW-striking normal faults are bound by NNW-striking transfer or strike-slip faults under N-S extension (after Etheridge and Wall, 1994). **b)** NE-SW compression (D_3) results in dextral strike-slip reactivation of the NNW-striking faults (Lorella, Tawallah and Emu Faults) and the formation of NW-striking reverse faults (Bauhinia Fault). The formation of a NW-trending contractional strike-slip duplex between the Tawallah and Lorella Faults during D_3 results in transpressional uplift of the western Tawallah Range.

interpreted to indicate that systematic variations between a dextral strike-slip and transtensional stress state occurred, given that the Batten Range was situated at a releasing bend along the Tawallah Fault during D_3 (Fig. 8.5). However, it is more likely that the D_3 secondary fault pattern in the Batten Range was controlled by the reactivation of pre-existing D_2 faults. It is therefore proposed that the generation of R, R' and P secondary faults during NE-SW compression was accompanied by the reactivation of pre-existing D_2 faults to form 'apparent' D_3 X shears.

Scrutton Range

In the Scrutton Range, the local D_3 structural geometry is characterised by a series of subsidiary fault-blocks that are separated by NE-striking oblique-dextral faults and bound by NW-striking reverse faults. By comparison with the deformational features formed during the emplacement of a competent and continuous thrust sheet (Mandl and Shippam, 1981), NE-striking oblique-dextral faults are interpreted to be tear faults and the NNW-striking reverse faults are thought to be secondary imbricate structures. In this model, tear faulting, secondary imbrication and fault propagation folding developed to accommodate excess shear strain during differential reverse displacement along the Bauhinia Fault. The juxtaposition of progressively younger Tawallah Group formations with McArthur Group stratigraphy towards the south along the Bauhinia Fault is consistent with this model.

Tawallah Range

The Lorella Fault and northern Tawallah Fault segment are the main structural features of the western Tawallah Range region, and respectively form the western and eastern margins of a Scrutton Volcanics/Yiyintyi Sandstone inlier. D_3 fault patterns in the Tawallah Range are interpreted to have formed by a combination of dextral simple shear on the Tawallah and Lorella Faults and horizontal shortening across a transpressional zone formed between the two major structures (contractional strike-slip duplex). The formation of a contractional strike-slip duplex between the Tawallah and Lorella Fault systems during D_3 is interpreted to have been controlled by the pre-existing, regional structural geometry (Fig. 8.5). The NW-striking Tawallah and Lorella Fault segments bisect a WNW-striking structure that was inferred to have been an extensional growth fault during basal Tawallah Group deposition (section 8.2). The WNW structural trend also constitutes one of the fundamental basement fracture orientations that have been recognised throughout the Proterozoic of Northern Australia (Plumb, 1979). Consequently, lateral shear fracture propagation between the Lorella and Tawallah dextral strike-slip systems during D_3 may have been controlled by a pre-

existing, WNW-trending zone of weakness in underlying basement and lower Tawallah Group rocks (Fig. 8.5).

Modification of the southern duplex margin by a NE-striking basement structure is also proposed to explain the change from SW- to NE-directed reverse displacement along the southern Lorella Fault segment. NE-directed displacement along the Lorella Fault is restricted to an isolated segment that parallels the region of NE-directed uplift in the Scrutton Range (Fig. 8.5). The fault segment is terminated by a NNE-trending oblique-sinistral transfer zone in central Tawallah Range, and by an unexposed NE-trending structure that extends from the southern margin of the Scrutton Range. The emplacement of the Scrutton Range fault-block during D_3 horizontal compression is therefore interpreted to have influenced the development of the southern duplex margin, with the NE-trending basement structure forming the southern boundary to NE-directed uplift in the study region (Fig. 8.5).

D_3 Fluid Flow

Quartz-hosted fluid inclusions in D_3 hydraulic fault breccias from the Batten Range have trapped moderate temperature (120° to 220°C), saline (< 20 eq wt. % NaCl) and oxidised fluids. Solutes are interpreted to have been sourced from the dissolution of halides, gypsum and/or anhydrite in deep-buried (2-3 km) Tawallah, McArthur and/or Nathan Group carbonates during interaction with hot (300°C), moderately saline (8-13 eq. wt.% NaCl) connate brines. During dextral strike-slip rupture, the brines ascended towards the surface along the Tawallah Fault and the network of secondary structures, boiling and precipitating hematite-quartz assemblages in breccia matrices and dilational veins. The fluids also mixed with cooler, less saline meteoric or connate waters. The presence of hot, saline and oxidised fluids in post-Roper brittle structures implies that there is great potential for late-stage epigenetic base-metal mineralisation in the southern McArthur Basin, particularly where reduced (graphite and/or pyrite bearing) sediments are juxtaposed against D_3 fault systems.

8.6 TECTONIC SETTING OF THE TAWALLAH GROUP

The structural, sedimentological, and geochemical characteristics of the Tawallah Group are consistent with an intracratonic setting for the early tectonic development of the southern McArthur Basin. The majority of the clastic Tawallah Group formations are interpreted to have accumulated in regionally extensive subaerial depositional systems, with subaqueous carbonate and clastic sedimentation comprising only a minor proportion of the succession. The igneous formations of the Tawallah Group have geochemical compositions typical of continental within-plate magmatism,

lending further support to an intracratonic tectonic model for the early evolution of the southern McArthur Basin. The Tawallah Group is interpreted to represent a Late Palaeoproterozoic intracratonic rift sequence that was deposited unconformably above post-Barramundian rock types of the North Australian transitional igneous suite (Scrutton Volcanics), and prior to thermal relaxation and deposition of overlying (sag-phase) McArthur Group carbonate and evaporite lithologies.

The dynamics of early intracratonic tectonism in the southern McArthur Basin is further constrained by the recognition of three distinct tectonic cycles within the Tawallah Group. The boundary between the basal and middle Tawallah Group sedimentary cycles is interpreted to mark a major change from an early basin architecture that was typified by regionally extensive sedimentary and volcanic depositional systems. Local uplift associated with D_1 compression at this boundary is considered to have controlled Wununmantyala Sandstone sedimentation, and locally influenced the depositional architecture of later carbonate and clastic formations. D_1 is also thought to have ended a period of rapid tectonic extension in the southern McArthur Basin, with slower extension rates subsequent to D_1 resulting in the production of smaller volume mafic magmas that locally intruded the Wollogorang Formation to form the Settlement Creek Volcanics and Gold Creek Volcanics. In the study region, the boundary between the middle and upper Tawallah Group cycles is recognised as a local disconformity, with an interpreted transition to marginal subaqueous and subaerial palaeo-depositional environments above the largely subaqueous Gold Creek Volcanics. Unlike the basal/middle Tawallah Group boundary, the disconformity between the Gold Creek Volcanics and Warramana Sandstone is not considered to correlate with a significant change in the local basin architecture. However, the boundary does mark the beginning of a regressional transition in the upper Tawallah Group that is tentatively attributed to the input of mafic material into the crust and associated elevation of the geothermal gradient during post-D_1 extension.

The influence of D_1 uplift on the local depositional architecture of middle and upper Tawallah Group formations makes it difficult to establish a possible orientation for tectonic extension during this period. The resolution of syn-depositional growth faulting in the middle and upper Tawallah Group is further complicated by the complex structural geometry developed along the Tawallah, Lorella and Bauhinia Faults during D_2 and/or D_3. However, local stratal geometries interpreted as 'growth' wedges adjacent to WNW-striking growth faults occur in the basal Tawallah Group stratigraphy (central Tawallah Range), and in the Masterton Sandstone (Batten Range).

The presence of WNW-striking growth faults during basal Tawallah and McArthur Group deposition is interpreted to indicate that the early extensional architecture of the southern McArthur Basin consisted of approximately E-W-trending rift compartments that were bound by N-S-trending transfer zones. A structural

geometry broadly similar to that proposed for the Lake Malawi Rift Zone by Scott *et al.* (1992) is envisaged, whereby small (< 50 km^2) individual rift compartments are bound by near dip-slip normal faults and subvertical oblique-slip or transfer faults. This interpretation is consistent with the tectonic model proposed for the southern McArthur Basin by Etheridge and Wall (1994), which was based on the presence of WNW-striking, syn-McArthur Group extensional faults adjacent to the Emu Fault Zone. A palaeogeographical model proposed for the Barney Creek Formation at the McArthur River Pb-Zn deposit by Hinman (1995) also had a structural architecture of E-W-striking extensional faults and N-S-trending transfer zones during McArthur Group times. It would appear therefore, that the geometry of basin-forming structures active during basal Tawallah Group sedimentation and volcanism was maintained after D_1, with N-S tectonic extension occurring until at least mid-McArthur Group times.

The most active extensional phase in the tectonic evolution of the southern McArthur Basin is considered to have occurred during Tawallah Group deposition, with the rate of tectonic extension progressively reducing prior to McArthur Group times. The Masterton Sandstone is interpreted to have been deposited in response to thermal relaxation following the cessation of post-D_1 magmatism. Deposition of the carbonate and evaporitic McArthur Group lithologies which overlie the Masterton Sandstone occurred during a period of more regionally distributed crustal extension, in an intracratonic sag-phase tectonic setting. Based on the lack of evidence for N-S-striking growth faults in the study region, the fundamental structural geometry of the southern McArthur Basin proposed here does not concur with the tectonic models of Plumb and co-workers (Plumb, 1979; Plumb and Wellman, 1987, Plumb 1994). However, the palaeostress-field orientations of D_2 and D_3 roughly correlate to Plumb's (1994) pre- and post-Roper deformation events respectively.

As this study has dealt primarily with the role of compressional deformation in the genesis of the southern McArthur Basin, the extensional architecture discussed here is simplistic and modelled in terms of in ideal orthogonally extending system (eg. Gibbs, 1990). The restriction of Tawallah Group surface exposure to the Batten Fault Zone, due largely to D_3 reactivation of N-S-trending fault zones, hinders any attempt at reconstructing the extensional structural geometry that was active during initial rifting in the southern McArthur Basin. The regional extent and geometry of the 'Tawallah Group rift' and the degree of oblique-slip accommodated by the fundamental basin-forming faults during N-S extension can be better constrained by the collection and interpretation of seismic data from the Batten Fault Zone.

Chapter 9 - Conclusions

CHAPTER 9 - Conclusions

9.1 OVERVIEW

The southern McArthur Basin consists of four main sedimentary packages. The basal Tawallah Group and overlying McArthur Group have been interpreted as the initial rift and sag cycles of intracratonic basin formation respectively (Plumb, 1994). The Tawallah Group consists of coarse-grained clastic lithologies, mafic igneous formations, minor carbonates and felsic volcanics, whereas the McArthur Group is characterised by finer-grained clastic and evaporitic carbonate sequences. The depositional age of the Tawallah Group is constrained between 1851 ± 7 Ma (Scrutton Volcanics 'basement'; R. Page, unpublished data) and 1713 ± 6 Ma (Tanumbirini Rhyolite; Haines *et al.*, 1993). Structural, sedimentological, volcanological and geochemical studies of the Tawallah Group were used to constrain, and assess existing models for, the early tectonic evolution of the southern McArthur Basin. This chapter summarises the main conclusions of the study, with the final section outlining a tectono-stratigraphic model for the early evolution of the southern McArthur Basin.

9.2 SEDIMENTARY CYCLES OF THE TAWALLAH GROUP

Three cycles of sedimentary deposition and igneous activity have been recognised in the Tawallah Group. Major changes in the structural basin architecture and/or palaeo-depositional conditions are interpreted to have occurred at the boundaries between each cycle.

The basal Tawallah Group package was formed during the initial extension-subsidence cycle in the southern McArthur Basin, with a transgressive transition from alluvial braidplain (Yiyintyi Sandstone and Sly Creek Sandstone) through braid-delta (Rosie Creek Sandstone) to shallow subaqueous (Aquarium Formation) depositional environments. An episode of subaerial mafic flood volcanism, equivalent in volume and aerial extent to the Columbia River flood basalts of North America, preceded Sly Creek Sandstone deposition (Seigal Volcanics).

The middle Tawallah Group package formed during a second extension-subsidence depositional cycle and transgressive phase, with a basal alluvial braidplain succession (Wununmantyala Sandstone) overlain by shallow subaqueous deposits (Wollogorang Formation). The Settlement Creek Volcanics and Gold Creek Volcanics, which intruded the lower carbonate and upper sandstone successions of the Wollogorang Formation respectively, are also included in the middle Tawallah Group package.

The regressive upper Tawallah Group package was deposited during a transition from nearshore (Warramana Sandstone) to braided fluvial sedimentary successions (Nyanantu Formation). Subaerial felsic volcanism preceded deposition of the Nyanantu Formation (Tanumbirini Rhyolite). The change from subaqueous (Wollogorang Formation) to marginal subaqueous/subaerial conditions is marked by a regressive conglomeratic lag deposit at the base of the upper Tawallah Group package.

9.3 GENESIS OF THE IGNEOUS TAWALLAH GROUP FORMATIONS

Mafic rocks of the Tawallah Group have sub-alkaline tholeiitic compositions. Immobile element concentrations are typical of within-plate tectonic settings, and multi-element variation patterns support a CFB affinity for Tawallah Group magmatism. The Seigal Volcanics are characterised by low TiO_2 and P_2O_5 concentrations relative to the younger mafic formations of the Tawallah Group. The Gold Creek Volcanics have enriched Nb and LREE, but depleted P_2O_5 concentrations compared to the Settlement Creek Volcanics.

Based on Zr/Nb, Y/Nb and REE relationships, the Settlement Creek and Gold Creek Volcanics are interpreted to have been derived from more enriched mantle sources than the Seigal Volcanics. This trend contrasts other CFB provinces, where eruptive products with N-type MORB compositions become increasingly abundant as rifting progresses (Crawford and von Rad, 1994). Enriched compositions in the younger mafic formations of the Tawallah Group are explained by proposing that progressively lower degrees of partial melting of an homogeneous asthenospheric mantle source occurred during magmatism. In this model, 20-30 % partial melting of an asthenospheric mantle source resulted in the production of large basalt volumes with 'depleted' compositions (Seigal Volcanics). The Settlement Creek Volcanics and Gold Creek Volcanics were derived by 10-15 % and 7-10 % partial melting of the same asthenospheric source respectively, so that smaller volumes of basalt/dolerite with more enriched compositions were produced. This model cannot explain, however, the anomalously high P_2O_5 and LREE concentrations of the Settlement Creek Volcanics relative to the Gold Creek Volcanics. An additional source component (enriched sub-continental lithosphere) is therefore suggested for the Settlement Creek Volcanics.

The Tanumbirini Rhyolite has immobile element concentrations comparable to similarly aged felsic volcanic suites elsewhere in Northern Australia (Fagan Phase; Rawlings, 1994). Possible correlates include the Peters Creek Volcanics (Lawn Hill Platform) and Fiery Creek Volcanics (Mount Isa Inlier), which are thought to have been derived from partial melting of lower crustal sources that formed during underplating of older tholeiitic magmas (Wyborn *et al.*, 1987).

9.4 STRUCTURAL HISTORY OF THE STUDY REGION

Brittle fault zones of varying magnitude are well developed in the Tawallah Group, and most are characterised by cataclastic deformation textures. A grain boundary sliding mechanism for local cataclastic deformation is proposed based on the microstructural study of a brittle fault zone in the Masterton Sandstone. Mesoscopic fault zone textures such as hydraulic fracture, hydraulic brecciation, veining and wall rock silicification are interpreted to have formed where significant fluid influx had occurred during deformation.

A deformation event hierarchy for the study region has been determined by calculating palaeostress tensors from fault-slip data collected in the Batten, Scrutton and Tawallah Ranges using the methods of Etchecopar *et al.* (1981). Results of the inverse palaeostress analyses were interpreted to indicate that three main compressional deformation phases characterised the structural history of the study region. D_1 involved E-W compression and was characterised by east-directed reverse displacement on the Tawallah Fault. Evidence for a pre-Wununmantyala Sandstone timing for D_1 includes;

- D_1 faults have been offset by D_2 and D_3 faults;
- D_1 faults only occur in the basal Tawallah Group sedimentary package;
- clasts of Scrutton Volcanics and basal Tawallah Group stratigraphy occur in the basal Wununmantyala Sandstone, consistent with intrabasinal uplift at that time;
- regional and pervasive silicification as present in the basal Tawallah Group sedimentary package, which contrasts with the unsilicified middle/upper Tawallah Group packages;
- cataclastic and/or hydraulic breccias are abundant along post-D_1 fault zones exposed in the basal Tawallah Group package.

D_2 post-dated Tawallah Group deposition, with NW-SE compression resulting in sinistral strike-slip deformation adjacent to the Tawallah and Lorella Faults. This event is tentatively correlated with syn-Barney Creek Formation transpression at the McArthur River Pb-Zn deposit (Hinman, 1995).

D_3 either terminated or post-dated deposition of the Roper Group, with NE-SW compression forming most of the structural features preserved in the study region. Orientations of D_3 secondary faults in the Batten Range are consistent with Mohr-Coulomb failure models of dextral simple shear, although deformation was accommodated to some extent by the reactivation of favourably orientated D_2 faults. In the Scrutton Range, NE-directed differential reverse displacement on the Bauhinia Fault during D_3 formed a series of subsidiary fault-blocks that were bound laterally by tear faults and deformed internally by imbricate structures. The generation of a D_3 contractional strike-slip duplex between the Tawallah and Lorella Faults resulted in transpressional uplift of the western Tawallah Range.

Quartz-hosted fluid inclusions in D_3 hydraulic fault breccias sampled from the Batten Range formed from moderate temperature (120° to 220°C), saline (< 20 eq wt. % NaCl) and oxidised fluids. The presence of late-stage hydrothermal fluids with these compositions implies that there is great potential for epigenetic base-metal mineralisation to have formed where reduced (graphite and/or pyrite bearing) sediments have been juxtaposed with the Tawallah Fault or similar D_3 fault systems.

9.5 TECTONO-STRATIGRAPHIC MODEL

The structural, sedimentological, and geochemical characteristics of the Tawallah Group are consistent with an intracratonic setting for the early tectonic development of the southern McArthur Basin. The basal Tawallah Group package was deposited during a period of rapid tectonic extension and was characterised by regionally extensive clastic depositional systems and widespread mafic volcanism. Rapid rates of tectonic extension resulted in high degrees of asthenospheric partial melting and the eruption of large-volume continental flood basalts (Seigal Volcanics). In the upper parts of the basal package, low-relief, shallow platform carbonates (upper Aquarium Formation) are interpreted to have been deposited across the southern McArthur Basin during a period of regional tectonic quiescence.

In the central Tawallah Range, a local stratal geometry interpreted as a 'growth wedge' occurs adjacent to a WNW-striking fault in basal Tawallah Group stratigraphy. This geometry is interpreted to indicate that deposition of the lower Tawallah Group was controlled by N-S-extension, and is consistent with the tectonic model proposed by Etheridge and Wall (1994) for McArthur Group times. An early extensional basin architecture comprising approximately E-W-trending rift compartments that were bound by trending transfer zones is therefore inferred for the initial depositional cycle of the southern McArthur Basin.

The transition from subaqueous (Aquarium Formation) to subaerial braidplain depositional environments at the base of the middle Tawallah Group package was controlled by D_1 uplift of lower Tawallah Group and Scrutton Volcanics stratigraphy along the N-striking Tawallah Fault system. In the study region, D_1 uplift resulted in the deposition of proximal braidplain deposits adjacent to the Tawallah Fault and more distal braidplain facies associations in the Scrutton Range (Wununmantyala Sandstone). In areas where sedimentation was not directly controlled by early intrabasinal uplift, shallow marine conditions may have prevailed at this stratigraphic interval.

Shallow subaqueous sediments (Wollogorang Formation) were deposited during a marine transgression when crustal extension and subsidence resumed. A reduction in the rate of tectonic extension is interpreted to have occurred following the D_1 compressional event, resulting in lower degrees of asthenospheric partial melting

and the formation of smaller-volume basalt/dolerite sequences (Settlement Creek and Gold Creek Volcanics). The upper Tawallah Group sedimentary cycle marks a regressive transition from the subaqueous settings of the Gold Creek Volcanics to marginal subaqueous and subaerial clastic depositional environments. Because evidence for compressional deformation is lacking, elevation of the ambient geothermal gradient during post-D_1 extension is proposed as a possible uplift mechanism for this regressive transition.

The Masterton Sandstone (basal McArthur Group) is interpreted to have been deposited in response to thermal relaxation following the regional uplift associated with upper Tawallah Group deposition and volcanism. It disconformably overlies the Wununmantyala Sandstone in the Batten and Tawallah Ranges, implying that the upper Tawallah Group package had been removed by erosion prior to McArthur Group deposition. An alternative possibility is that these regions remained as topographic highs and sites of non- or restricted deposition during middle/upper Tawallah Group sedimentation and intrusive/volcanic activity, which occurred in adjacent, topographically lower areas.

Identification of syn-depositional growth faulting in the middle and upper Tawallah Group packages has been complicated by the influence of D_1 uplift on their local depositional patterns. However, the occurrence of a 'growth wedge' stratal geometry in the Masterton Sandstone (Batten Range) is interpreted to indicate that the geometry of basin-forming structures active during basal Tawallah Group sedimentation and volcanism was maintained after the cessation of D_1. Sedimentary deposition was therefore controlled by N-S tectonic extension until at least McArthur Group times.

Based on the absence of volcanics with N-MORB affinities in the southern McArthur Basin, intracontinental extension did not proceed to the stage where new oceanic crust was developed. Instead, failure of rifting resulted in the deposition of finer-grained clastic and evaporitic carbonate lithologies (McArthur Group) in a sag-phase tectonic setting characterised by broad crustal extension.

In conclusion, the palaeo-depositional architecture of the Tawallah Group was controlled by major NNW- and WNW-striking faults during both the extensional and compressional phases of basin formation. These 'fundamental' structural trends are likely to have also influenced McArthur and Nathan Group depositional geometries, with anomalous thickening of potential host lithologies for base-metal mineralisation occurring at their intersections. Their resolution by geological or geophysical means would be an important consideration in any exploration program intended for the southern McArthur Basin.